PHD Thesis

Development of a coagulation coefficient measurement device (CMD) for the measurement of the coagulation coefficient of nanoparticles in the size range from 10 to 1000 nm

Dipl.-Ing. Bernhard Andreas Heiden

Graz, 7th of January 2006

written at the

Institute for Internal Combustion Engines and Thermodynamics
Traffic and Environment Section
Graz University of Technology

Advisors:

Ao.Univ.-Prof. Dipl.-Ing. Dr. techn. Peter Johann Sturm

Adjunct Prof. Dr. Athanasios G. Konstandopoulos

Acknowledgements

My sincerest thanks go to all who have contributed to this work. First of all is Ao. Univ.-Prof. Dr. techn. Peter Sturm who had the initial idea of investigating this very fundamental problem of aerosol technology. He was the primary person responsible for the sponsorship by the FVT (Forschungsgesellschaft für Verbrennungskraftmaschinen und Thermodynamik), which made the experiments, necessary for this kind of basic research[1], possible. His generosity with time insight and friendship both personal and professional are well known and it is to him I am most indebted. I am also indebted to Adjunct Prof. Athanasios Konstandopoulos who was willing to be my associate advisor, in spite of his very busy schedule, especially as he is one of the experts in this reemerging field of nanoparticle research. The head of the Institute for Internal Combustion Engines and Thermodynamics and all my colleagues are due my thanks, especially Univ.-Prof. Dr. techn. Rudolf Pischinger, em. Univ.-Prof. Dr. techn. Helmut Eichelseder, Ao.univ. Prof. Dr. Raimund Almbauer, Dipl.- Ing. Dr. Gerhard Pretterhofer for discussing ideas, Dipl.-Ing. Dr. Hannes Rodler for helping with instruments and social integration in the group as well as Dipl.-Ing. Michael Bacher, my co researchers, Mag. Dr. Dietmar Öttl, Dipl.-Ing. Christian Kurz, Mag. Marlene Hinterhofer, Mag. Silvia Vogelsang and the secretary Sabine Hartinger, Sabine Minarik and Alexandra Stiermair. I enjoyed also the cooperation with the group under the direction of Univ.-Prof. Dr. techn-Stefan Hausberger especially Dipl.-Ing. Martin Rexeis, Dipl.-Ing. Thomas Vuckovic, Dr. Jürgen Blasnegger, Dipl.-Ing. Michael Zallinger. My thanks also go to Dipl.-Ing. Dieter Engler, who introduced me in the use of the SMPS and CPC and all the other particulate measurement equipment from the institute as well as to the former assistant Dipl.-Ing. Dr. Mario Ivanišin for scientific exchange. Additionally I would like to thank the staff of the

[1] This sampling system has been completely founded by the FVT (Research society of combustion engines and thermodynamics) at the Institute for Internal Combustion Engines and Thermodynamics of the University of Technology Graz.

laboratory for the help in the mechanical setup, especially Siegfried Gimpl, Günter Rumpf for manufacturing parts of the CMD and indeed all others who are to numerous to mention.
Dipl.-Ing. Helmut Wurm from National Instruments is due a special thank for fruitful, repeated and personal assistance concerning the Labview Hard- and Software integration. My diploma students Dipl.-Ing. Emil Bakk and Bernd Brugger are due thanks for having supported the work of the CMD by their enthusiasm and work around the clock to prepare the measurements in Munich and at the AVL Graz. Dr. Armin Messerer is due thanks for the measurements at the TU-Munich. Dr. Schindler of the AVL is due thanks for the support with the measurements with the CAST. My old friend Dipl.-Ing. Günter Jaritz is due many thanks for building the electrical circuits of the CMD and discussing ideas as also for measurement assistance in Munich. I am also indebted to Dr. Werner Schaffenberger who helped me in the theoretical segment in clarifying the mathematical concepts. My thanks also go to Mr. Steven Fowler, M.H. for editing the text for American English.
Last but not least, my personal thank goes to my wife, Bianca, who listened to my long discussions about this topic, and who continually gave me motivation. As she is expecting at the time of this writing our first child who is according to the last ultra sound a baby.
I dedicate this work to our son.

Kurzfassung

Da die Luftverschmutzung von Nanopartikeln im Größenbereich von 10 bis 1000 nm einen großen Einfluss auf die menschliche Gesundheit hat und der Dispersionsprozess von der Emissionsquelle bis zur Immissionssenke noch nicht sehr gut prognostiziert werden kann, ist es notwendig das Wachstumsverhalten von Aerosolen weiter zu untersuchen. Zu diesem Zweck wurde ein mobiles Koagulationsmessgerät (CMD) entwickelt. Dieses dient dazu den Koagulationskoeffizienten K von Aerosolen mit einem Durchmesser zwischen 10 und 1000 nm zu messen. Dabei ist K ist ein grundlegendes Maß für das Wachstum von Aerosolen. Ein konstanter Konzentrationsaerosolreaktor, der aufgrund des veränderlichen Volumens unterschiedliche Größenverteilungsmessungen ein und desselben Aerosols ermöglicht, wurde zum ersten Mal gebaut, getestet und mit LABVIEW prozessautomatisiert. Eine bestehende Theorie, die auf der allgemeinen dynamischen Gleichung (GDE) basiert, wurde für das CMD angepasst und, unter Berücksichtigung von Koagulation und Diffusion, auf die Form einer speziellen logistischen Gleichung gebracht. Die Anzahlkonzentrationsabnahmemessung erlaubt zusammen mit der entwickelten Theorie die Auswertung des Koagulationskoeffizienten mit einer Reihe von verschiedenen Methoden. Die sich daraus ergebenden Koagulationskoeffizienten sind weitgehend kohärent mit Werten aus der Literatur. Die zwei kontinuierlichen Konzentrationsmessmethoden, ergaben in Bezug auf die zwei diskontinuierlichen Methoden für den Grenzfall kurzer Zeiten einen im Mittel um den Faktor 5 höheren Koagulationskoeffizienten. Die Ursache könnten Fluktuationen des Koagulationskoeffizienten oder eine unterschiedliche Aerosolverdünnung sein. Zukünftiger Forschungsinhalt ist die Anwendung der Messmethoden des CMD auf die Unterscheidbarkeit von Aerosolen, Partikelform und einen allgemeinen Koagulationskoeffizienten.

Abstract

As air pollution of nanoparticles in the size range of 10 to 1000 nm has a high impact on human health and the dispersion of these particles can not be predicted very well, clarification of growth of aerosols is necessary. For this purpose a mobile coagulation measurement device (CMD) was developed. It aimed at measuring of the coagulation coefficient K of aerosols in the diameter size range between 10 and 1000 nm, where K is a basis quantity for the kinetic of aerosols. A constant concentration aerosol reactor has been built, tested and automated with LABVIEW for the first time, allowing for a variable volume and time dependent size distribution or concentration measurements of the same aerosol. A theory was adapted for the CMD based on the fundamental general dynamics equation (GDE), which reduces to the form of a special logistic equation, taking coagulation and diffusion into account. The measurement of the number concentration decay and of their distribution allows, together with the developed theory, for the evaluation of the coagulation constant with a number of different methods. The resulting coagulation coefficients reflected the values from the literature. The two continuous concentration measurement methods yielded, compared to the two discontinuous methods, for the limiting case of short times, an average 5 times higher coagulation coefficient. The cause might have been fluctuations of the coagulation coefficient or the influence of different aerosol dilution. Future research areas are the application of the measurement methods of the CMD to the distinction of aerosols, particle form and to a general coagulation coefficient.

CONTENT

Acknowledgements ... 3
Kurzfassung ... 5
Abstract ... 7
CONTENT ... 9
Introduction ... 13
List of principal symbols ... 15
INDICES ... 20
Theory ... 21
Problem formulation ... 21
Aerosol characterization ... 22
I.1.1 On the lognormal size distribution interpretation ... 22
I.1.2 Application to fractal aggregates ... 23
I.1.3 The lognormal size distribution ... 24
Aerosol dynamics relevant for the coagulation coefficient ... 25
I.1.4 General Dynamics Equation (GDE) ... 25
I.1.5 Diffusions coefficient D ... 28
I.1.6 Coagulation coefficient K ... 29
I.1.6.1 Smoluchowski equation ... 29
I.1.6.2 Approximation of applicability of the Smoluchowski Equation ... 30
I.1.7 Determination of the coagulation coefficient K ... 32
I.1.7.1 Theory of loss by coagulation and diffusion ... 32
I.1.7.2 Method (1) - Constant Volume Batch Reactor (CV) for short times ... 34
I.1.7.3 Method (2) - Constant Volume Batch Reactor (CV) for long times ... 36
I.1.7.4 Method (4) - Constant Concentration Reactor (CC) for long times ... 36
I.1.7.5 Method (3) - Constant Concentration Reactor (CC) for short times ... 39
I.1.8 Predicted application of the measurement of the quantity K ... 41

I.1.8.1 Fractal dimension determination ... 41
I.1.8.2 Primary particle diameter ... 43
Description of the CMD ... 45
Principle of operation of the CMD ... 45
Setup of the CMD ... 46
I.1.9 System setup ... 46
I.1.9.1 Standard SMPS system ... 46
I.1.9.2 CMD system ... 47
I.1.10 Settler ... 50
I.1.11 Effective flow rate ... 51
I.1.11.1 Settler volume determination ... 52
I.1.11.2 Total time calculation ... 56
I.1.11.3 Pressure drop ... 56
I.1.11.4 Pressure and temperature dependence ... 58
I.1.11.5 Gas dependence ... 63
Operation of the CMD ... 63
I.1.12 Path concept ... 63
I.1.13 Operation concept ... 64
I.1.13.1 Complex operation types ... 65
I.1.13.2 Simple operation types ... 67
I.1.14 Labview software implementation ... 69
I.1.14.1 Structure ... 69
I.1.14.2 Main menu ... 70
I.1.14.3 Initialization ... 71
I.1.14.4 Measurement ... 73
Fundamental considerations ... 77
I.1.15 Reactor characterization ... 77
I.1.16 Residence times ... 78
I.1.16.1 Overall residence time for measurement ... 79
I.1.16.2 Settler ... 81
I.1.16.3 DMA ... 83
I.1.16.4 CPC ... 86
I.1.17 Dilution ... 87

I.1.17.1 Dilution in the CPC ... 87
I.1.17.2 Dilution due to incomplete filling ... 88
I.1.18 Impaction, deposition and other effects ... 88
Measurements of the coagulation coefficient with the CMD ... 91
Monodisperse aerosols ... 91
I.1.19 Control measurement ... 95
I.1.20 Results: Smoluchowski coagulation plot ... 96
Polydisperse aerosols ... 97
I.1.21 Measurement of the coagulation coefficient of polydisperse aersols by means of a size distribution measurements - Incense Measurements ... 97
I.1.22 Measurement of the coagulation coefficient of polydisperse aersols by means of a number distribution measurement ... 101
I.1.22.1 Polydisperse Coagulation I (Method 4) ... 101
I.1.22.2 Polydisperse Coagulation II (Method 3) ... 105
Conclusions ... 111
Theory of coagulation and diffusion ... 111
Coagulation Measurement Device (CMD) ... 112
Coagulation coefficient ... 114
Outlook ... 115
Literature ... 117
FIGURES ... 121
TABLES ... 127
INDEX ... 131
Appendix A Detailed specifications ... 133
Tubes ... 133
Detailed residence times ... 134
Settler ... 136
Appendix B Visual Basic (VB) programs determining the lognormal size distribution ... 137
Appendix C Labview 7.1 software implementation of the CMD ... 141
Detailed main front panel ... 141
Software hierarchy ... 141
CMD Stepper motor control ... 145
Software variables in the Labview 7.1 implementation ... 146

Devices and corresponding programs 152

Introduction

1.) The <u>coagulation measurement device</u> (CMD) is the core unit referred to in this work. The aim of such an instrument is to measure the kinetics of coagulation of nanoparticle aerosols. It was my aim to build a portable instrument for measuring the coagulation coefficient in the nanoparticle size range. In the literature, measurements of the coagulation of nanoparticles were often made during the last century. The measurements were made mainly with particle number concentration measurements (Husar 1971; Rooker and Davies 1979) or even with particle number size distribution measurements (Schnell and others 2004). Some kind of closed batch reactor is the usual method of measuring the coagulation kinetics, because an aerosol cannot easily be kept constant in concentration. For example large bags were often used with a large volume to surface ratio, allowing for increasing neglect of wall diffusion. All of these methods show the problem of being physically very large and, therefore, not portable. Scaling down the size of the reactor, the aerosol volume sampled cannot be neglected compared to the volume of the settler[2]. For a closed, constant volume reactor this means that the pressure drops. To compensate for this I developed the *constant concentration reactor*[3] allowing for a theoretically constant thermodynamic state with respect to pressure and temperature.

The experimental work for the building of the CMD with a constant concentration reactor and the commercial SMPS System (Scanning Mobility Particulate Sizer System) from TSI has been done in the Laboratory of Internal Combustion Engines and Thermodynamics at the University of Technology in Graz from 2004 to 2005, where the programming and process automation was implemented with the Labview Software.

[2] Aerosol batch reactor or container for coagulation (in general any reaction) and subsequent particle concentration measurement.

[3] Constant concentration refers to an ideal (not real existing) state of no coagulation and no deposition to the reactor walls.

There have been made two diploma theses on the CMD (Bakk 2005; Brugger 2005) looking at the fail-safe analysis of the CMD, and on routines for the normal measurement mode of the CMD.

This thesis consists of four main chapters. The first refers to the theoretical background of the system, the underlying physics, the theory of simultaneous coagulation and diffusion first adapted for the concept of the constant concentration reactor and its derivation for practical application.

The second chapter contains the description of the CMD. What it consists of, the basic components, experiments related to the build CMD and application diagrams when measuring with the CMD to keep overview of the basics of the CMD system. The principles of operation are explained as well as the practical use of the Labview software I developed for the CMD during development.

The third chapter contains a selection of experiments demonstrating the principal use of the CMD for different concepts of measurement the coagulation coefficient. Main applications are the measurement of the mono- and polydisperse coagulation coefficient, with different methods.

The listing is not complete as the CMD is intended to be used as research instrument. E.g. with additional hardware, the temperature dependency or additional reactor type equivalent measurements[4] could be investigated.

In the Appendices additional information is given for the detailed specifications of some key elements of the CMD, visual basic programs for calculating the logarithmic normal distribution from experimental data and an overview over the Labview program hierarchy.

[4] Other than the constant concentration reactor; e.g. Continuously Stirred Tank Reactor (CSTR) with variable residence time (see section I.1.18).

List of principal symbols

Var	Description	Unit
#	Particle(s)	~
[]	Denotes units inside the brackets	~
Λ	Lacunarity	~
A	"Area"	~
AIMS	Aerosol instrument manager software of the standard SMPS system (e.g. DMA 3081 and CPC 3010)	~
$A_{SETTLER}$	Inner surface area of the settler inside	m^2
ASF	Flow sensor ASF1430 from Sensirion	~
ASP	Differential pressure sensor from Sensirion ASP1400	~
B	Second virial coefficient	~
bool	Boolean	~
C	Cunningham-Knudsen-Weber-Millikan correction factor for the diffusion coefficient	~
CAST	Soot particle generator for production of defined particle number concentrations from Matter-Engineering www.matter-engineering.com	~
CC	Cumulative Counts since the last measurement from the CPC	-
CC	Constant Concentration reactor	~
CMD	Coagulation measurement device	~
CNC	Condensation nuclei counter	~
CPC	Condensation particle counter	~
c_s	Terminal settling velocity	m/s
c_{sf}	Terminal settling velocity of fractal particles	m/s
CSTR	Continuously Stirred Tank Reactor	~
CT	Cumulative Time of the last measurement from the CPC	s
CV	Constant volume reactor	~
D	Diffusion coefficient	m^2/s
D_f	Fractal dimension	~
$d_{i\_SETTLER}$	Inner diameter of the settler	m
dm	Differential mass	kg
d_m	Mean settler diameter	m
d_m	Collision diameter – distance between the centers of two molecules	m
DMA	Differential mobility analyzer	~
dN	Differential particle concentration	$\#/cm^3$
dN0	Differential particle concentration of CPC measurement	$\#/cm^3$
dN00	Differential particle concentration of CPC dilution air	$\#/cm^3$
$d_{o\_SETTLER}$	Outer diameter of the settler	m

Var	Description	Unit
D_p	Diffusion coefficient of particle with diameter d_p	m^2/s
d_p	Diameter of Particle	nm
D_{p0}	Diffusion coefficient of particle with primary diameter d_{p0}	m^2/s
d_{p0}	Diameter of primary particle of a fractal aggregate	nm
dp_1	Pressure drop impactor (cm H2O)	cm H2O
dp_2	Pressure drop across the bypass orifice	mm H20
dp_3	Differential pressure of ASP1400 (CMD settler)	Pa
d_{pg}	Geometric mean diameter of particle	nm
dp_{max}	Diameter of Particle MAXimum that could be measured with SMPS	nm
dp_{min}	Diameter of Particle MINimum that could be measured with SMPS	nm
DRVi	i=1..3 manual needle valves	~
dV	Differential volume	cm^3
EK-H2	Evaluation Kit EK-H2 from Sensirion; microcontroller access kit for the humidity sensors. The sensor SHT75 was used.	~
Ft	With of one fold of the settler	m
Fz	Number of fold of the settler	~
g	Gravitational constant	m/s^2
GDE	General dynamics equation	~
Gilibrator 2	Calibration bubble flow meter from Sensidyne	~
GMEAMOD	Variable in the CMD program for setting the *operation*	~
h	Diffusion layer thickness	m
HASOTEC	Company for the used stepper motor hardware www.hasotec.com	~
HCX001A6V	Absoluter pressure sensor from SensorTechnics	~
I	Particle current according to nucleation law	
INNOFLEX	Company for settler production www.faltenbalg.de	~
K	Coagulation coefficient	cm^3_gas/(#*s)
k	Boltzmann constant: $k=R/N_A=1.38*10^{-23}$	J/K
K_a	Apparent coagulation coefficient	cm^3_gas/(#*s)
K_{ac}	**A**pparent coagulation coefficient for constant **c**oncentration reactor	cm^3_gas/(#*s)
K_m	Mean coagulation coefficient	cm^3_gas/(#*s)
K_p	Coagulation coefficient of particle with diameter d_p	cm^3_gas/(#*s)
K_{p0}	Coagulation coefficient of primary particle with diameter d_{p0}	cm^3_gas/(#*s)
L	Length	Length
L	Particle wall diffusion frequency	1/s
$L_{\_Settler\_min}$	Settler minimum size due to folds	m
L_0	Particle wall diffusion frequency for constant concentration reactor	1/s
L_{0m}	Mean L_0	1/s
LABVIEW	Labview 7.1 Software from National Instruments www.ni.com	~
L_{DMA}	DMA Characteristic Length	m
L_{max}	Settler maximum actual size	m
L_{min}	Settler minimum actual size	m
LMS	Least mean squares fit	~
lpm	Liter per minute	~

Var	Description	Unit
m.v.	Measurement value	~
Mathcad®	Mathematic software package from Mathsoft www.mathsoft.com	~
Matter-Engineering	www.matter-engineering.com	~
MDP	Monodisperse particle diameter	nm
MG	Molecular weight	kg/mol
N	Number of scan intervals	-
N	Particle concentration	$\#/cm^3$
N_∞	Total particle concentration	$\#/cm^3$
$n(v), n(\bar{v})$	Volume distribution	$\#/(L^3\_particle*L^3\_gas)$
n_0	Initial number concentration	$\#/cm^3$
N_0	Initial total particle concentration	$\#/cm^3$
N_A	Avogadro constant $N_A=6.022*10^{23}$	#_gas/mol
NBR	Antistatic rubber mixture of the settler from INNOFLEX	~
n_d	Particle size distribution function	$\#/(cm^3*nm)$
NI	National Instruments (see Labview)	~
N_p	Number of particles in a fractal aggregate	~
$N_{p,\ primary}$	Total number of primary particles in volume V	~
NSM	number of single measurements	-
n_{tot}	Total particle counts since last measurement	#
operation	A series of paths see I.1.13	~
p	Pressure	mbar
p_0	Ambient air pressure	mbar
p_1	Absolute pressure (SMPS sensor)	mbar
p_2	Absolute pressure sensor CMD (settler)	mbar
path	Valve setting leading to a fluid path in the CMD see I.1.12	~
p_s	Standard pressure (1013mbar)	mbar
Q	Effective constant flow rate of the settler as a function of the stepper motor velocity	lpm=l/min
R	Gas constant: R=8.31441	J/(mol*K)
r^2	Pearson's regression coefficient	~
r_d	Is proportional to dN; The actual particle concentration of the CPC	$\#/cm^3$
Re	Reynolds number	~
Re_x	Local Reynolds number	~
rgbx	Command code SMCard SM41 (HASOTEC)	~
r_{i_DMA}	DMA Inner Radius	m
r_{o_DMA}	DMA Outer Radius	m
ROTDRV1	Rotations of needle valve DRV1	Rot(ations)
rpm	Rotations per minute	~
RS232	Serial interface	~
RSV	Unidirectional valve	~
S	Surface area	m^2
S/V	Surface area to volume ratio of the settler	m^2/m^3
Sc	Schmidt number	~
sccm	Standard cubic centimeter	~
SCT	SCan Time in seconds. Scan time for one size distribution	s

Var	Description	Unit
	measurement	
SEM	Scanning electron microscopy	~
Sensidyne	www.sensidyne.com	~
Sensirion	www.sensiorion.com	~
SensorTechnics	www.sensortechnics.com	~
sff	Safety factor for increasing filling time	~
SHT75	Humidity sensor form Sensirion (see also Sensirion)	~
Sh_x	Local Sherwood number	~
SM-41-PCI	PCI Interface card from HASOTEC for stepper motor control	~
SMPS	Scanning mobility particulate sizer	~
SMPS 3081	Standard SMPS system from TSI containing the classifier 3081, the DMA 3080 and the CPC 3010	~
SPFA	Speed factor for the stepper motor	~
t	Time	s, min
T	Temperature	°C
T_1	Cabinet temperature	°C
T_2	Sheath flow temperature	°C
T_3	Bypass flow temperature	°C
T_4	CPC Condenser temperature	°C
T_5	CPC Saturator temperature	°C
T_6	ASP temperature	°C
T_7	CMDC temperature Pt100	°C
T_8	CMD Balg: Humidity temperature sensor on EK-H2	°C
t_{CLEAN}	Time for STEP Cleaning of the CMD Balg	s
t_{COAGUL}	Time for STEP coagulation	s
td	Residence time of the CPC 3010 and the standard tubing from the SMPS DMA to the SMPS CPC.	s
td'	Calculated td	s
tf	Is the residence time in the SMPS DMA from the AIMS software tf is the same as τ_3	s
t_{FILL}	Time for STEP filling the probe into the CMD Balg	s
t_{MEAS}	Time for STEP Measurement with the SMPS	s
T_s	Standard temperature (20°C)	°C
TSI	TSI Aerosol Instrumentation Company (www.tsi.com)	~
t_{total}	Time total	s
t_{total}	Total time of measurement x; total time of all measurements of one settler probe	min
u	Velocity, bulk velocity	L/time ;m/s
UV	Ultraviolet radiation	~
v	Volume of particle	m^3
V	(Gas) Volume	m^3,length^3
v, $\bar{v}$	Volume	L^3
V/S	Volume to Surface area ratio of the settler	m^3/m^2
v_0	Volume of primary particle of an fractal aggregate	m^3
V_0	Volume of air in the path between SMPS DMA & SMPS CPC	l
V_{0S}	Volume of air in the path between SMPS DMA & SMPS CPC according to AIMS software and standard setting	l
$V_{0S'}$	Calculated V_{0S}	l

Var	Description	Unit
V_1	Volume of air in the path between settler and SMPS in	l
V_2	Volume of air inside the SMPS between input and DMA	l
V_3	Volume inside the SMPS DMA	l
V_4	Volume of air in the path between SMPS and CPC for the CMD	l
V_5	Volume of air in the path between settler and CPC for settler measurement mode without DMA volume	l
V_6	Volume of gas in the CPC 3010 in the sample flow line between inlet and laser particle measurement in the CPC	l
V_7	(Total) Effective volume in the settler that can be pressed out	l
V_{70}	Total gas volume of the settler or when the settler is in the end switch position on the bottom.	l
V_{7min}	Settler rest volume when empty	l
V_9	Volume of air in the path between settler and CPC in (part of path 4)	l
v_b	Bulk velocity of the particles	m/s
v_{BALG}	Velocity of "BALG"	Upm
v_d	Minimum volume	l
Vi	i=1..8 magnetic two way valves	~
vi	Virtual instrument – this is a program module in Labview	~
vi’	See vi	~
V_{max}	Maximum volume of the settler	l
VMi	i=1..2 manual two way ball valves	~
V_{min}	Effective minimum volume of the settler	l
v_{MOT}	Motor control velocity (from SM card) - appr. motor velocity	Upm
V_p	(Gas) Flow rate	l/min
V_{p1}	Sample Flow rate SMPS	lpm
V_{p2}	Sheath Flow rate SMPS	lpm
V_{p3}	Bypass Flow rate SMPS	lpm
V_{p4s}, V_{p4}	Flow rate ASF Sensor	sccm, lpm
V_{p6}	Flow rate of the CPC dilution air	Lpm
V_{p7}	Identical with Q;	lpm
x_i	i=1..3 Cartesian coordinates x,y,z	L (length)
x_q	Transformation factor between dN and dN/dlog(d_p)	~
ZIMM	Company for machine components and elements www.zimm-austria.com	~
ΔL	Difference between L_{max} and L_{min}	m
α	Leakage ratio	~
$\alpha°$	*Contraction number*	~
β	Particle transfer coefficient	m/s
β_x	Local particle transfer coefficient	m/s
β	Collision frequency function	cm^3_gas/(#*s)
δ	Flow rate percentage increase	~
ϕ_1	Relative humidity sensor CMD	%
γ	Settler correction of d_m for real volume	[time/time]
γ	Total time ratio: t/t_{total}	~
κ	Differential pressure correction factor	~
λ	Mean free path of the gas	m
μ	Dynamic viscosity	kg/(m*s)

Var	Description	Unit
ρ_g,ρ	Gas density	kg/m^3
ρ_L	Density of air	kg/m^3
ρ_p	Particle density	kg/m^3
σ_g	Geometric standard deviation	~
τ	Residence time	s
τ_{CPC}	Residence time in the CPC 3010	s
τ_i	Residence time according to V_i i=0..6;9	s
τ_{tot}	Total residence time for settler measurement from the settler to the CPC	s
τ_{tot0}	Total residence time for settler measurement from the DMA to the CPC for SMPS measurement setup (standard SMPS measurement)	s
τ_{trans}	Total residence time for settler measurement from the DMA to the CPC for CMD measurement setup	s
τ_I	Time d_p is shifted to concentration because of residence time between DMA and CPC	s
τ_{II}	Time the raw data are shifted to the beginning of measurement mode	s
ζ	Sample to sheath flow volume ratio of the DMA	~

INDICES

Index	Description
B	Bulk
D	Distribution
F	Fractal
L	Leakage, air
M, m	Mean
max	Maximum
min	Minimum
P	Particle
P0	Referring to primary particle
s,S	Standard
tot	Total
u	Infinite volume

Theory

Problem formulation

Combustion generated nanoparticles are a main concern for air pollution and its health risks. There are still open questions about the *residence time*[5] in the atmosphere and the *laws of growth* of nanoparticles, which are typically found in the transition regime[6] in the size range between approximately 10 nm and one micrometer. It is not well understood in a theoretical sense, especially concerning coagulation. For this problem there are mainly two approximations at the end of this range, one of statistical thermodynamics and one deduced out of the Einstein approximation for Brownian motion (Friedlander 2000).

Both regimes together can be expressed as coagulation kernel β or K in the Smoluchowski equation in the transition regime by interpolation first accomplished by Fuchs (Fuchs 1989).

Measurement of physical quantities in the transition regime is both important for understanding the underlying physics and the atmospheric processes. Experimental investigations of particle evolution are available for special cases of aerosols and a limited number of physical quantities. The basic description for this process is given by the Smoluchowski equation (Smoluchowski 1917), which is part of the GDE[7] or equation (0-17).
The aim of the work is to investigate the physical process of coagulation in the transition regime in a systematic and flexible way, as for this purposes no standard measuring procedure is available. To fill this gap, an aerosol coagulation coefficient measurement device (CMD) has been developed to measure systematically the coagulation coefficient, which corresponds to the coagulation kernel of the Smoluchowski equation. By means of this a more precise and mobile measurement of the coagulation coefficient comes into reach, with the future goal of establishing it as standard measurement quantity (Heiden and Sturm 2005).

[5] See section I.1.16 for definition.

[6] This is where the Knudsen number is about 1 (see section I.1.5 for Knudsen number definition).

[7] General dynamics equation.

Aerosol characterization

I.1.1 On the lognormal size distribution interpretation

A very useful form to describe the distributions of nanoaerosols is to use the lognormal size distribution. It fits for the most parts of unimodal sources very well. Up to now there has been no theoretical explanation for this, though a good overview is given in (Friedlander 2000; Hinds 1999). In the following a short deduction for the relation between the quantities $dN/dlog(d_p)$ and dN, with respect to dV/dlog(dp) is given.

The most important function is the *continuous size distribution*. When dN [#/cm^3_gas] is the number of particles per unit volume of gas given in the diameter range d_p to $d(d_p)$ this can be formulated as:

$$dN = n_d \cdot (dp) \cdot d(dp) \tag{0-1}$$

In this defining equation, $n_d(d_p,t)$ [#/(cm^3_gas*nm_particle)] is the *particle size distribution function* for the general case. With reference to the units, that means that particles are related to a certain air volume, which equates to a size *particle concentration* and a characteristic length for the particles.

It is now of importance to relate these basic quantities to the common $dN/dlog(d_p)$ interpretation of the particles.

The variable dN refers to the particle concentration in a size interval, which can be measured directly with a CPC/CNC[8], this is normally then plugged into the $dN/dlog(d_p)$ interpretation. Differentiating the general equation for the relation between the natural and the decadic logarithm (0-2) gives (0-3).

$$\ln(d_p) = \ln 10 \cdot \log(d_p) \tag{0-2}$$

$$\frac{1}{d_p} \cdot d(d_p) = \ln 10 \cdot d\log(d_p) \tag{0-3}$$

Together with (0-1) the transformation equation for the two distributions is given in (0-4).

$$\frac{dN}{d\log(d_p)} = n_d \cdot d_p \cdot \ln(10) = n_d \cdot d_p \cdot 2.3 \tag{0-4}$$

To calculate now the relation between dN and dN/dlog(dp) it is at first unsatisfactory to calculate n_d from (0-4) and then dN from (0-1) leading to fluctuations of the transformed equation. To avoid fluctuation we introduce a mean value $x_{q,}$ where the index i corresponds to

[8] **C**ondensation **P**article **C**ounter; **C**ondensation **N**uclei **C**ounter

the measured values of the size distribution and Δd_{pi} is the mean difference between the diameters.

$$x_q = \frac{1}{m}\cdot\sum_{i=1}^{m}\frac{d_{p_i}\cdot\ln(10)}{\Delta d_{p_i}} = \frac{1}{m}\cdot\sum_{i=1}^{m}\frac{d_{p_i}\cdot 2.3}{\Delta d_{p_i}} \qquad \begin{array}{ll} \Delta d_{p_i} = \dfrac{d_{p_{i+1}} - d_{p_{i-1}}}{2} & i = 2..m\text{-}1 \\ \Delta d_{p_i} = d_{p_{i+1}} - d_{p_i} & i = 1 \\ \Delta d_{p_i} = d_{p_i} - d_{p_{i-1}} & i = m \end{array} \tag{0-5}$$

Then we get a practical formula for the transformation of the distributions dN and dN/dlog(dp):

$$\frac{dN}{d\log(d_p)} = dN\cdot x_q \tag{0-6}$$

By means of the definition of a spherical particle, the relation between the $dN/d\log(d_p)$ and $dV/d\log(d_p)$ is maintained. Defining the volume V

$$V = \int 1\,dV = \int n_d\cdot\frac{d_p^{\,3}\cdot\pi}{6}\,d(d_p) \tag{0-7}$$

we get together with (0-3) $dV/d\log(d_p)$ as a function of d_p and n_d:

$$\frac{dV}{d\log(d_p)} = \frac{\ln(10)\cdot\pi\cdot d_p^{\,4}\cdot n_d(d_p)}{6} = 1.2056\,d_p^{\,4}\cdot n_d(d_p) \tag{0-8}$$

Assuming constant density ρ_p the mass distribution follows out of (0-8):

$$\frac{dm}{d\log(d_p)} = \rho_p\cdot\frac{dV}{d\log(d_p)} \tag{0-9}$$

I.1.2 Application to fractal aggregates

When we want to use (0-8) for any particle form which can be described with the fractal dimension D_f we first look at the common definition of the fractal dimension for particle diameters[9]:

$$N_p = \frac{v}{v_0} = A\cdot\left(\frac{d_p}{d_{p_0}}\right)^{D_f} \tag{0-10}$$

N_p is the number of particles in one aggregate, v the volume of the particle, v_0 the volume of the primary particle A, the lacunarity, d_p the overall diameter of the particle, d_{p0} the primary particle diameter and D_f the fractal dimension. A is usually set for a constant of one, which leads to deviations of the description for small aggregates. We then get the fractal volume of the particle:

$$v = A \cdot \frac{\left(d_{p_0}\right)^3 \cdot \pi}{6} \cdot \left(\frac{d_p}{d_{p_0}} \right)^{D_f} \tag{0-11}$$

Substituting now (0-11) in (0-7) and using again (0-3) we get the more general solution for $dV/d\log(d_p)$:

$$\frac{dV}{d\log\left(d_p\right)} = A \cdot \frac{\ln(10) \cdot \pi}{6} \cdot \left(d_{p_0}\right)^{3-D_f} \cdot d_p^{\,D_f+1} \cdot n_d\left(d_p\right) = 1.206 \left(d_{p_0}\right)^{3-D_f} \cdot d_p^{\,D_f+1} \cdot n_d\left(d_p\right) \tag{0-12}$$

It can be remarked that different methods of particle sampling lead to different particle size distribution functions with reference to their density.

I.1.3 The lognormal size distribution

The lognormal size distribution is a good approximation for a lot of unimodal nanoaerosols, although the reasons are not well understood. It is a distribution which appears as a normal distribution when the x-axis has the logarithmic scale. It can be written as size distribution function in the form:

$$n_d\left(d_p\right) = \frac{N_\infty}{\sqrt{2 \cdot \pi} \cdot d_p \cdot \ln\left(\sigma_g\right)} \cdot e^{\left[\frac{-\left(\ln\left(d_p\right) - \ln\left(d_{pg}\right)\right)^2}{2 \cdot \ln\left(\sigma_g\right)^2} \right]} \tag{0-13}$$

N_∞ [#/cm^3] is the total particle concentration, σ_g the geometric standard deviation and d_{pg} the geometric mean diameter.

The distribution function n_d is related with (0-4) to $dN/d\log(d_p)$. For a given $dN/d\log(d_p)$ the total number concentration N_∞ can be calculated with the following equation:

$$N_\infty = \frac{1}{\ln(10)} \sum_{i=1}^{n-1} \frac{\left(\frac{dN}{d\log\left(d_p\right)} \right)_{i+1} - \left(\frac{dN}{d\log\left(d_p\right)} \right)_i}{\ln\left[\frac{\left(\frac{dN}{d\log\left(d_p\right)} \right)_{i+1}}{\left(\frac{dN}{d\log\left(d_p\right)} \right)_i} \right]} \cdot \ln\left(\frac{d_{p_{i+1}}}{d_{p_i}} \right) = \frac{1}{\ln(10)} \sum_{i=1}^{n-1} mdN_i \tag{0-14}$$

---

[9] e.g. (Mandelbrot 1987); (Friedlander 2000)

The index i goes from 1 to n-1 where n is the number of samples for the distribution, and mdN is the mean differential distribution. The geometric mean diameter d_{pg} and the geometric standard deviation σ_g can then be calculated from the experiments with:

$$d_{pg} = e^{\sum_{i=1}^{n-1} \ln\left(\frac{d_{p_{i+1}} - d_{p_i}}{\ln\left(\frac{d_{p_{i+1}}}{d_{p_i}}\right)}\right)} \tag{0-15}$$

$$\sigma_g = e^{\sqrt{\sum_{i=1}^{n-1} \left(\ln\left(\frac{d_{p_{i+1}} - d_{p_i}}{\ln\left(\frac{d_{p_{i+1}}}{d_{p_i}}\right)}\right) - \ln(d_{pg})\right)^2}} \tag{0-16}$$

In the Appendices, visual basic programs for gaining the lognormal size distribution parameters from grouped experimental data for $dN/d\log(d_p)$ or $dN(d_p)$ are printed.

Aerosol dynamics relevant for the coagulation coefficient

I.1.4 General Dynamics Equation (GDE)

The aerosol dynamics in general can be described by the GDE in (0-17), according to (Friedlander 2000)[10]. It can describe the motion and the growth process of the particulates. N_∞ is the total particle concentration, usually, and also in my experiments, measured with the CPC. In equation (0-17) it is looked at the volume distribution which is integrated from a minimum volume v_d to infinite volume u.

In the first term dN_∞/dt the time dependence of the total size concentration is given. The second term describes the change of particles due to convective motion of the particles with the bulk velocity v_B which pass the observed volume in the time interval dt. The index i corresponds to Einstein's sum convention.

$$\frac{d}{dt}N_\infty + v_B \cdot \frac{\partial}{\partial x_i} N_\infty = \int_{v_d}^{u} \frac{d}{dv} I \, dv + \frac{\partial^2}{\partial x_i^2} \int_{v_d}^{u} D \cdot n(v) \, dv + \frac{1}{2} \cdot \int_{v_d}^{u} \int_0^{v} \beta(\bar{v}, v - \bar{v}) \cdot n(\bar{v}) \cdot n(v - \bar{v}) \, d\bar{v} \, dv \ldots$$
$$+ - \int_{v_d}^{u} \int_0^{v} \beta(v, \bar{v}) \cdot n(v) \cdot n(\bar{v}) \, d\bar{v} \, dv - \frac{d}{dx_3} \int_{v_d}^{u} c_s \cdot n \, dv \tag{0-17}$$

The third term describes the nucleation, where the variable I is the particle current according to a nucleation law. The fourth term describes the diffusion losses, e.g. through wall deposition by wall collision, with D the diffusion coefficient and n=n(v) the particle size

[10] p. 311 ff.

distribution for the volume. The fifth and sixth term describes the coagulation with β as the *collision frequency function*[11]. The fifth term describes the gaining of particles of dv due to growth from the collision of particles with smaller diameter (particle with volume $d\overline{v}$ collide with particles with volume $d(\overline{v}-v)$), whereas the sixth term describes the loss of particles with volume dv due to all collisions of particles with volume $d\overline{v}$ that collide with particles with volume dv. The seventh term describes the loss due to the gravitational settling of spherical particles, where c_s is the terminal settling velocity, gained from the Stokes law (Friedlander 2000)[12] also considering the buoyant forces:

$$c_s = \frac{d_p^{\,2} \cdot g}{18 \cdot \mu} \cdot \left(\rho_p - \rho_g\right) \tag{0-18}$$

ρ_p and ρ_g are the particle and gas density, d_p is the diameter of the particle and μ is the viscosity of the gas. Replacing the volume of the particle by the fractal volume defined by (0-10) the terminal settling velocity c_{sf} can be gained for fractal particles:

$$c_{sf} = A \cdot \left(\frac{d_p}{d_{p0}}\right)^{D_f - 3} \cdot c_s \tag{0-19}$$

The fractal particle contrary to a spherical one leads to a drastic decrease in particle settling velocity as the fractal dimension is always ≤ 3 and the particle size d_p/d_{p0} increases. This is also shown for illustration in Figure 1 for A=1, different particle size ratios dp/dp_0 and fractal dimensions D_f. This can be also observed for macro fractal particles like snow flakes or springs.

[11] β is also called coagulation kernel.

[12] p. 15; this equation is a result of the gravity, buoyant and Stokes resistant forces.

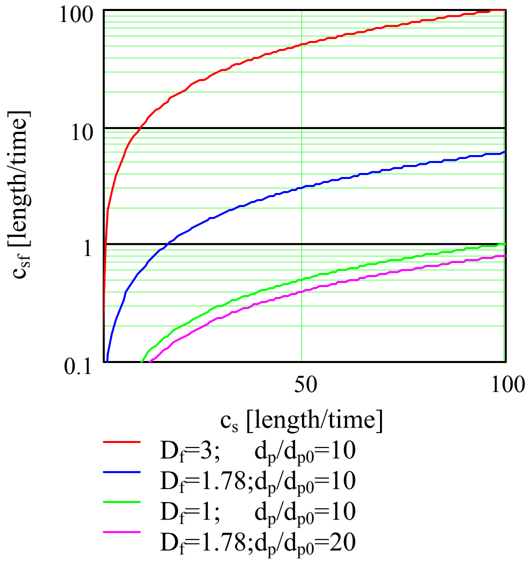

Figure 1 Corrected settling factor c_{sf} for fractal particles as a function of the settling velocity c_s for spherical particles. Decreasing fractal dimension D_f and decreasing particle size d_p leads to a decreasing settling velocity. The value D_f=1.78 is the value for Brownian coagulation in the three dimensional space often applied for soot particles (Jullien and Botet 1987) p.88.

For our application, the GDE can be simplified. The first term stays as we regard the time dependency. The convective forces can be neglected as there was no stirring experiment and the gas motion velocity v can be neglected Re<<10[13]. Nucleation effects are assumed to be neglected, as the thermodynamic state (p, T, V) stays constant. This effect can not be neglected, when there is evidence of a condensable vapor and hence nucleation. The nucleation rate is highly nonlinear with temperature. Therefore this quantity has to be observed very accurately in the case of possible nucleation.

It is assumed, that the diffusion losses cannot be neglected as well as the coagulation. The gravitational settling can be neglected for nanoparticles below 1 µm, as the observed ones, especially in relative short time ranges.

The resulting equation of the particle concentration in time, dependant on the wall deposition and the coagulation is given as:

[13] In practical this condition is fulfilled best near the walls in the diffusion boundary layer, where the later derived theory of loss by coagulation and diffusion is applied. In the bulk the Reynolds number Re is about 1 to 10

$$\frac{d}{dt}N_\infty = \frac{\partial^2}{\partial x_i^2}\int_{v_d}^{u} D\cdot n(v)\,dv + \frac{1}{2}\cdot\int_{v_d}^{u}\int_{0}^{v} \beta(\bar{v}, v-\bar{v})\cdot n(\bar{v})\cdot n(v-\bar{v})\,d\bar{v}\,dv \,...$$
$$-\int_{v_d}^{u}\int_{0}^{v} \beta(v,\bar{v})\cdot n(v)\cdot n(\bar{v})\,d\bar{v}\,dv \tag{0-20}$$

Neglecting the coagulation leads to:

$$\frac{d}{dt}N_\infty = \frac{\partial^2}{\partial x_i^2}\int_{v_d}^{u} D\cdot n(v)\,dv \tag{0-21}$$

When the surface to volume ratio S/V is large enough then the deposition on the wall can be neglected equation (0-20) is leading to:

$$\frac{d}{dt}N_\infty = \frac{1}{2}\cdot\int_{v_d}^{u}\int_{0}^{v} \beta(\bar{v}, v-\bar{v})\cdot n(\bar{v})\cdot n(v-\bar{v})\,d\bar{v}\,dv \,...$$
$$-\int_{v_d}^{u}\int_{0}^{v} \beta(v,\bar{v})\cdot n(v)\cdot n(\bar{v})\,d\bar{v}\,dv \tag{0-22}$$

I.1.5 Diffusions coefficient D

The Diffusion coefficient for particles in air according to the Einstein relation can be gained from (0-27):

$$D = \frac{k\cdot T\cdot C}{3\cdot\pi\cdot d_p\cdot\mu} \tag{0-23}$$

C is the *Cunningham-Knudsen-Weber-Millikan correction factor*:

$$C = 1 + Kn\cdot\left(1.257 + 0.4\cdot e^{\frac{-1.1}{Kn}}\right) \tag{0-24}$$

$$Kn = \frac{\lambda}{\frac{d_p}{2}} \tag{0-25}$$

C is an empirical function of the Knudsen number. The Knudsen number as defined below is the ratio of the mean free path of the gas λ and the particle radius $d_p/2$. The mean free path of the gas is:

$$\lambda = \frac{MG}{\sqrt{2}\cdot N_A\cdot\rho\cdot\pi\cdot {d_m}^2} \tag{0-26}$$

MG is the molecular weight; N_A is the Avogadro constant, ρ the density of the gas and d_m the *collision diameter* of the gas[14]. For air the collision diameter d_m=3.7*10^{-10} [m]. For standard air[15] the mean free path is 0.066 [µm] e.g.(Hinds 1999) p.21.

The usually defined diffusion constant is a function of two materials, describing the material flux of one material into the other, according to Fick's equation. In general the diffusion depends on all the components of the medium in which diffusion occurs. For the usual diffusion constant referring to two components as for the multicomponent pendant it is to be expected that C will depend on the gas in which particles are suspended and hence is not valid for gases other than air. There is also a temperature dependence of the diffusion coefficient which is not included in the Cunningham correction factor (equation (0-24)), as the experiments were done at room temperature (Rudyak and Krasnolutskii 2001; Rudyak and Krasnolutskii 2002).

In the above mentioned papers, Rudyak and Krasnotlutskii have introduced a new approach for determining the temperature dependent particle diffusion coefficient, taking into account that one gas particle interacts with multiple surface particles. It would be of scientific interest to study this effect in temperature regions above and below room temperature on the diffusion coefficient as the link to the coagulation coefficient.

I.1.6 Coagulation coefficient K

I.1.6.1 Smoluchowski equation

The coagulation constant K[16] is defined as[17]:

$$K = \frac{4 \cdot k \cdot T}{3 \cdot \mu} \cdot C = 4 \cdot \pi \cdot d_p \cdot D \tag{0-27}$$

k is the Boltzmann constant, T the absolute temperature, μ the dynamic viscosity and C the Cunningham correction factor. There is a relation between the coagulation constant and the particle diffusion constant in the Brownian regime.

---

[14] Distance between the centers of two colliding molecules

[15] p=1.013 [bar] and T=293 [K]

[16] K is also called coagulation coefficient, collision frequency β see section I.1.4 or coagulation kernel.

[17] There is confusion in the literature about the factor of two in the coagulation coefficient. According to (Rooker and Davies 1979) this is due to an error in the theoretical derivation.

The Smoluchowski equation (Smoluchowski 1917) for monodisperse coagulation can then be written as equation (0-28) which is a special case for the GDE regarding only coagulation with a constant coagulation coefficient K.

$$\frac{d}{dt} N_\infty = -K \cdot N_\infty^{\ 2} \tag{0-28}$$

N_∞ is the particle concentration for the complete size distribution over time. The solution is,

$$N_\infty = \frac{N_0}{1 + t \cdot K \cdot N_0} \tag{0-29}$$

where t is the coagulation time and N_0 is the initial particle concentration.

I.1.6.2 Approximation of applicability of the Smoluchowski Equation

Equation (0-29) is depicted in Figure 2, for the coagulation constant $K=54*10^{-10}$ according to (Rooker and Davies 1979), and can be used for a rough determination of the particle concentration over the time, given an initial particle concentration. This is useful for approximation of the particle concentration decay after the coagulation time t. The measured coagulation constant will vary around the first approximation, depending on the temperature and the different types of aerosols.

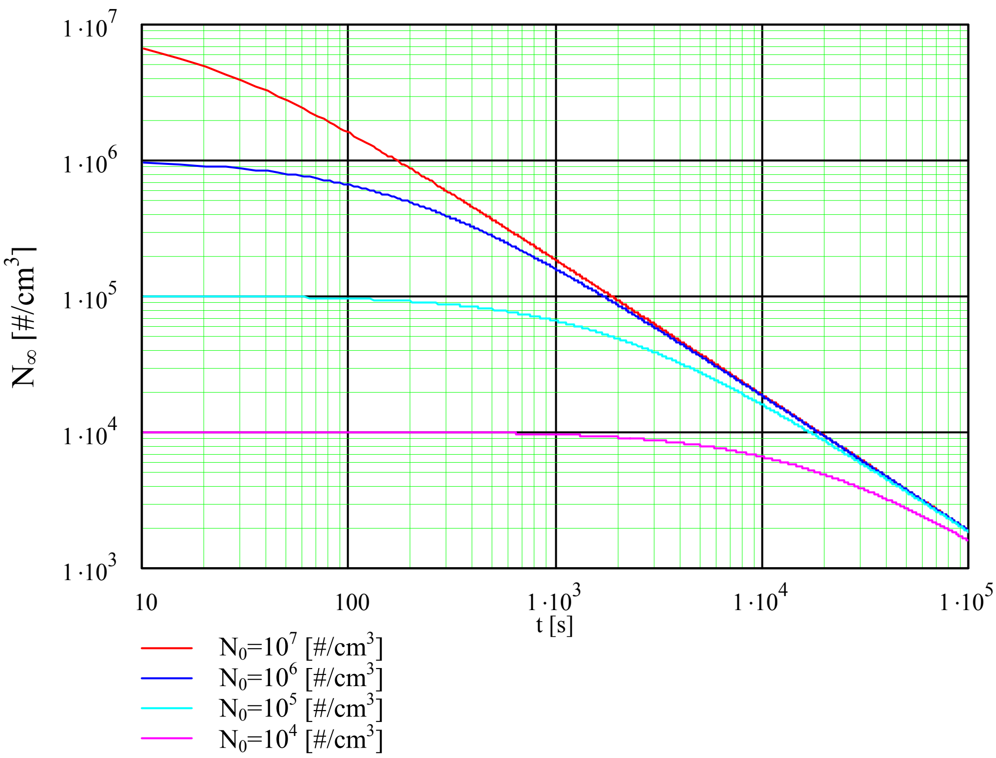

Figure 2 Solution of the Smoluchowski equation for different initial concentration and a constant coagulation coefficient $K=54*10$ [cm^3/s].

As it is necessary to have a difference in concentration measurement to determine the coagulation coefficient, it is useful to compare the initial concentration with the actual concentration over time. Hence we define the *concentration decrease* α:

$$\alpha = \frac{N_\infty}{N_0} \qquad (0\text{-}30)$$

Together with (0-29) we get the following equations for N_∞ and N_0:

$$\alpha\left(N_0, t\right) = \frac{1}{1 + t \cdot K \cdot N_0} \qquad (0\text{-}31)$$

$$\alpha\left(N_\infty, t\right) = 1 - t \cdot K \cdot N_\infty \qquad (0\text{-}32)$$

Equations (0-31) and (0-32) are depicted in Figure 3 for four different coagulation times t, for a fixed coagulation coefficient K. The dotted curves depict the initial concentration N_0 according to (0-31) the lined curves the concentration N_∞ according to (0-32) after a certain coagulation time t.

Given a desired concentration $N_0=2*10^5$ [#/cm^3] and a desired concentration decrease α the end concentration $N_\infty=1.2*10^5$ [#/cm^3] after the coagulation time of 600 [s] can be gained by following the black arrows.

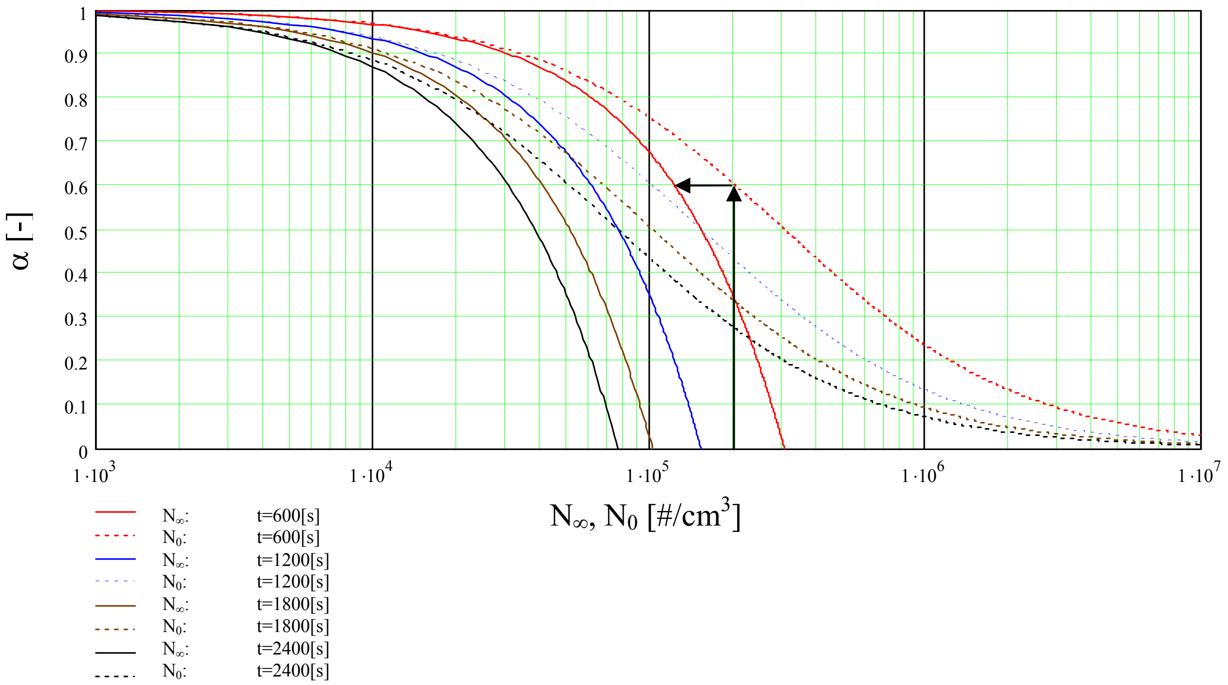

Figure 3 Solution of the Smoluchowski equation for a different concentration decrease α and the corresponding actual as the initial particle concentration N and N_0; Different coagulation times t are used as a parameter. The coagulation coefficient is constant $K= 54*10^{-10}$ [cm^3/s].

I.1.7 Determination of the coagulation coefficient K

I.1.7.1 Theory of loss by coagulation and diffusion

The general dynamics equation can be simplified for a constant coagulation coefficient K, as it is done in the Smoluchowski equation (0-27). Fick's second law of diffusion can be written for diffusion only applying a constant diffusion coefficient with respect to particle size and using the coordinate independent Laplace operator:

$$\frac{d}{dt}N_\infty = -D\cdot\Delta N_\infty = -\mathrm{div}\left(D\cdot \mathrm{grad}\left(N_\infty\right)\right) \tag{0-33}$$

The particle concentration gradient dN_∞/dt is hence proportional to the divergence of the gradient of N_∞ which is also:

$$N_\infty = \frac{N_\#}{V} \tag{0-34}$$

$N_\#$ are the total particles and V is the reference volume. Assuming natural convection in the coagulation reactor (CMD) a diffusion layer of thickness h remains, in which only diffusion takes place. This assumption corresponds to the "*two film theory*" for mass transport (Pflügl and Rentz 2000)[18]. If the particle concentration is zero on the wall and N_∞ in the core of the coagulation reactor then the gradient is constant over the whole surface:

$$\mathrm{grad}\left(N_\infty\right) = \frac{N_\infty}{h} \tag{0-35}$$

When we now equate the flux of the particles from the container volume V through the surrounding surface S according to the Gauss integral law the diffusion results in:

---

[18] p. 182; Corresponding to this theory, the concentration gradient is linear from a constant value at the wall (layer) to a constant concentration in the core. A constant velocity u from the bulk to the wall and no velocity boundary layer is regarded. In this case the *particle transfer coefficient* β=D/h. To take into account also the velocity boundary layer, the "Grenzschicht Theorie" (boundary layer theory), for the flow over a plate, can be applied, leading to a different solution for laminar and turbulent flow, which is also dependent on the length of the plate (settler actual effective length). For laminar flow β_x is proportional to $D^{2/3}$ (from exact solution $Sh_x=0.332*Re_x^{1/2}*Sc^{1/3}$). For turbulent flow β_x is proportional to $D^{0.57}$ (from exact solution $Sh_x=0.0296*Re_x^{4/5}*Sc^{0.43}$), with $\beta_x=D/x*Sh_x$, where D is the particle diffusion coefficient, Sh_x the local particle Sherwood number β_x*x/D, x the actual length coordinate parallel to the flow direction, Sc the Schmidt number ν/D, and Re_x the local Reynolds number u*x/ν.

$$\frac{d}{dt}N_\infty = -\frac{1}{V}\cdot\int \operatorname{div}\left(D\cdot\frac{N_\infty}{h}\right)dV = -\frac{1}{V}\cdot\int D\cdot\frac{N_\infty}{h}\,dS \tag{0-36}$$

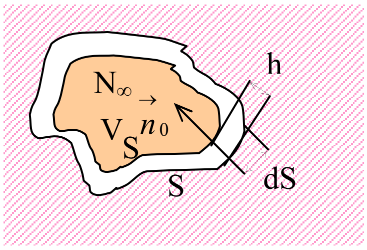

Figure 4 Principal surface, volume and particle concentration relation of the settler

The solution of equation (0-36) is,

$$\beta = \frac{D}{h} \tag{0-37}$$

$$L = \frac{S}{V}\cdot\frac{D}{h} = \frac{S}{V}\cdot\beta \tag{0-38}$$

$$\frac{d}{dt}N_\infty = -\frac{S}{V}\cdot\frac{D}{h}\cdot N_\infty = -\frac{S}{V}\cdot\beta\cdot N_\infty = -L\cdot N_\infty \tag{0-39}$$

where β [m/s] is the *particle transfer coefficient* in analogy to the mass transfer coefficient, and L [1/s] is the *particle wall diffusion frequency*. The equation is valid for a small diffusion layer of thickness h compared to the characteristic length of the reactor.

Simplifying (0-20) and introducing of (0-39) leads to

$$\frac{d}{dt}N_\infty = -\left(K\cdot N_\infty^{\;2} + L\cdot N_\infty\right) \tag{0-40}$$

which describes simultaneous coagulation and deposition. K is the coagulation coefficient and L is the previously defined particle wall diffusion frequency. Equation (0-40) can also be identified with the logistic equation (Soldov and Ochkov 2005)[19] which is a general equation for growth limited by saturation. The growth corresponds to the coagulation coefficient; the saturation corresponds to the loss due to wall diffusion. Equation (0-40) is the base equation of the four methods listed in Table 1 and derived in the next sections for gaining the coagulation coefficient K. Method (1) is the method derived from Rooker and Davies, where method (2) is the more general solution of method (1) for long residence times. Methods (1)&(2) are valid for a constant volume batch reactor (CV), whereas methods (3)&(4) are valid for the constant concentration (CC) coagulation reactor[20] used in this work. Method (1)

---

[19] p.10ff

[20] Definition see section I.1.15 p. 77

and (3) are used for short times and (2)&(4) for long time measurement of an aerosol.

Table 1 Methods of the determination of the coagulation coefficient K; CV denotes the constant volume and CC the constant concentration reactor;

Method	*Restrictions*	*Description*	*Reactor type*
(1)	$t \rightarrow 0$	Method of Rooker and Davies (Rooker and Davies 1979)	CV
(2)	t: 0..∞ (general method)	Like method of Rooker and Davies adapted for long times	CV
(3)	$\gamma \rightarrow 0$	Method developed in this work for the constant concentration reactor and analogous to method (1)	CC
(4)	γ: 0..∞ (general method)	Method developed in this work for the constant concentration reactor and analogous to method (2)	CC

I.1.7.2 Method (1) - Constant Volume Batch Reactor (CV) for short times

According to Rooker and Davies (Rooker and Davies 1979), a method for determining the coagulation equation can be derived. First an apparent coagulation coefficient K_a is introduced:

$$K_a = K \cdot \left(1 + \frac{L}{K \cdot N_\infty}\right) \tag{0-41}$$

This coagulation coefficient appears in the settler due to deposition on the wall and due to coagulation. In the case of an infinite surface, K_a becomes K. For practical application only K_a can be measured directly. Under the assumption that K_a is constant, which is true for short coagulation times, relative to the concentration, equation (0-40) can be written as follows:

$$\frac{d}{dt} N_\infty = -K_a \cdot N_\infty^{\,2} \tag{0-42}$$

This can be integrated like the Smoluchowski equation (0-28),

$$\frac{1}{N_{t2}} - \frac{1}{N_{t1}} = K_a \cdot (t_2 - t_1) \tag{0-43}$$

where t_i (i=1,2) denote two different times with constant K_a. In the Smoluchowski plot ($1/N_\infty$ is plotted against t) this can be seen when K_a is a straight line. K_a is dependent on the particle concentration $N_{\infty,}$ and as $K \approx N_\infty^{\,2}$ and $L \approx N_\infty$ K_a will differ, for different wall diffusion characteristics.

Equation (0-41) can now be integrated for constant K and L, by making a decomposition into partial fractions and using the defining equation (0-41) for K_a and for times t_i (i=1,2):

$$-L\cdot(t_2 - t_1) = \int_{t_1}^{t_2} \frac{1}{N_\infty}\, dN_\infty - \frac{K}{L}\cdot\int_{t_1}^{t_2} \frac{1}{\frac{K}{L}\cdot N_\infty + 1}\, dN_\infty = \ln\left(\frac{1+\frac{L}{K\cdot N_{t1}}}{1+\frac{L}{K\cdot N_{t2}}}\right) = \ln\left(\frac{K_{a,\,t1}}{K_{a,\,t2}}\right) \tag{0-44}$$

Hence,

$$K_{a,\,t2} = K_{a,\,t1}\cdot e^{L\cdot(t_2 - t_1)} \tag{0-45}$$

According to Rooker and Davies, this equation cannot be used for evaluation of L, as the assumption that L and K are constant is not valid over long periods of time, and K_a is a function of L.

For short periods of time K_a is constant for different particle concentrations N_∞. This leads to the following experimental method: Having one material of nanoparticles dispersed in a gas[21] with different particle concentrations the apparent coagulation coefficients can be calculated as slopes in the Smoluchowski plot ($1/N_\infty$ against t). Then from equations (0-38) and (0-41) the coefficients L, K, β, and h can be calculated:

$$L = \frac{K_{a,\,t2} - K_{a,\,t1}}{\frac{1}{N_{t2}} - \frac{1}{N_{t1}}} \tag{0-46}$$

$$K = K_{a,\,t1} - \frac{L}{N_{t1}} = K_{a,\,t2} - \frac{L}{N_{t2}}$$

$$\beta = L\cdot\frac{V}{S}$$

$$h = \frac{D}{L}\cdot\frac{S}{V}$$

If there are more than two apparent coagulation coefficients K_a available for the experiments, then K_a is plotted as a function of the initial particle concentration N_∞. The least mean squares fit of equation (0-41) yields to the coefficients for L and K and with equation (0-46) also to β and h.

To fulfill the conditions of the theory the size of the dimensions of the coagulation container has to be large compared to the diffusion layer h. Otherwise the geometry of the container has also to be taken into account in equation (0-36).

---

[21] Most commonly air

I.1.7.3 Method (2) - Constant Volume Batch Reactor (CV) for long times

For the case that the coagulation times are long and hence K_a is not constant any more, the detailed solution of equation (0-45) has to be calculated. This is done by inserting (0-41) in equation (0-45). The total particle concentration N_∞ can then be calculated as a function of time t, setting t_2=t and t_1=0 and N(t)=N_0 as:

$$N_\infty(t) = \frac{L}{K\cdot\left[\left(1+\frac{L}{K\cdot N_0}\right)\cdot e^{L\cdot t}-1\right]} \tag{0-47}$$

I.1.7.4 Method (4) - Constant Concentration Reactor (CC) for long times

The method of Rooker and Davies was applied for evaluation of the coagulation coefficient. The surface to volume ratio is in the same order of magnitude for the built CMD than that of Rooker and Davies. The main difference is that the volume is variable as the CMD is a *constant concentration reactor* (see section I.1.15, p.77). The CMD allows for a coagulation coefficient K determination by means of a single concentration measurement or the examination of the particle concentration decrease for the apparent coagulation coefficient K_a.

Mathematically the volume of the *constant concentration reactor* can be described by (0-48). For obtaining the equation describing the concentration as a function of time coagulation and diffusion the volume in (0-40) has to be replaced by:

$$V(t) = V_{70} - Vp_7\cdot t \tag{0-48}$$

V_{70} is the initial total volume of the settler, Vp_7 is the constant settler flow due to geometrical considerations and t is the time the measurement takes place.

In section I.1.11 it is derived that Vp_7 is inverse proportional to t_{total}[22]. Assuming that the volume for the empty settler is very small compared to the initial settler volume then Vp_7 is also approximately proportional to V_{70}. Defining the *total time ratio* γ,

$$\gamma = \frac{t}{t_{total}} \tag{0-49}$$

equation (0-48) can be written as:

$$V(t) = V_{70}\cdot(1-\gamma) \tag{0-50}$$

[22] Total time for emptying the settler.

We define L_0 according to equation (0-51) as a function of the initial conditions. These are the surface to volume ratio S/V_{70} (see Table 2) and the *particle transfer coefficient* β or S/V_{70}, the Diffusion coefficient D and the diffusive layer h.

$$L_0 = \frac{S}{V_{70}} \cdot \frac{D}{h} = \frac{S}{V_{70}} \cdot \beta \tag{0-51}$$

With equation (0-51) L can be written in equation (0-52) as a function of γ and a constant particle wall diffusion frequency L_0.

$$L(\gamma) \equiv \frac{L_0}{1-\gamma} \tag{0-52}$$

The governing equation for the constant concentration reactor can be yielded inserting equation (0-52) into (0-40) and substituting t according to equation (0-49):

$$\frac{d}{d\gamma} \frac{N_\infty}{t_{total}} = -\left(K \cdot N_\infty^{\ 2} + \frac{L_0}{1-\gamma} \cdot N_\infty \right) \tag{0-53}$$

t_{total} is constant for a measurement as the sample flow rate Vp_4 is constant and can be gained from equation (0-11).

To solve equation (0-53) we substitute N_∞ with y^α in equation (0-53). From this we see that α=-1. As a consequence we substitute N_∞ with y^{-1} in equation (0-53) yielding the following inhomogeneous differential equation:

$$\frac{d}{d\gamma} y \cdot \frac{1}{t_{total}} - \frac{L_0}{1-\gamma} \cdot y = K \tag{0-54}$$

The solution for the homogenous part is,

$$y_h = C \left(\frac{1}{1-\gamma} \right)^{L_0 \cdot t_{total}} \tag{0-55}$$

where the variable C is the integration constant. Making the variation of constants and inserting the in homogenous solution yields an equation for C:

$$\frac{d}{d\gamma} C = K \cdot t_{total} \cdot (1-\gamma)^{L_0 \cdot t_{total}} \tag{0-56}$$

After integration C is:

$$C = -\frac{K \cdot t_{total} \cdot (1-\gamma)^{L_0 \cdot t_{total}+1}}{L_0 \cdot t_{total} + 1} \tag{0-57}$$

After insertion in equation (0-55) and simplification the particular solution is:

$$y_p = -\frac{(1-\gamma) \cdot K \cdot t_{total}}{L_0 \cdot t_{total} + 1} \tag{0-58}$$

The complete solution is then the superposition of homogenous and inhomogeneous solution and resubstitution of N_∞:

$$\frac{1}{N_\infty} = y = y_p + y_h = (1-\gamma)^{-L_0 \cdot t_{total}} \cdot C - \frac{(1-\gamma) \cdot K \cdot t_{total}}{L_0 \cdot t_{total} + 1} \tag{0-59}$$

With the initial condition $N_\infty = N_0$ and $\gamma = 0$ the integration constant C gets:

$$C = \frac{1}{N_0} + \frac{K \cdot t_{total}}{L_0 \cdot t_{total} + 1} \tag{0-60}$$

Simplification of equation (0-59) and (0-60) yields for N_∞:

$$N_\infty = \frac{L_0 \cdot t_{total} + 1}{(1-\gamma) \cdot K \cdot t_{total} \cdot \left[\frac{1 + \frac{1}{K \cdot N_0} \cdot \left(\frac{1}{t_{total}} + L_0 \right)}{(1-\gamma)^{L_0 \cdot t_{total} + 1}} - 1 \right]} \tag{0-61}$$

This is the predicted concentration for a complete measurement run from $\gamma = 0$ to $\gamma = 1$, and simultaneous coagulation and diffusion. Equation (0-61) is shown in Figure 5 for different initial particle concentrations N_0, and typical constant values for K and $L = L_0$ for the experiments of Rooker and Davies.

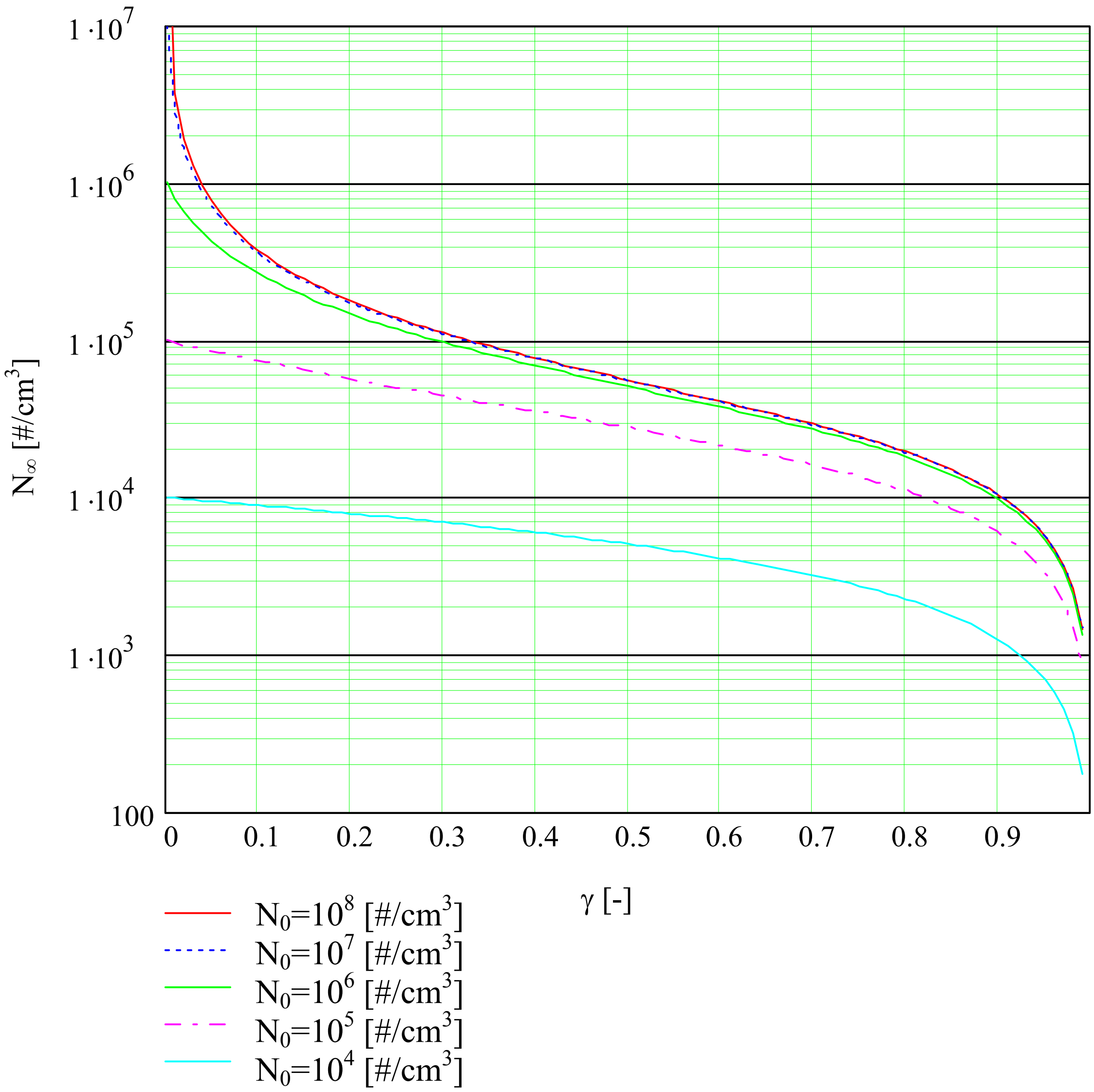

*Figure 5 Solution of the logistic equation for the constant concentration reactor for different initial concentrations N_0 and a constant emptying time t_{total} =75 [min] and the constants L_0=1.89*10^{-4} [1/s] and =56.7*10^{-10}[cm^3/s] according to equation (0-61)*

I.1.7.5 Method (3) - Constant Concentration Reactor (CC) for short times

For method (3) the initial concentration decay is regarded. Successive dilution and measurement of the probe gives different initial concentrations. Again equation (0-61) can be applied for evaluation of the coefficients L_0 and K.

A linearization can be made in analogy to the method of Rooker and Davies, as different initial concentrations lead to almost linear concentration decay when the time t or γ is small. The first order Taylor development of equation (0-61) in γ is:

$$N_{\infty}(\gamma) = N_0 - \left(K \cdot N_0^2 + L_0 \cdot N_0\right) \cdot t_{total} \cdot \gamma \tag{0-62}$$

Subsequent derivation in γ yields to:

$$\frac{d}{d\gamma}N_{\infty}\cdot\frac{1}{t_{total}} = -\left(K\cdot N_0^{\;2} + L_0\cdot N_0\right) \tag{0-63}$$

After resubstitution of γ with equation (0-49), substitution of L_0 with L and N_0 with N_∞ equation (0-40) is obtained. This is the basis equation for the general theory for loss by coagulation and diffusion.

In analogy to equation (0-41) an apparent coagulation coefficient can be introduced:

$$K_{ac}\left(N_0\right) = K\cdot\left(1 + \frac{L_0}{K\cdot N_0}\right) \tag{0-64}$$

Combining equations (0-63) and (0-64) yields equation (0-65).

$$K_{ac}\left(N_0\right) = -\frac{\frac{d}{d\gamma}N_\infty}{N_0^{\;2}\cdot t_{total}} \tag{0-65}$$

As a result for small times or when γ→0 K_{ac} is a function of the declining particle concentration slopes, the total measurement time $t_{total,}$ which is a function of sample flow, and the initial particle concentration N_0.

A least mean squares fit for equation (0-64) for all different N_0 and one coagulation run with this method gives then the coagulation coefficient K and the variable L_0 for the settler, or the constant concentration reactor in general.[23]

I.1.7.5.1 Graphical method

From equation (0-65) a graphical method[24] for determination of the coagulation coefficient can be derived. For γ→0, equivalent with the beginning of the measurement, when t→0, equation (0-65) can further be simplified to:

$$\frac{d}{dt}N_{\infty} = -K_{ac}\cdot N_0^{\;2} \tag{0-66}$$

As for t→0 the concentration N_∞ is equal to the initial concentration N_0 this results in

$$\frac{1}{N_0\cdot\Delta t} = K_{ac} \tag{0-67}$$

,

which can be interpreted geometrically according to Figure 6. The apparent coagulation coefficient K_{ac} is inverse proportional to the area spanned by the initial concentration N_0 and

[23] See section I.1.15 p. 77

[24] Which is also applicable for the simplified calculation of the coagulation coefficient K.

the time Δt gained by section of the tangent in N_0 with the x-axis[25]. The resulting apparent coagulation coefficient K_{ac} is then a function of the initial concentration N_0. With least mean squares fit of equation (0-64), the coagulation coefficient K and the diffusion frequency L_0 results.

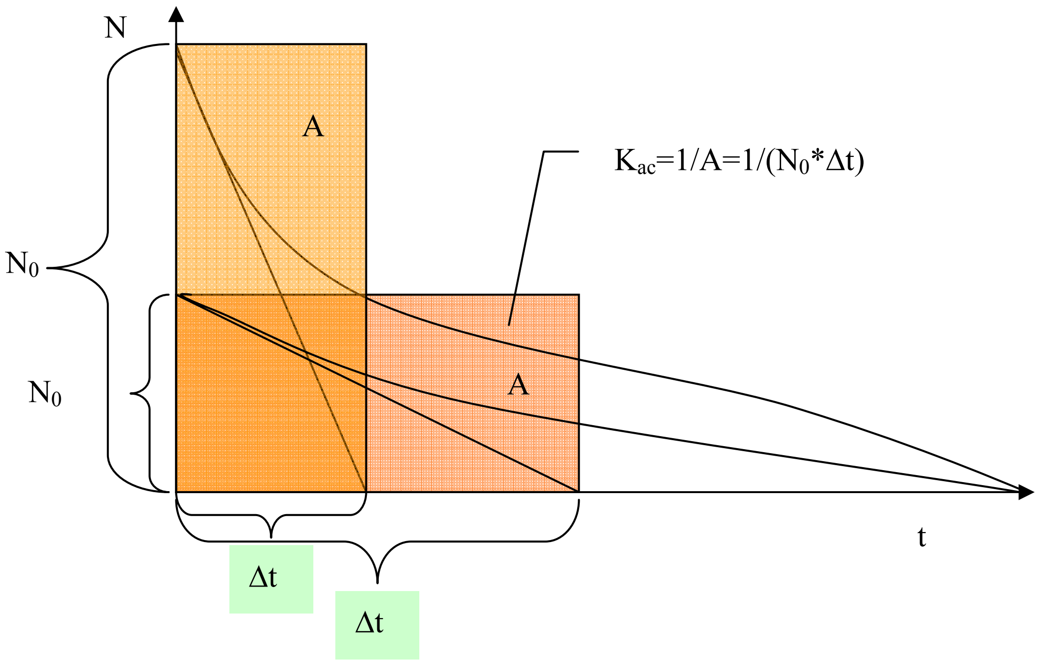

Figure 6 Graphical method to determine the apparent coagulation coefficient K_{ac} according to equation (0-67). The method is described in the text.

I.1.8 Predicted application of the measurement of the quantity K

As the coagulation constant K is determined experimentally, other quantities can be calculated. To characterize the fractal properties of particles a method for determination of the fractal dimension D_f and the primary particle d_{p0}, is sketched shortly. The experimental results for K as the resulting D_f, and dp_0 can then be compared with numerical simulations for the evolution of fractal aggregates in this field, see e.g. (Kostoglou and Konstandopoulos 2001).

I.1.8.1 Fractal dimension determination

The way of determining the fractal dimension shall be described in short. In the Brownian regime[26] the equation (0-27) can be transformed for two different particle diameters to:

---

[25] This is a result of the tangent in equation (0-66) for $\gamma \rightarrow 0$.

[26] Particles (much) larger then the mean free path λ, or where the Stokes-Einstein relation for the diffusion coefficient is valid.

$$\frac{d_{p1}}{d_{p2}} = \frac{K(d_{p1})\cdot D(d_{p2})}{K(d_{p2})\cdot D(d_{p1})} \tag{0-68}$$

Both the coagulation constant and the diffusion constant are a function of the particle diameter. For this purpose the coagulation constant has to be measured for monodisperse particles. Next the definition equation of the fractal particles (0-10) can be put for this condition to:

$$\frac{N_{p1}}{N_{p2}} = \left(\frac{d_{p1}}{d_{p2}}\right)^{D_f} \tag{0-69}$$

Together with (0-68) and solving for the fractal dimension D_f we get:

$$D_f = \frac{\ln\left(\frac{N_{p1}}{N_{p2}}\right)}{\ln\left[\frac{K(d_{p1})\cdot D(d_{p2})}{(K(d_{p2})\cdot D(d_{p1}))}\right]} \tag{0-70}$$

Assuming, that no particle loss at the wall occurs, that $N_{\infty,i}$ is referred to the same volume V and no primary particles are generated, then the number of all primary particles $N_{p,primary}$ in a closed volume V stays constant for fractal growth[27]. Let be the index i=1 the state at t and i=2 the state t+Δt, then according to equation (0-71) the gas particle concentration $N_{\infty,i}$ decreases whereas the average particle number N_{pi} in each fractal particle increases, and the total primary particle concentration $N_{\infty,primary}$ is constant for coagulation neglecting other particle losses. Equation (0-71) is then for this case the population balance equation for primary particle concentration $N_{\infty,primary}$, which is defined by the ratio of the total number of all primary particles $N_{p,primary}$ and the reference volume V.

$$N_{p1}\cdot N_{\infty,1} = N_{p2}\cdot N_{\infty,2} = \frac{N_{p,primary}}{V} = N_{\infty,primary} = \text{const} \tag{0-71}$$

As N_{pi} is inverse proportional to the particle concentration for coagulation the unknown ratio for N_{pi} is:

$$\frac{N_{p1}}{N_{p2}} = \frac{N_{\infty,2}}{N_{\infty,1}} \tag{0-72}$$

For a coagulating aerosol equation (0-70) can then be written[28]:

---

[27] This is also the case when the particle concentration N_∞ stays constant.

[28] This is only valid for ideal particle coagulation without other particle losses; for the case of additional losses equation (0-71) has to be modified accordingly.

$$D_f = \frac{\ln\left(\frac{N_{\infty,2}}{N_{\infty,1}}\right)}{\ln\left[\frac{K\left(d_{p1}\right)\cdot D\left(d_{p2}\right)}{\left(K\left(d_{p2}\right)\cdot D\left(d_{p1}\right)\right)}\right]} \tag{0-73}$$

With equation (0-73) the fractal dimension D_f can be solved for two paired monodisperse coagulation constants $K(d_{pi})$, the particle concentrations $N_{\infty,i}$, and the diffusion constants $D(d_{pi})$ according to equation (0-23).

This method is only an approximation, as for the coagulation necessarily a polydisperse aerosol is developing. Therefore, it is not possible to determine the declining concentrations for one monodisperse aerosol with known concentrations, although monodisperse coagulation constants can be measured for monodisperse aerosols with different diameters. The effects of deposition may have also significant influence, which can be taken into account e.g. by equation (0-61).

I.1.8.2 Primary particle diameter

To characterize a fractal particle it is necessary to know the primary particle diameter dp_0. It can be measured most commonly by electron microscopy or online with the optical dispersion quotient process (Zahoransky and others 2000).

When the primary particle diameter d_{p0} and also the fractal dimension D_f is known, N_p can be calculated from the definition equation (0-10) for a particle of size d_p. With the diffusion coefficient D_p the coagulation coefficient K_p for the particle of size d_p and the diffusion coefficient of the primary particle D_{p0}, the coagulation coefficient of the primary particle can be calculated with equation (0-74).

$$K_{p0} = K_p \cdot \frac{D_{p0}}{\left(\exp\left(\frac{\ln\left(N_p\right)}{D_f}\right)\cdot D_p\right)} \tag{0-74}$$

Evaluation of different coagulation coefficients K_p for different particle diameters d_p result in the same coagulation coefficient $K_{p0.}$ In an iterative process a new primary particle d_{p0} can be assumed, leading to a better adaptation of the experimental values of K_p and the resulting K_{p0} in equation (0-74).

Description of the CMD

In this chapter the CMD will be introduced, first by its principles of operation, its physical, mechanical and electrical systems and total system setup over some fundamental issues with the software implementation of the whole CMD system.

Principle of operation of the CMD

The CMD system is a complete system of several measurement instruments combined through the LABVIEW integration process. The basic setup of the CMD is shown in Figure 7.

The first basic instrument for the CMD system is an instrument to measure the *particle size distribution.* For this purpose the SMPS 3081[29] (scanning mobility particulate sizer) was used with DMA (differential mobility analyzer) technology, and the CPC (condensation particle counter).

The second system is the settler system of the CMD, mainly a *constant concentration reactor*. One possible operation is as follows: First one sample is vacuumed into the settler. Then the time needed for decay of particle number concentration – the residence time for reaction (coagulation sedimentation, settling) – is measured. A (smaller) sample is taken from the settler. The last to steps are repeated n times. The difference between the measured concentrations, measured with the modified standard SMPS system, gives us evidence about the decay in concentration and hence the coagulation constant. The constant concentration reactor is therefore tunable in time and gives evidence about the real time behavior of coagulation of aerosols, especially in cases when the volume tends to infinity. Concerning experimental setup a limited volume has to be taken into account.

[29] SMPS system from TSI containing the classifier 3081, the DMA 3080 and the CPC 3010.

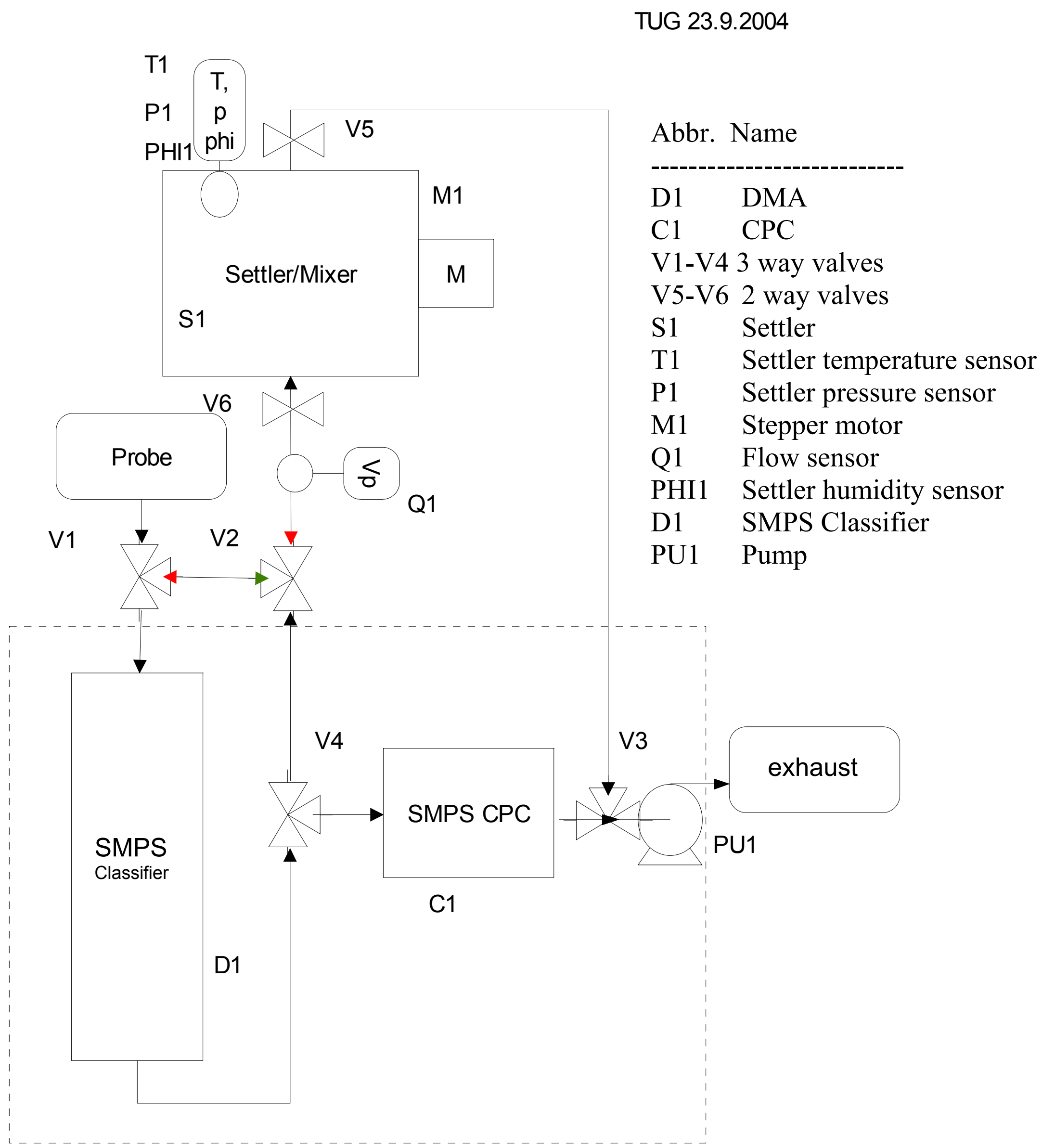

Figure 7 Basic Setup of the CMD

Setup of the CMD

I.1.9 System setup

The system used in this work consists mainly of two self contained systems: The *standard SMPS system* - used for comparison - and the introduced new *CMD system*.

I.1.9.1 Standard SMPS system

The standard SMPS system as stand alone application is depicted in Figure 8. First, there is first the SMPS classifier unit, with the orange case including the recycle flow sheath air control system and the DMA. The yellow case depicts the DMA unit transforming the polydisperse aerosol into a monodisperse one. Ambient air that passes the clean air filter

RLF2 is mixed with the monodisperse output of the transformer. This diluted particle concentration is then counted with the CPC (condensation particle counter) (Ivanišin and others 2005).

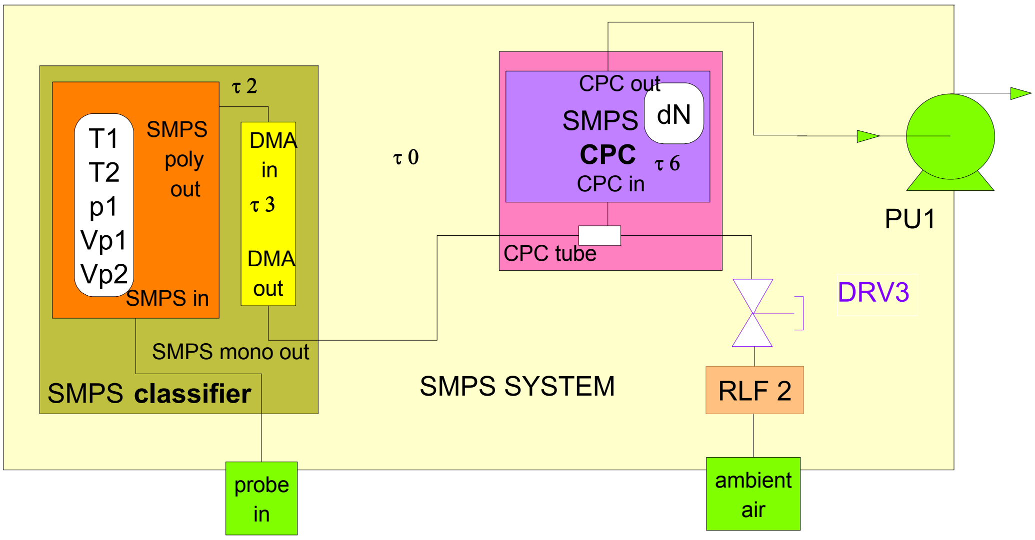

Figure 8 Flow chart of the standard SMPS system

I.1.9.2 CMD system

In the CMD system (Figure 9) the SMPS system is integrated. There are three basic subsystems with an optional fourth:

1. The Settler system
2. The Valve system
3. The SMPS system
4. An alternative measurement system e.g. for particle or mass concentration

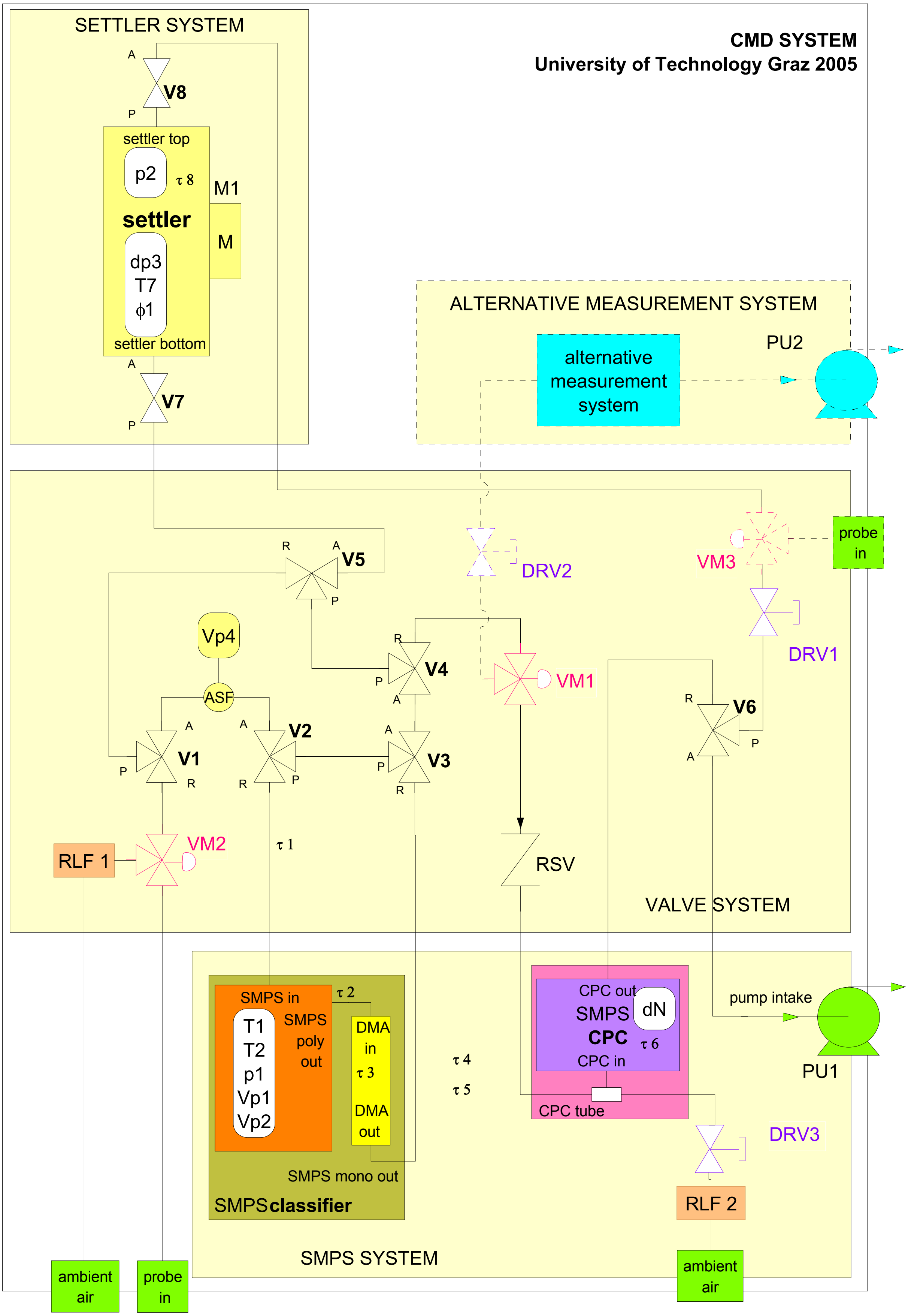

Figure 9 Flow chart of the CMD system

In the actual setup the SMPS system and the valve system is in one case, and the settler system in another[30]. The whole CMD system and its individual components are described in (Bakk 2005; Brugger 2005) in detail.

The settler system is a system with a constant concentration reactor also known as "the accordion"[31]. It is a variable volume reactor whose volume is varied by a stepper motor M1 (Figure 9) with connected gear[32]. On the top and on the bottom there are magnetic valves V7, V8 for shutting in the aerosol probe to maintain a constant thermodynamic state of the aerosol system. A total pressure sensor p_2 is mounted on the top. A differential pressure d_{p3}, a temperature T_7 and a humidity sensor ϕ_1 is mounted on the bottom of the settler.

The valve system consists of the magnetic two way valves V1-V6 and the flow sensor V_{p4}, which is passed in the most of the paths. The flow sensor has a high measurement accuracy, as has been shown by comparison to a primary bubble flow meter (Bakk 2005; Brugger 2005). Two manual ball valves VM1-VM2 also have been integrated. They allow for (VM2) the optional filtering the inlet air of the whole system through the filter RLF1, and thereby cleaning the whole system, which is important for cleaning the settler and for (VM1) measurement with an alternative measurement system instead of the CPC. The regulating needle valve DRV1 is used to manually set up the filling flow rate of the settler. A one direction valve (RSV) to protect the CPC has also been integrated (Brugger 2005)[33].

The SMPS standard system - consisting of the DMA classifier, CPC and the pump - has been modified by extending the connecting tube from "SMPS mono out" to "CPC tube" with the valve system, as well as the SMPS sample inlet "SMPS in". The needle valve DRV1 together with a clean air filter RLF2 is regulating the sample flow that is vacuumed from the DMA and the filter RLF2 through the CPC. The temperatures for the cabinet T_1, for the sheath flow recycle T_2, as well as the absolute pressure in the classifier unit p_2 and the flow rates for the sample flow V_{p1} and the sheath flow V_{p2} are measured and transmitted via the serial interface to the monitoring PC and continuously logged for the measurement mode. The same takes place with the particle size concentration dN[34] of the CPC.

---

[30] The settler system can be fully closed for future temperature regulation.

[31] Oral note of A. Konstandopoulos, Zurich 2005

[32] The gear system is from ZIMM, www.zimm-austria.com: Specifications: BG:SHZ-02-LR, miniature spindle lifting gear i=12:1, 0.25mm / rotation

[33] For normal operation this valve is recommended to be removed because of high particle losses.

[34] This is the parameter rd of the CPC or the actual measured particle concentration [#/cm^3]

I.1.10 Settler

The basic parameters of the coagulation *settler* are given in Table 2 and shown in Figure 10. The inner and outer diameters are given with $d_{i\_SETTLER}$ and $d_{o\_SETTLER}$. The length $L_{\_SETTLER}$ is the outer size of diameter. The width of one fold Ft of the settler calculates from the difference of the diameter divided by two. The number of folds Fz is L_{max} divided by Ft according to the producer[35]. The length of the the minimal volume is restricted to the thickness of the folds and is approximately: $L_{\_SETTLER\_min}$=Fz*2.5/1000. The settler area $A_{SETTLER}$ is defined by (0-1).

$$A_{SETTLER} = \left[Fz \cdot 2 \cdot \left(d_{o\_SETTLER}^{\;2} - d_{i\_SETTLER}^{\;2} \right) + 2 \cdot d_{i\_SETTLER} \right] \cdot \frac{\pi}{4} \tag{0-1}$$

Table 2 Main settler parameters

	Name	*Description*	*Value*	*Unit*
specification	producer	Innoflex	~	[~]
	material	NBR-rubber; 1mm (temp. resistant - 90°C)	~	[~]
	Product	S21177; Scheibenbalg[36] 144-204-500-144-144	~	[~]
	$d_{i\ SETTLER}$	Inner diameter	0.144	[m]
	$d_{o\ SETTLER}$	Outer diameter	0.204	[m]
	$L_{\_SETTLER}$	Length	0.5	[m]
	Ft	Width of folds	0.030	[m]
	Fz	Number of folds	14	[~]
	$L_{\ SETTLER\ min}$	Minimum size due to folds (.05m)	0.036	[m]
	$A_{SETTLER}$	Inner surface	0.500	[m^2]
actual setup	d_m	Theoretical mean diameter	0.174	[m]
	γ	Correction of d_m for real volume	0.833	[~]
	L_{min}	Minimum actual size	0.003	[m]
	L_{max}	Maximum actual size	0.428	[m]
	ΔL	L_{max}-L_{min}	.0425	[m]
	d_7	Effective inner diameter	0.145	[m]
	$d_{7'}$	Outlet diameter for pressure difference	0.006	[m]
	V_7	Effective measured press out volume	7.0	[l]
	V_{7min}	Rest volume	0.05	[l]
	V_{70}	Actual total volume	7.05	[l]
	V_{70}/S	Volume to surface ratio	0.0140	[m^3/m^2]
	S/V_{70}	Surface to volume ratio	71	[m^2/m^3]

[35] The settler is a standard “Faltenbalg” (bellow) from Innoflex. The material is made of NBR-rubber which is made of special antistatic mixture; the advantage is that particles will not be attracted due to static charge; the disadvantage is that the settler is not resistant to UV radiation or ozone.

[36] Bellow

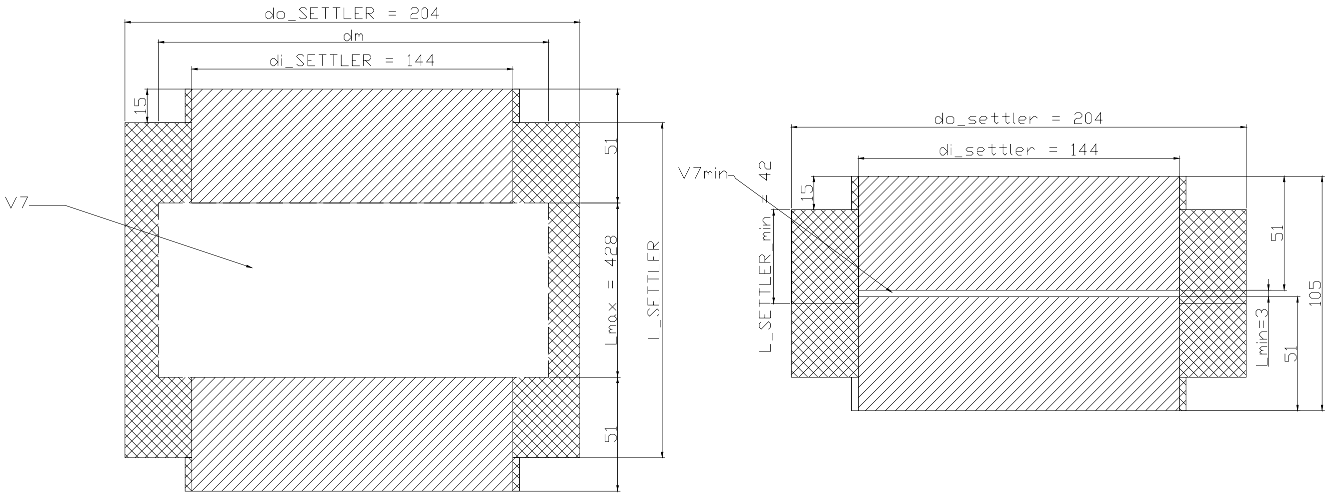

Figure 10 Settler in the end switch positions

For the actual setup the approximated mean diameter d_m is corrected with the numerically derived γ resulting in the effective settler diameter d_7. L_{min} and L_{max} are the lengths in the end positions of the settler[37]. The volumes of the settler are defined in (0-21). The effective volume that can be used for a number of measurements is V_7. It is the volume that can be pressed out by the stepper motor. The minimum volume is V_{7min}. The actual total free volume of the settler is V_{70} which is relevant for filling the settler.

$$V_7 = \left[\left(d_m \cdot \gamma \cdot L_{max}\right)^2 + d_{i\_SETTLER}{}^2 \cdot L_{min}\right] \cdot \frac{\pi}{4} \cdot 10^3$$

$$V_{7min} = d_{i\_SETTLER}{}^2 \cdot \frac{\pi}{4} \cdot L_{min} \cdot 10^3 \qquad (0\text{-}2)$$

$$V_{70} = V_{7min} + V_7$$

The ratio between total area and volume "V/S" and "S/V" are given for comparison with other experiments. They can also be used to compare measurements with the actual settler with a different S/V ratio, and hence a different deposition to coagulation ratio.

I.1.11 Effective flow rate[38]

An experiment was set up to measure the flow rate Vp_4[39] over time while pressing out the

[37] When the end switches are pressed, or when the settler has its actual maximum or minimum possible volume

[38] The relations for the leakage flow dilution in this section are restricted to path 3 (see section I.1.12). For a different path different relations are to be expected, especially for the quantities α and V_{pL} whereas V_{p7} should stay constant (quantities are explained later in this section).

[39] With the ASF1430 flow sensor from SENSIRION (www.sensirion.com).

total volume of the settler. The input parameter SPFA (selection of constant speed factor)[40] for the stepper motor control is only dependent on the stepper motor hardware. As output, the flow rate Vp_4 and the total time t_{total} needed to press out the effective settler volume was measured. The results are given in Figure 11. Drawing a line from the chosen SPFA[41] to the pink line and then going down to the brown curve yields the total time t_{total} and the flow rate V_{p4}. In Figure 11, the maximum deviations of the mean value for the flow rate measurement are also given. The start and stop measurement values, including acceleration of the flow rate, were not regarded for the mean value.

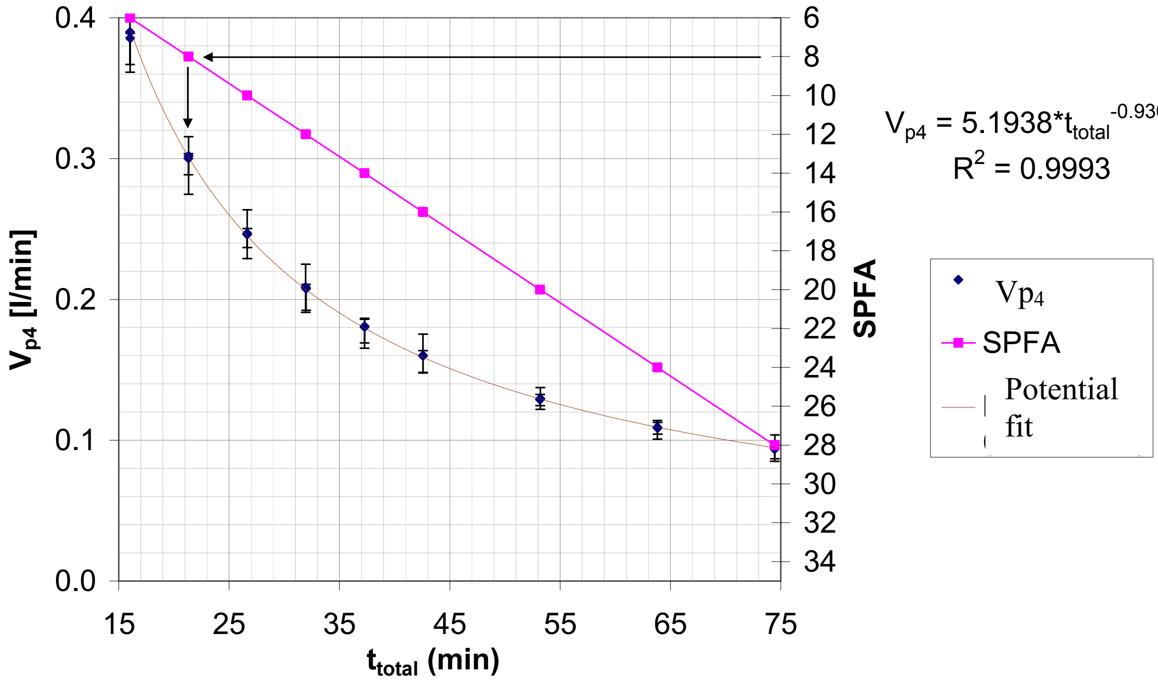

Figure 11 Flow rates Vp_4 of the flow sensor ASF 1430 for different times of emptying and filling the settler; The parameter SPFA denotes the speed factor of the stepper motor in the LABVIEW software. It is proportional to the stepper motor steps per time unit.

I.1.11.1 Settler volume determination

Assuming a settler volume V_7 leading to the *settler exhaust flow* Vp_7 when compressed. Vp_7 is only determined by the movement of the stepper motor and the connected gear, therefore it is

---

[40] The speed factor is the software parameter needed for the HASOTECH (www.hasotech.com) stepper motor control card. As it is approximately proportional to a defined number of steps per time unit, the SPFA is nearly linear with time.

[41] Is needed as input parameter in the LABVIEW Software and is proportional to the number of steps with the stepper motor

very accurate. Vp_7 induces the *sample flow* Vp_4 and also the *leakage flow* Vp_L[42] described by:

$$Vp_7 = Vp_4 + Vp_L \tag{0-3}$$

The inferred leakage flow Vp_L together with the sample flow Vp_4 is depicted in Figure 12 and Table 3, as sample and settler flow.

The volume flow Vp_7 can also be calculated from geometric considerations only. Taking the maximum range of the settler ΔL and the effective settler diameter d_7 the volume flow can be calculated,

$$Q = Vp_7 = \frac{1}{4} \cdot \Delta L \cdot d_7^{\,2} \cdot \frac{\pi}{t_{total}} \tag{0-4}$$

$$\approx Vp_{70}/t_{total}$$

which can also be used to calculate the total time t_{total} with given volume flow. The volume flow Q of the settler is constant over temperature, as it is completely defined by geometry.

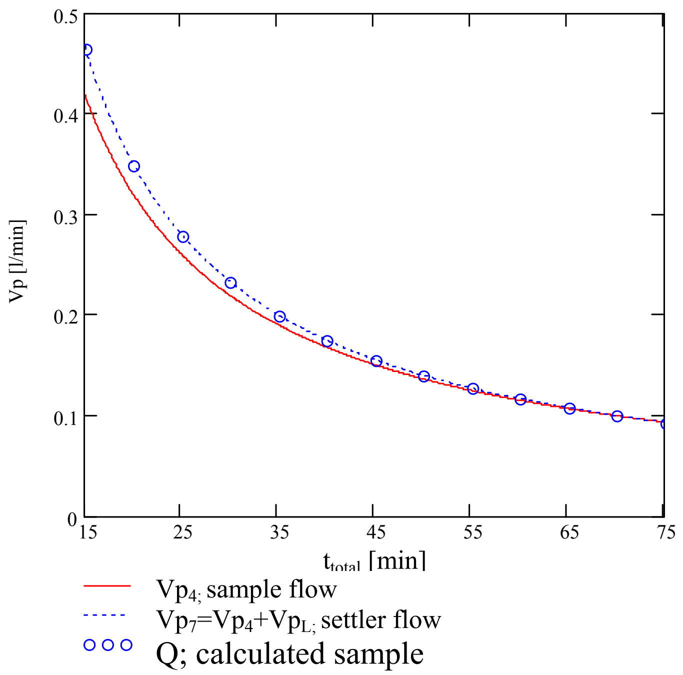

Figure 12 Settler flow rates as a function of the total time for pressing out the complete settler volume; Vp_4 is according to the measurement in Figure 11; The measured flow together with the calculated leakage flow Vp_7 (see text) is shown with the blue dotted line and shows a good accordance with the volume flow Q calculated from the settler geometry according to equation (0-4).

The total volume of the settler V_7 can be divided into the volume V_{7a} according to the sample flow and the volume V_{7b} according to the leakage flow, described in the next sections.

[42] This equation is only valid when the densities ρ_4,ρ_7 are constant

I.1.11.1.1 Sample flow

The effective flow rate experiment was used, according to Figure 13 and (0-5), for the determination of the total effective settler volume V_{7a}[43], where ρ_4 is the density at the

$$V_{7a} = Vp_4 \cdot \frac{\rho_4}{\rho_7} \cdot t_{total} \tag{0-5}$$

flow sensor or approximately in the SMPS and ρ_7 the density in the settler[44].

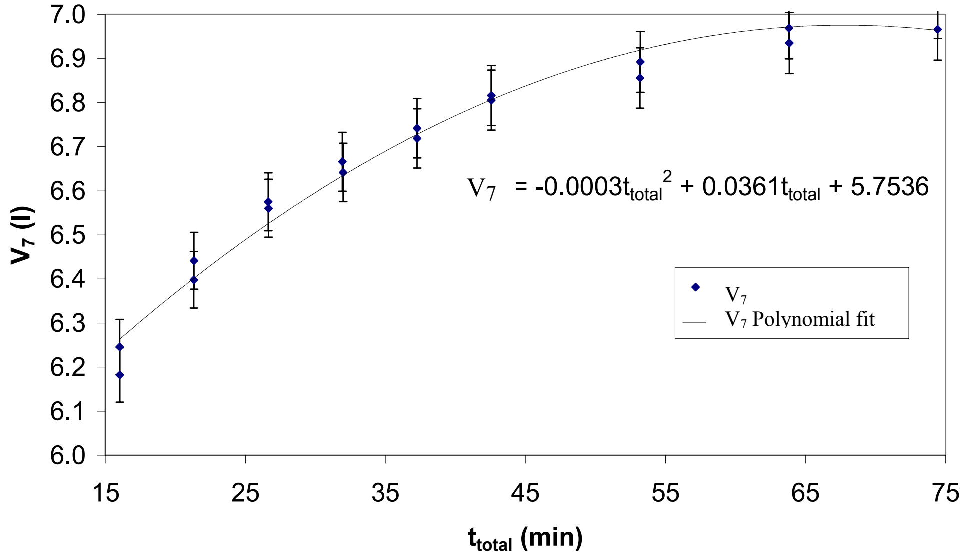

Figure 13 Calculation of the total effective settler volume according to the measurement in Figure 11 and equation (0-5).

The error for the ASF measurements is +-1 % of the measurement value, and is also shown in Figure 13. A constant straight line should have been expected. The curved shape indicates a leakage somewhere in the measurement line although none had been expected as intensive testing had been performed. The sequence of the measurements had no influence on the curve shape, which means that the leakage flow is reproducible. The approximated volume of the settler, achieved for the maximum measured total time t_{total} is V_7=7[l], for all measurements. This was inferred from the decreasing *leakage flow* for long periods depicted in Figure 12[45].

I.1.11.1.2 Leakage and total flow

To consider a leakage flow we define the *leakage ratio* α where Vp_L is the leakage flow rate:

---

[43] When there is no leakage then $V_{7a}=V_7$

[44] For constant states $\rho_4/\rho_7=1$; the densities can be calculated with the later defined viral equation.

[45] The real volume is probably slightly higher, as can be calculated from the dimensions of the settler.

$$\alpha = \frac{Vp_L}{Vp_4} \tag{0-6}$$

The continuity equation can then be fulfilled according to Figure 14:

$$Vp_7 = \frac{\rho_4}{\rho_7} \cdot Vp_4 \cdot (1 + \alpha) \tag{0-7}$$

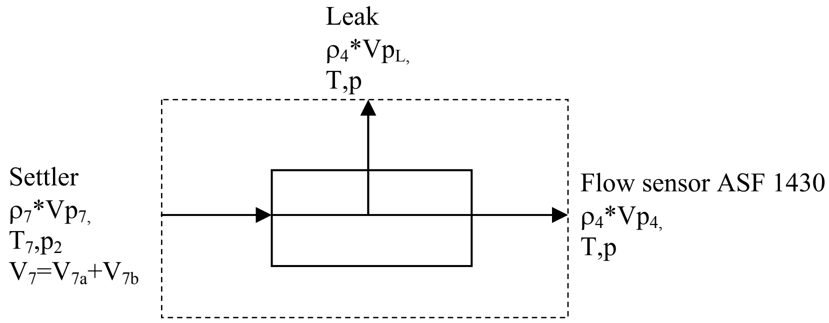

Figure 14 Scheme of the settler flow Vp_7 the leakage flow Vp_L and the measured flow Vp_4 for the mass balance

When we take into account that the total volume of the settler must be the integral of the total measurement time t_{total} according to,

$$V_7 = \int_0^{t_{total}} Vp_7 \, dt = Vp_7 \cdot t_{total} \tag{0-8}$$

where the flow rate Vp_7 can be regarded constant over the time t_{total}, as also the measured sample flow Vp_4 is constant over time, neglecting the flow acceleration we can write (0-7) for the settler volume total V_7

$$V_7 = Vp_4 \cdot (1 + \alpha) \cdot \frac{\rho_4}{\rho_7} \cdot t_{total} \tag{0-9}$$

In the limiting case of no leakage flow α=0 and (0-9) is reduced to (0-5). From (0-9) α can be resolved which is needed for the temperature adaptation of the flow rate[46]:

$$\alpha = \frac{V_7 \cdot \rho_7}{Vp_4 \cdot \rho_4 \cdot t_{total}} - 1 \tag{0-10}$$

The results from the experiments for α and other parameters are shown in Table 3 for $t_{total.}$ The real flow rate in the settler Vp_7 can then be calculated by the known α and (0-7).

[46] See also section I.1.11.4 p.58

Table 3 t_{total}=time for one run of the effective flow rate experiments; α=leakage ratio; Vp_4=sample flow rate; Vp_7=settler flow rate; dp_3=differential pressure settler; T_7=temperature settler, mean T_{7m}=298.3 [K]; mean p_{2m}=.9819 [bar]; $\rho_4=\rho_7$=1.147 [kg/m^3] orange values are extrapolated;

t_{total}	[min]	5	10	15	20	25	30	35	40	45	50	55	60	65	70	75
α	[-]	0.207	0.151	0.119	0.096	0.079	0.066	0.054	0.045	0.036	0.029	0.022	0.016	0.010	0.005	0
Vp_4	[l/min]	1.162	0.610	0.418	0.320	0.260	0.219	0.190	0.168	0.150	0.136	0.125	0.115	0.107	0.100	0.094
Vp_7	[l/min]	1.403	0.701	0.468	0.351	0.281	0.234	0.200	0.175	0.156	0.140	0.128	0.117	0.108	0.100	0.094
dp_3	[Pa]	3.301	1.498	0.944	0.680	0.527	0.428	0.359	0.309	0.270	0.239	0.215	0.194	0.177	0.163	0.151
T_7	[°C]	25.3	25.3	22.8	23.0	24.3	25.5	26.3	26.4	25.9	25.3	24.9	24.9	25.4	26.2	26.5

I.1.11.2 Total time calculation

The time needed for emptying the settler t_{total} as a function of the measured sample flow Vp_4 can be seen in Figure 11 and calculated according to the polynomial fit equation there. Alternatively t_{total} can be calculated from equation (0-7) and (0-4) according to,

$$t_{total} = \frac{\rho_7}{\rho_4} \cdot \frac{\Delta L \cdot d_m^2 \cdot \pi}{(1+\alpha) \cdot Vp_4 \cdot 4} \qquad (0\text{-}11)$$

t_{total} is then constant for one coagulation experiment, supposing constant sample flow and constant settler and ambient temperatures. α is a function of the sample flow Vp_4 and the actual leakage according to Table 3 and the defining equation (0-6).

I.1.11.3 Pressure drop

The pressure drop dp_3 for the total times was measured at the settler outlet, for “breathing in” (move UP) and “out” (move DOWN). The results are shown in Figure 15. There is a very small pressure difference of maximal ~0.9 [Pa] which has negligible influence on the density change of air. There is a hysteresis indicating that the breathing in is easier than the breathing out. A very good approximation can be given with a potential fitting although the measurement took place at very low pressure differences[47], and the whole experiment lasted several days. In addition similarity can be seen compared to the volume flow measurement. Indeed there exists proportionality between pressure drop and volume flow[48], hence the pressure drop measurement can also be used for volume flow measurement[49]. A short method for determining the settler and the sample flow is introduced in the following.

[47] The measurement range of the differential pressure sensor is ±100 [Pa].

[48] The ASF 1430 sensor from Sensirion uses this relationship.

[49] e.g. after calibration with the *bubble flow meter*.

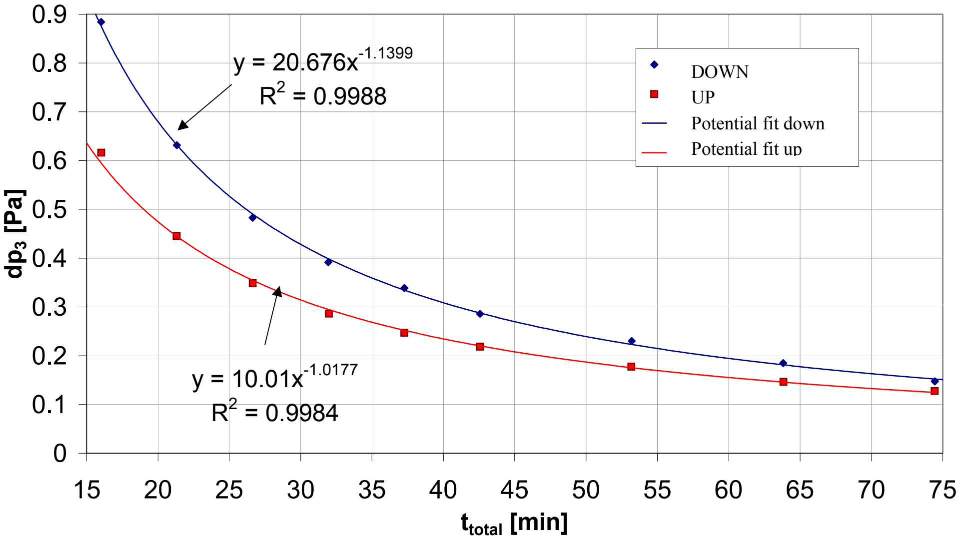

Figure 15 Pressure difference measurements for the sensor ASP 1400 for different times of emptying and filling the settler.

I.1.11.3.1 Sample flow determination from the pressure difference measurements

When we assume no leakage flow from the settler to the ambient air, and no friction we can calculate, from the Bernoulli equation, the settler flow Vp_7, which will occur according to the measured pressure difference $\Delta p = dp_3$:

$$Vp_7 = \sqrt{\frac{|\Delta p|}{\rho_7} \cdot \frac{d_7^{\,4} \cdot 2 \cdot \left(\frac{\pi}{4}\right)^2}{\frac{1}{\alpha^2 \cdot \left(\frac{d_{7'}}{d_7}\right)^4} - 1}} \qquad (0\text{-}12)$$

The effective settler inner and outer diameters[50] are d_7 and d_7' respectively. The density is ρ_7 for isothermal differential pressure measurement and α° is the *contraction number* e.g. according to (Oertel 2001)[51]. Equation (0-12) can be simplified with the assumption that $d_7 >> d_{7'}$ leading to:

$$Vp_7 = \alpha\sqrt{|\Delta p|} \cdot \frac{d_{7'}^{\,2} \cdot \pi}{2 \cdot \sqrt{2 \cdot \rho_7}} \qquad (0\text{-}13)$$

To allow for the measured flow including leakage flow a *differential pressure correction factor* κ is introduced. Equation (0-13) then becomes:

[50] At the differential pressure measurement site.

[51] p.153

$$Vp_7 = \alpha\left(|\Delta p|\right)^{\frac{1}{2}+\kappa} \cdot \frac{d_{7'}^{2} \cdot \pi}{2\sqrt{2 \cdot \rho_7}} \tag{0-14}$$

With this equation from the differential pressure measurement the volume flow in the settler Vp_7 can be calculated. Assuming no density difference between settler and flow measurement also the sample flow rate Vp_4 can be calculated[52]. The fitted parameters for (0-14) and the pressure drop (Figure 15) are given in Table 4 for the state in Table 3.

Table 4 Parameters of equation (0-14) to determine the settler flow Vp_7 and the sample flow Vp_4 from pressure difference $dp_3=\Delta p$ of Figure 15.

Flow rate	Δp	$\alpha°$	κ
Vp_7	UP	0.3258	0.4826
	DOWN	0.2197	0.3773
Vp_4	UP	0.2822	0.4142
	DOWN	0.1957	0.3162

I.1.11.4 Pressure and temperature dependence

I.1.11.4.1 Virial equation

The general pVT[53] behavior of *real* air can be described with the virial equation in (0-15), where B is the *second cross virial coefficient* of the N_2-O_2 air mixture which is -6.6 [cm^3/mol] according to (Dymond and Smith 1980). ρ is the density of the gas, MG the molecular weight, R the general gas constant and p the pressure.

$$\rho = \frac{MG}{2B} \cdot \left(\sqrt{1 + \frac{4 \cdot B \cdot p}{R \cdot T}} - 1\right) \tag{0-15}$$

The advantage of the virial equation is that the mixture rules can be inferred from statistical mechanics. In the literature mostly coefficients for pure gases and mixtures of two gases can be found. Virial coefficients for mixtures for three or more components are difficult to find.

I.1.11.4.2 Pressure differences

When we take (0-5) and apply (0-15) we can draw the conclusion that a pressure change of 1 [mbar] leads to 1% volume change of the settler. A differential pressure of this order of

[52] Taking also the leakage flow according to equation (0-9) into account

[53] Pressure, Volume, Temperature

magnitude is much higher than the measured differences (see e.g. Figure 15), hence, it is not of importance for the flow rates.

I.1.11.4.3 Temperature

Temperature changes have a greater influence on the settler gas volume V_7. A gas volume change of 1% at *standard state*[54] can be affected by ~3 [K] temperature difference. As the physical settler volume is constant, this leads to an increased/decreased sample flow Vp_4 in the measurement mode which has to be considered.
Under normal operation the temperature is constant in the settler as during the measurement in the SMPS, CPC. In case of future investigations of aerosols at higher than ambient temperatures, two cases can be investigated: A.) The probe is heated up in the settler B.) The settler is filled with an aerosol above ambient temperature. In both cases the aerosol is kept at a constant temperature and afterwards cooled down by a heat exchanger. In the following, method B is described more extensively.

I.1.11.4.4 Constant temperature settler and SMPS system difference measurement

As, due to safety reasons[55], the SMPS measurement is only possible up to a temperature of 50 [°C]. Higher temperature measurements have to be cooled down for particle concentration measurement.
The settler flow rate Vp_7 is physically determined by the stepper motor and consequently constant for all temperatures, at the same pressure (see also Table 3). First the aerosol is sampled at an above ambient temperature, then the valves are closed and the temperature is kept constant. Making a size distribution measurement, the flow is cooled down. The pressure stays approximately constant, but the density increases leading to a net lower sample flow rate Vp_4. The time t_{total} - e.g. for the effective flow rate experiment see p.51 ff. - stays the same. The *apparent particle concentration* increases as the volume flow is lower than at the original temperature in the settler. The total particles measured stay the same, the referred volume changes. For these reasons it can be concluded that for a given temperature difference between settler and SMPS-system $\Delta t=T_7-T_2$ the particle concentration has to be corrected[56].

---

[54] T_s=20 [°C] ,p_s=1013 [mbar]

[55] The radioactive source mounting could be damaged.

[56] In this consideration no particle concentration change due to particle loss (deposition, coagulation etc.) or formation (nucleation etc.) has been regarded.

→ **CONCLUSION**

A positive temperature difference between settler and sample flow will lead to a decreased sample flow and an increased particle concentration and vice versa.

→ **METHOD FOR GAINING PARTICLE CORRECTION**

For correcting the particle concentration, the first equation (0-7) is resolved for Vp_4 according to the temperature difference Δt, which is implicitly described with the density and the virial equation (0-15). Vp_7 and α are constant for each t_{total} according to Table 3. The calculated Vp_4 should then be identical with the measured one. The *flow rate correction factor* δ+1 is then Vp_7/Vp_4 which is also the correction factor for the real particle concentration. The *flow rate percentage increase* δ can then be written:

$$\delta = \frac{Vp_7}{Vp_4} - 1 = (1+\alpha)\cdot\frac{\sqrt{1+\frac{4B\cdot p_1}{R\cdot T_2}}-1}{\sqrt{1+\frac{4B\cdot p_2}{R\cdot T_7}}-1} - 1 \qquad (0\text{-}16)$$

p_1,T_2 is the pressure temperature state in the SMPS cabinet which is approximately the same as at the ASF 1430 sensor. p_2, T_7 is the state in the settler for the pressure and temperature and α is the experimental correction factor from Table 3, which is constant for a constant temperature at the flow sensor $T_4 \approx T_2$ and the leak at ambient air T_L.

In Figure 16 and Table 5 the dependency of the measured flow rate from the settler flow rate is given for different temperatures in the settler T_7 and a constant T_4=20°C according to (0-7). In Figure 17 and Table 6 the percentage increase of the flow rate Vp_4 is given, to calculate the flow rate Vp_7 or to calculate the percentage increase of the particle concentration in the settler for T_4=20°. The basic equation for this calculation is equation (0-16).

As can be seen δ=α in Table 6 and Vp_4 in Table 5 equals to Vp_4 in Table 3 for T_4=20°C and T_7=20°C, as this is the isothermal case.

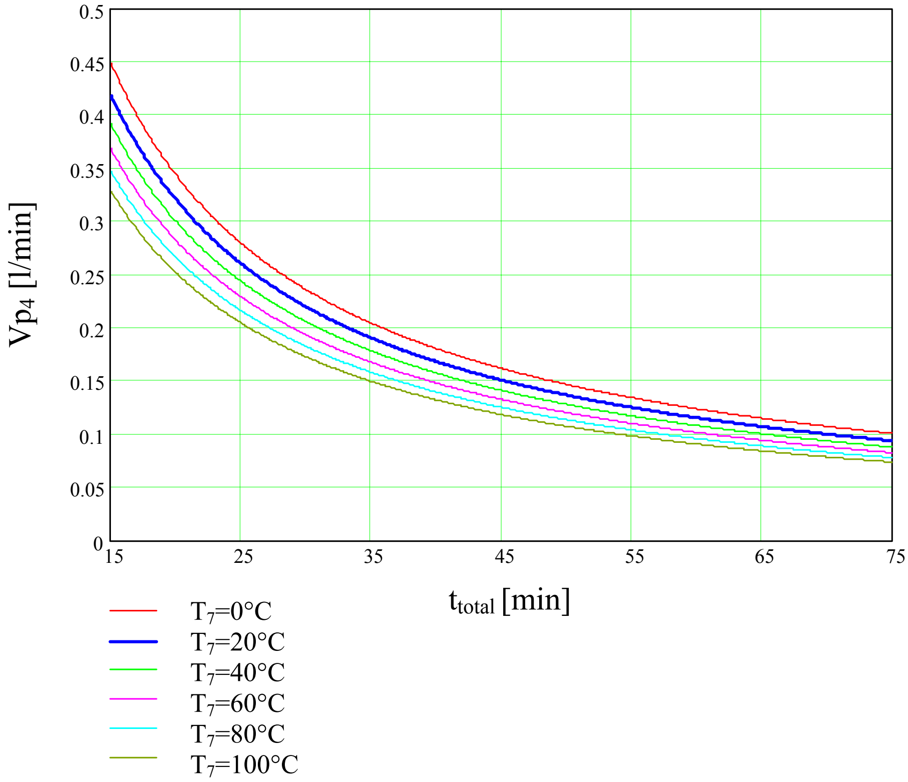

Figure 16 *Volume flow Vp_4 at T_4=20°C as a function of different settler temperatures T_7 and the total measurement time t_{total}. The ambient temperature T_2 is also 20°C.*

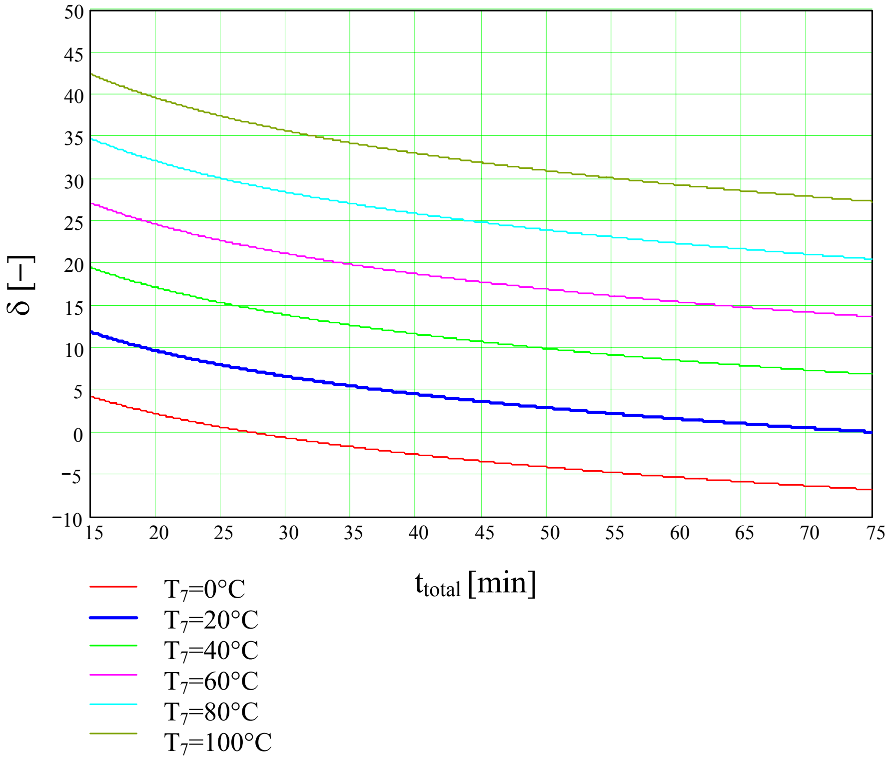

Figure 17 *δ in % at T_4=20°C as a function of different settler temperatures T_7 and the total measurement time t_{total} . The ambient temperature T_2 is also 20°C.*

Table 5 *Vp_4 at T_4=20°C as a function of the settler temperature T_7 and the total measurement time t_{total} and Vp_7=const according to Table 3*

t_{total}	[min]	15	20	25	30	35	40	45	50	55	60	65	70	75
T_7=0°C		0.449	0.343	0.279	0.235	0.204	0.180	0.161	0.146	0.134	0.124	0.115	0.107	0.100
T_7=10°C		0.433	0.331	0.269	0.227	0.197	0.174	0.156	0.141	0.129	0.119	0.111	0.103	0.097
T_7=20°C		**0.418**	**0.320**	**0.260**	**0.219**	**0.190**	**0.168**	**0.150**	**0.136**	**0.125**	**0.115**	**0.107**	**0.100**	**0.094**
T_7=30°C		0.404	0.309	0.251	0.212	0.184	0.162	0.145	0.132	0.121	0.111	0.103	0.096	0.090
T_7=40°C		0.391	0.299	0.243	0.205	0.178	0.157	0.141	0.128	0.117	0.108	0.100	0.093	0.088
T_7=50°C	[l/min]	0.379	0.290	0.236	0.199	0.172	0.152	0.136	0.124	0.113	0.104	0.097	0.090	0.085
T_7=60°C		0.368	0.281	0.229	0.193	0.167	0.148	0.132	0.120	0.110	0.101	0.094	0.088	0.082
T_7=70°C		0.357	0.273	0.222	0.187	0.162	0.143	0.129	0.117	0.107	0.098	0.091	0.085	0.080
T_7=80°C		0.347	0.266	0.216	0.182	0.158	0.139	0.125	0.113	0.104	0.096	0.089	0.083	0.078
T_7=90°C		0.337	0.258	0.210	0.177	0.153	0.135	0.121	0.110	0.101	0.093	0.086	0.080	0.075
T_7=100°C		0.328	0.251	0.204	0.172	0.149	0.132	0.118	0.107	0.098	0.090	0.084	0.078	0.073

Table 6 *δ in % at T_4=20°C as a function of T_7 and the total measurement time t_{total};Vp_7 is const according to Table 3.*

t_{total} [min]	15	20	25	30	35	40	45	50	55	60	65	70	75
T_7=0°C	4.2%	2.2%	0.6%	-0.7%	-1.7%	-2.7%	-3.5%	-4.2%	-4.8%	-5.4%	-5.9%	-6.4%	-6.8%
T_7=5°C	6.1%	4.0%	2.4%	1.1%	0.1%	-0.9%	-1.7%	-2.4%	-3.0%	-3.6%	-4.2%	-4.7%	-5.1%
T_7=10°C	8.0%	5.9%	4.3%	2.9%	1.8%	0.9%	0.1%	-0.6%	-1.3%	-1.9%	-2.4%	-2.9%	-3.4%
T_7=15°C	9.9%	7.8%	6.1%	4.8%	3.6%	2.7%	1.9%	1.1%	0.4%	-0.2%	-0.7%	-1.2%	-1.7%
T_7=20°C	**11.9%**	**9.6%**	**7.9%**	**6.6%**	**5.4%**	**4.5%**	**3.6%**	**2.9%**	**2.2%**	**1.6%**	**1.0%**	**0.5%**	**0.0%**
T_7=25°C	13.8%	11.5%	9.8%	8.4%	7.2%	6.3%	5.4%	4.6%	3.9%	3.3%	2.7%	2.2%	1.7%
T_7=30°C	15.7%	13.4%	11.6%	10.2%	9.0%	8.0%	7.2%	6.4%	5.7%	5.0%	4.4%	3.9%	3.4%
T_7=35°C	17.6%	15.2%	13.5%	12.0%	10.8%	9.8%	8.9%	8.1%	7.4%	6.8%	6.2%	5.6%	5.1%
T_7=40°C	19.5%	17.1%	15.3%	13.9%	12.6%	11.6%	10.7%	9.9%	9.2%	8.5%	7.9%	7.3%	6.8%
T_7=45°C	21.4%	19.0%	17.2%	15.7%	14.4%	13.4%	12.5%	11.6%	10.9%	10.2%	9.6%	9.1%	8.5%
T_7=50°C	23.3%	20.9%	19.0%	17.5%	16.2%	15.2%	14.2%	13.4%	12.6%	12.0%	11.3%	10.8%	10.2%
T_7=55°C	25.2%	22.7%	20.8%	19.3%	18.0%	16.9%	16.0%	15.1%	14.4%	13.7%	13.1%	12.5%	11.9%
T_7=60°C	27.1%	24.6%	22.7%	21.1%	19.8%	18.7%	17.8%	16.9%	16.1%	15.4%	14.8%	14.2%	13.6%
T_7=65°C	29.0%	26.5%	24.5%	23.0%	21.6%	20.5%	19.5%	18.7%	17.9%	17.2%	16.5%	15.9%	15.4%
T_7=70°C	30.9%	28.3%	26.4%	24.8%	23.4%	22.3%	21.3%	20.4%	19.6%	18.9%	18.2%	17.6%	17.1%
T_7=75°C	32.8%	30.2%	28.2%	26.6%	25.2%	24.1%	23.1%	22.2%	21.4%	20.6%	20.0%	19.3%	18.8%
T_7=80°C	34.8%	32.1%	30.0%	28.4%	27.0%	25.9%	24.8%	23.9%	23.1%	22.4%	21.7%	21.1%	20.5%
T_7=85°C	36.7%	34.0%	31.9%	30.2%	28.8%	27.6%	26.6%	25.7%	24.8%	24.1%	23.4%	22.8%	22.2%
T_7=90°C	38.6%	35.8%	33.7%	32.0%	30.6%	29.4%	28.4%	27.4%	26.6%	25.8%	25.1%	24.5%	23.9%
T_7=95°C	40.5%	37.7%	35.6%	33.9%	32.4%	31.2%	30.1%	29.2%	28.3%	27.6%	26.8%	26.2%	25.6%
T_7=100°C	42.4%	39.6%	37.4%	35.7%	34.2%	33.0%	31.9%	30.9%	30.1%	29.3%	28.6%	27.9%	27.3%

I.1.11.5 Gas dependence

The settler flow Vp_7 is independent of the gas and constant, as it is physically determined by the geometry and the stepper motor control. The volume flow Vp_4 may vary due to a different pressure difference and hence a different leakage flow. The flow sensor for the flow Vp_4 has to be calibrated for the gas. This can be done, e.g., with a settler measurement (ideally) without leakage flow. Gas mixtures can be calculated, e.g., with equation (0-16), which is of importance for the leakage flow mixture calculation or, e.g., the complex operation “Polydisperse Coagulation II” (see section 0).

Operation of the CMD

I.1.12 Path concept

For the measurement of the particle concentration over time the path concept has been established. It denotes a certain configuration of the valves, leading to a fluid path in the tubing of the CMD. The path the fluid takes according to the setting of the valves is shown in Table 7, with the names according to Figure 9.

Table 7 CMD paths: green=filling or cleaning; orange=settler measuring; blue=like standard SMPS measuring

Path	Short name	Detailed path
1	Probe Fill Mono	Probe in→V1→ASF→V2→SMPS classifier→V3 →V4→V5→V7→Settler→V8→V6→PU1→exhaust
2	Probe Measure[57]	Probe in→V1→ASF→V2→SMPS classifier→V3 →V4→CPC→V6→PU1→exhaust
3	Settler Measure	Settler→V7→V5→V1→ASF→V2→SMPS classifier→V3 →V4→CPC→V6→PU1→exhaust
4	Settler Count	Settler→V7→V5→V1→ASF→V2→V3→V4→CPC→V6 →PU1→exhaust
5a	Probe Fill Poly	Probe in→VM2→V1→ASF→V2→V3→V4→V5→V7 →Settler→V8→V6→PU1→exhaust
5b	Settler Clean	Ambient air→RLF1→VM2→V1→ASF→V2→V3→V4→V5→V7 →Settler→V8→V6→PU1→exhaust
6	Probe Count	Probe in→V1→ASF→V2→V3→V4→CPC→V6→PU1→exhaust

The six paths are as follows:

1. The path “Probe fill mono” serves to fill the settler with a probe of a specified diameter MDP (monodisperse particle diameter)[58]. The air flow is vacuumed in through the SMPS classifier. The particle diameter of the DMA is set to the monodisperse filling diameter MDP with the CMD software.

[57] Or waiting for coagulation, deposition, sedimentation etc.

[58] Monodisperse means that the particle size distribution has a very narrow standard deviation.

2. “Probe measure” is the standard path. It corresponds to the standard SMPS measurement with different residence times compared with the standard tubing and without valves in between.
3. “Settler measure” is the path for measuring the particle size distribution of the CMD. The pressed volume - achieved by the stepper motor motion - into the sampling line is the same as that one vacuumed off. The number and mass concentration in an ideally inert reactor stays constant without any reaction.
4. The path “Settler count” serves to measure the total particle concentration.
5. The path “Probe fill poly” is used to fill the settler with a polydisperse aerosol, cleaning with ambient aerosol (a) or for cleaning with particle free air (b).[59]
6. The path “Probe count” is used to measure the number concentration of the aerosol, like measuring with the CPC alone.

The colors in Table 7 depict the differences in operation. The standard measurement paths comparable with the Standard SMPS system setup are blue. Filling or cleaning paths are green, and settler measuring paths are orange.

The Labview implementation of the paths is shown in Figure 18.

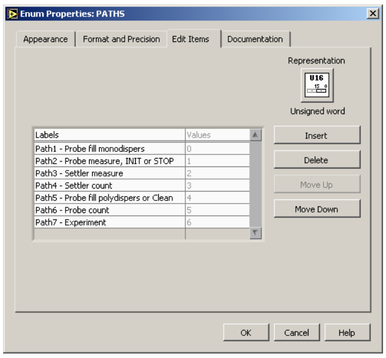

Figure 18 Labview implementation of the paths of the CMD

I.1.13 Operation concept

The paths have to be operated in a certain sequence, to get the right measurement series for calculation of the coagulation or deposition. There are now ten types of operation, stored in the variable GMEAMOD. The LABVIEW implementation is shown in Figure 19. They can

[59] Concerning the actual computer control the paths 5a and 5b are equal as VM2 is a manual valve.

be assigned to the complex or simple type according to Table 8. Complex denotes that several paths are used for accomplishing the operation.

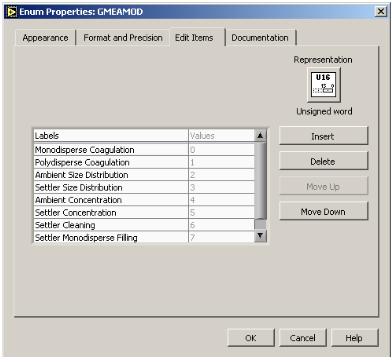

Figure 19 Labview implementation of the operations of the CMD

Table 8 Operations of the CMD

Operation	*name*	*type*
1	Monodisperse Coagulation	Complex
2	Polydisperse Coagulation	Complex
3	Ambient Size Distribution	Simple
4	Settler Size Distribution	Simple
5	Ambient Concentration	Simple
6	Settler Concentration	Simple
7	Settler Cleaning	Simple
8	Monodisperse Filling	Simple
9	Polydisperse Coagulation I	Complex
10	Polydisperse Coagulation II	Complex

Each operation is explained in detail in the following sections.

I.1.13.1 Complex operation types

The actual complex operation types are depicted in Figure 20 and Figure 21, the bold words denote the operations. They are:

1. Monodisperse Coagulation and
2. Polydisperse Coagulation.
3. Polydisperse Coagulation I
4. Polydisperse Coagulation II

I.1.13.1.1 Mono- and Polydisperse Coagulation

The flow chart for the first two operations 1 & 2 is shown in Figure 20. For the operation “Monodisperse Coagulation” first the settler is cleaned with path 5. Either the clean air filter RLF1 is used setting the manual valve VM2 or ambient air is filled into the settler. The subsequent step is to fill the probe into the settler, setting a monodisperse diameter MDP at the DMA. For the operation “Polydisperse Coagulation” the settler is first filled with a polydisperse probe at the "probe in" air inlet with path 5. Then with path2 the valves V7-V8 are closed to keep a constant settler probe. Then enough time is given to allow for the coagulation in the settler.

For mono- and polydisperse coagulation measurement (complex operation 1 & 2) the sequence is now the same; first measuring the particle size distribution in path3, then waiting for coagulation. This procedure is done NSM (number of simple (single) measurements) times until the actual measurement is NSMA=NSM. The settler is then cleaned and returns to the starting end position.

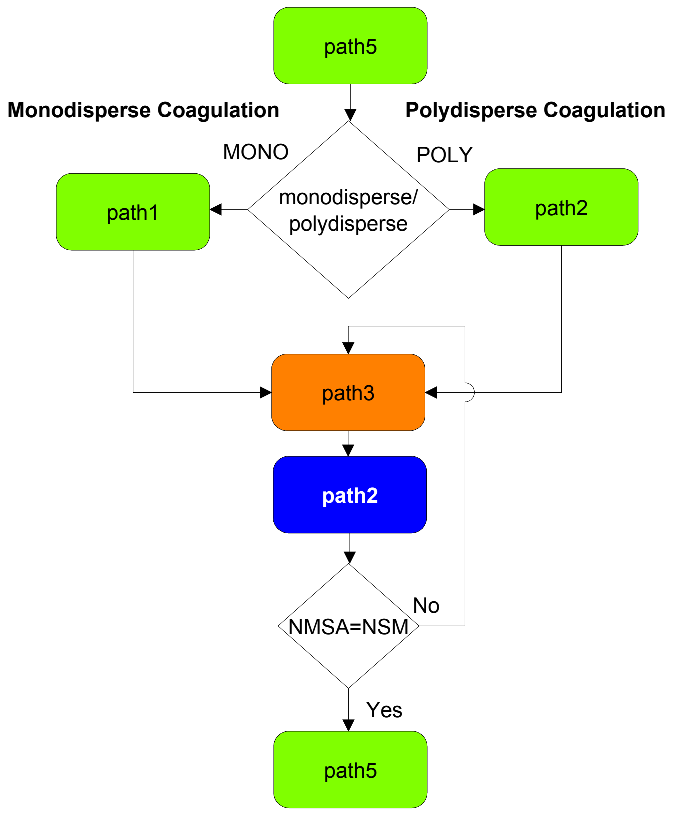

Figure 20 The complex operations "Monodisperse Coagulation" and "Polydisperse Coagulation"

I.1.13.1.2 Polydisperse Coagulation I,II

The operations "Polydisperse Coagulation I" and "-II" use only the concentration measurements with the CPC without using the SMPS classifier. Hence with this method only the coagulation of a polydisperse aerosol can be determined.

The flow chart is depicted in Figure 21. First in both operations the settler is cleaned, and filled with path 5. This can be accomplished by first applying the single operation "Settler Cleaning", then switching the manual valve VM2 to "probe in". After filling path 5 the manual valve VM2 should be switched to the clean air filter again.

Then the particle concentration is measured with path 4. For the operation "Polydisperse Coagulation I" this is done when the settler volume has been emptied, then the initial state is reestablished. For the operation "Polydisperse Coagulation II" a certain time smaller than t_{total} for the counting measurement has to be entered in the Labview software for path 4. Path 5a serves then as dilution of the settler with clean ambient air, while the stepper motor is driving to the starting initial position[60].

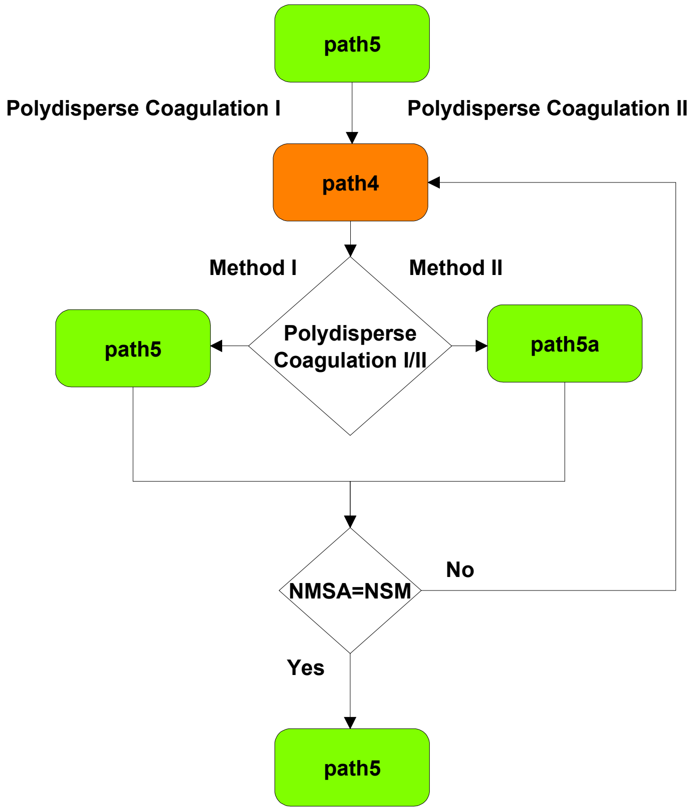

Figure 21 Complex operations Polydisperse Coagulation I and II

The complex operation "Polydisperse Coagulation I" and "Polydisperse Coagulation II" refer directly to the theoretical justified coagulation coefficient retrieving methods given in I.1.7.4 and I.1.7.5 respectively. This theoretical foundation is then used in the experimental part in chapter 0 for evaluation of the coagulation coefficient.

I.1.13.2 Simple operation types

The simple operation types are denoted by the application of one path to one operation. They are depicted in Figure 22, with the operations in bold. Each operation can be repeated NSM

[60] For the operation "Polydisperse Coagulation I" it is recommended for the current setting to make only one single measurement, as the filling operation has to be accomplished manually by VM2.

times. They can be used to measure a set of measurements manually, or e.g. for filling, cleaning etc. In general a complex operation should be implemented, when the sequence of paths is known, to fully use the capabilities of the LABVIEW automation. This is very important for reproducibility.

- The "Ambient Size distribution" operation measures the size distribution that can also be measured with the standard SMPS system. The residence time between SMPS classifier and CPC is longer, hence the parameter td. The residence time τ_4 (Figure 8) instead of τ_0 (Figure 9) has to be taken.

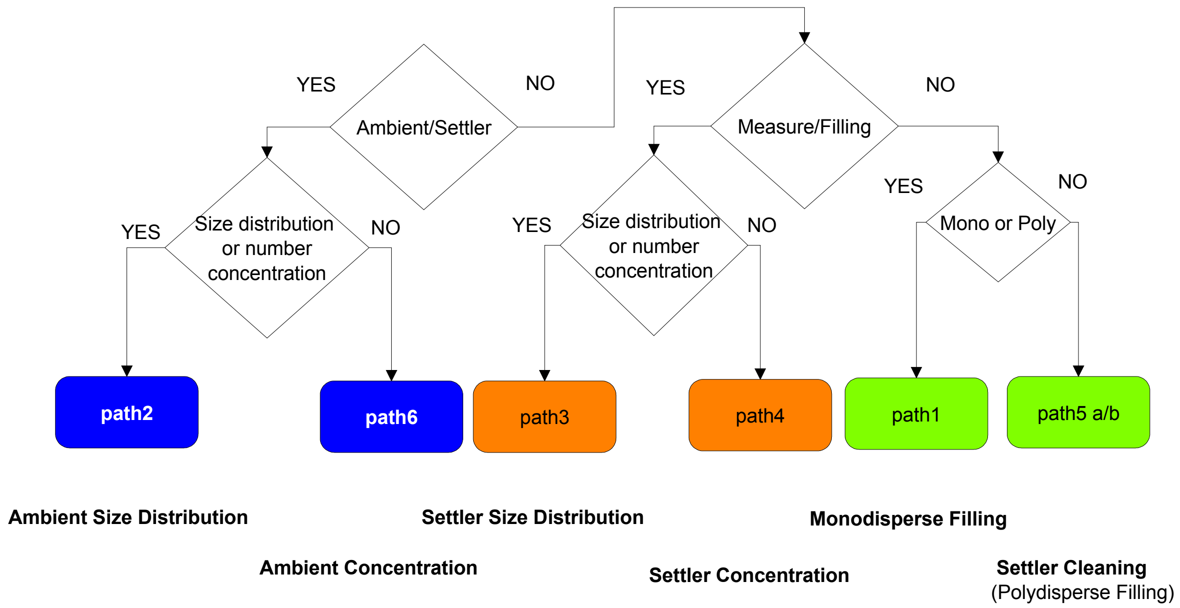

Figure 22 Decision chart for the simple operations of the CMD denoted with bold letters.

- The "Ambient Concentration" operation measures the total number concentration of the CPC from the ambient in, without any other device.
- The operation "Settler Size Distribution" measures size distribution from the settler, like in the complex paths individually.
- The operation "Settler Concentration" measures the particle number concentration of the settler alone.
- "Monodisperse Filling" denotes the filling of the settler with a monodisperse particle source.
- The operation "Settler Cleaning" denotes the cleaning with the clean air filter as noted above in the complex operation (setting by manual valve VM2). This operation can also be used to fill the settler with an aerosol at the "probe in" inlet, which is polydisperse or monodisperse in dependence of the aerosol source.

I.1.14 Labview software implementation

Implementation of the CMD integrates all valves, sensor measurements, the stepping motor control and the measurement instruments like the SMPS[61] or the CPC of the Labview software. Additional hardware can be implemented by adding modules into the Labview platform.

In this section first a short overview is given of the most important features that were used for programming the LABVIEW main application. More details of the programming language can be found in (Jamal and Hagestedt 2001; National Instruments 2003; National Instruments 2004). Then an overview of the most important programming features and the main program modules[62] is given: The main[63]-, initialization-[64] and measurement-[65] program.

I.1.14.1 Structure

The basic principle is to program in modules. The detailed software implementation and the variables definition is given in the appendix and on the accompanying CD. The implemented CMD program makes use of the following features of Labview:

- Modules
- State Machines
- Parallel Processing

I.1.14.1.1 Modules

Modules, so called vi's (**v**irtual **i**nstrument) split the task in logical operations, and they aim at keeping the overview over the total program architecture.

The modules were programmed for the sensors, the valves, and the measurement instruments first. For example, the previously introduced path concept was applied first in the basis valve control program.

---

[61] SMPS 3081: System from TSI containing the classifier 3081, the DMA 3080 and the CPC 3010

[62] In Labview, the subroutines are called sub-vi, each program is called a vi. The name refers to the file extension *.vi and means "virtual instrument".

[63] CMDC_Menu.vi

[64] CMDC_Initialization.vi

[65] CMDC_Measurement.vi

The modules build the basis of the programming hierarchy, which have been built into a hierarchy of state machines and parallel processes for simultaneous measurement.

I.1.14.1.2 State Machines

A state machine is a LABVIEW program with certain architecture. It is implemented in a CASE programming structure. Different states are switched to, using a CASE for each state. The path and the operation concept were used as base for the state machine programming. The State machine is also useful in general program structuring. Different programs branching from the main program are also states of a state machine e.g. the main menu in Figure 23.

I.1.14.1.3 Parallel Processing

The exact parallel processing is implemented in LABVIEW with “while loops” by means of “notifiers”, that are exchanging data between the while loops. These can trigger simultaneous measurement start, which is important for exact parallel measurement of the sensor and instrument data.

One exception is the serial measurement. Four instruments and sensors are plugged to one serial interface card. These are: SMPS, CPC, ASF, ASP. They respond in the same sequence as denoted, because the used serial card is not capable of parallel processing. As a consequence the minimum time interval of all measurements in parallel is approximately 3[s], which can be reduced by switching of sensors[66].

I.1.14.2 Main menu

The main menu can be seen in Figure 23. In this case each button denotes a separate state in the state machine. There are four programs that can be called:

1.) *Initialization*: This program serves for initialization and control of all sensors the stepper motor and the valves.
2.) *File*: This program chooses the measurement protocol file. A standard file “Testxx.xls” can be chosen by the button Standard file.
3.) The button “*All measurements”* calls the sub-vi “CMDC Measurement”

[66] Variable SM in Figure 50

4.) Coagulation Coefficient is not yet programmed, and should serve for the automatic statistical evaluation of the measurements including the calculation of the coagulation coefficient.

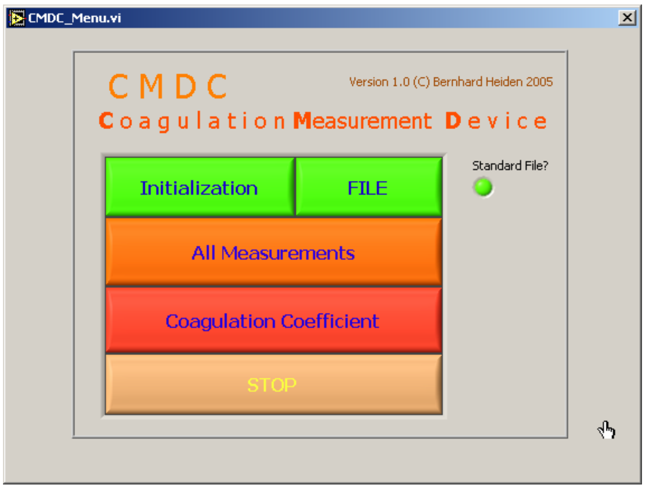

Figure 23 Main application window of the CMD-Program: „CMDC_Menu.vi“

I.1.14.3 Initialization

The program window for the Initialization vi is shown in Figure 24. There are initialization and or control programs for the CMD accessible. The programs are briefly described as follows:

SMPS

INIT: This program initializes the sheath flow rate of the SMPS

BASIS: Most of the measurement values available from the SMPS can be seen. They are read out from the SMPS microcontroller via RS232 (serial interface). They are identical with the information available at SMPS display.

CPC STATE: Reads all the measurement values available for the CPC via RS232.

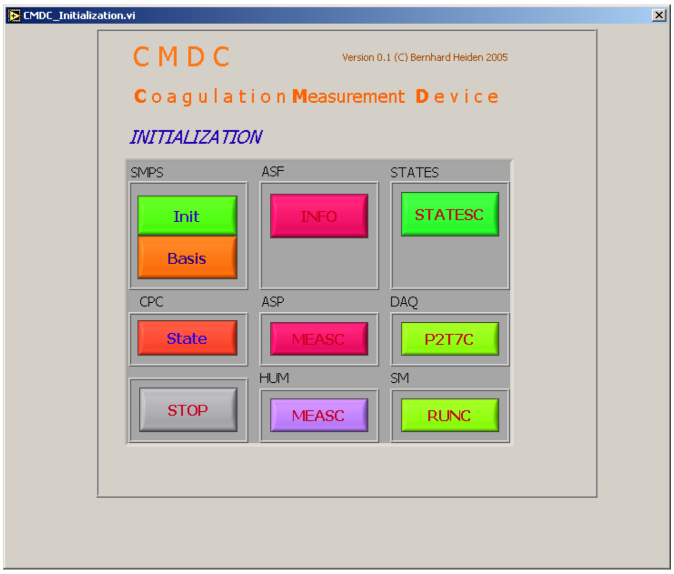

Figure 24 *Application window of the CMD-Program: „CMDC_Initialization.vi“*

ASF	INFO: Reads out the information of the ASF flow sensor via RS232
ASP	MEASC: Makes a measurement of the ASP differential pressure sensor via RS232
HUM	MEASC: Makes a measurement of the humidity sensor SHT75 via RS232. The evaluation kit EK-H7 is used for the microprocessor control and serial connection with the sensor.
STATES	STATESC: Is used to test the different paths in section (I.1.12), setting the valves to the corresponding states.
DAQ	P2T7C: Data Acquisition Hardware from NI (National Instruments) SC-2345 (Signal conditioning). A Pt 100 platinum sensor T_7 and the pressure sensor HCX001A6V p_2 from the settler are accessed (see Figure 9).
SM	RUNC: Stepper motor control program. The different modes of accessing the stepper motor can be tested. The stepper motor control program from HASOTEC[67] (see Figure 54) has to be started before main program execution. It has to be taken care that the valves are in the right position (right path), before running the program. In case of continuous running of the stepper motor, the end switches from the settler can be used to stop the running of the stepper motor.

[67] The program “SM4xDRV.EXE” is the driver program of the HASOTEC SM-41 PCI card for the stepper motor control. This program has to be started and closed once before access in LABVIEW is possible.

I.1.14.4 Measurement

This is the main program for the CMD. All measurement automation tasks can be accomplished with this program. The control window can be seen in Figure 25. As this window contains all important information for measuring, it will be explained in detail, beginning with the variable name.

PATH: In the first deactivated line the path including the name of the protocol file previously chosen can be seen. It can not be changed.

COMMENT: In the next line a comment can be inserted for each measurement. It appears in the protocol file in the first line for each measurement that has been started with the start button.

ROTDRV: Number of rotations set by the manual valve DRV1. The number to flow rate relationship is attached at DRV1 on the instrument which is also shown as result of the calibration measurements (Figure 26, p. 82).

GMEAMOD: A dropdown list can be accessed in the variable *GMEAMOD*. Here all the operations possible can be chosen for the measurement (see section I.1.13). The operation that can be seen is the complex operation “Monodisperse Coagulation”.

TIMER: The variable timer on the left side is deactivated, as the timer is chosen on the right side, explained later.

NSM: denotes the number of single (simple) measurement performed. Concerning simple measurements the number of these is denoted.

NSMA: is the actual count number of NSM.

SF (starting flag) is true when a measurement is running otherwise false.

TTOTAL: The total calculated measurement time due to the setting in seconds.

TTOTALA: The total actual measurement time in seconds that has passed.
PATHS: Denotes the actual path that is set.

PATHi: i=1..6 time information and control of the different paths; Each line is only active when the corresponding path is actually set. The STOP buttons STPi can end the control of the actual path. The path times are:

1: TMFILL/TFILLA: The monodisperse filling time and actual time of path

2: TCOAGUL/TCOAGULA: The monodisperse filling time and actual time of path

3: TSMEAS/TSMEASA: Settler measuring path and actual time of path

4: TCOUNT/TCOUNTA: Settler counting time and actual time of path

5: TPFILL/TPFILLA: Polydisperse filling or settler cleaning time and actual time of path

5a: TDILUTE/ TDILUTEA: Settler diluting time and actual time of path

6: TPCOUNT/TPCOUNTA: Polydisperse counting time and actual time of path

V1-8: Depicts the actual setting of the valves ON/OFF=LIGHT GREEN/DARK GREEN together with the path.

SPFA: is the setting of the speed of the stepper motor, either turning the button or setting the value. The speed factor SPFA corresponds to a flow rate shown in Figure 11 p.52.

MB?: Is a LED for showing the activity of the stepper motor.

STOPIL: Stops the run of the stepper motor; once stopped it cannot be started again in the same run

UP/DOWN: switch in the Stepper motor control cluster: This switch determines the direction of the stepper motor for path 3. In normal operation the switch is down for normal measurement. In the filling path 5 the stepper motor goes to the starting position.

DPMIN/DPMAX: Minimum/Maximum diameter set at the SMPS for scanning mode in nm. This setting is only effective when the SDR (Select Diameter Range) switch is set to manual

SDR: (Select Diameter Range) Switch of setting the diameter range to AUTO or manual. Auto denotes that the particle size range is set automatically according to the SMPS setting based on settings an measurement values for flow rate V_{p1} and the

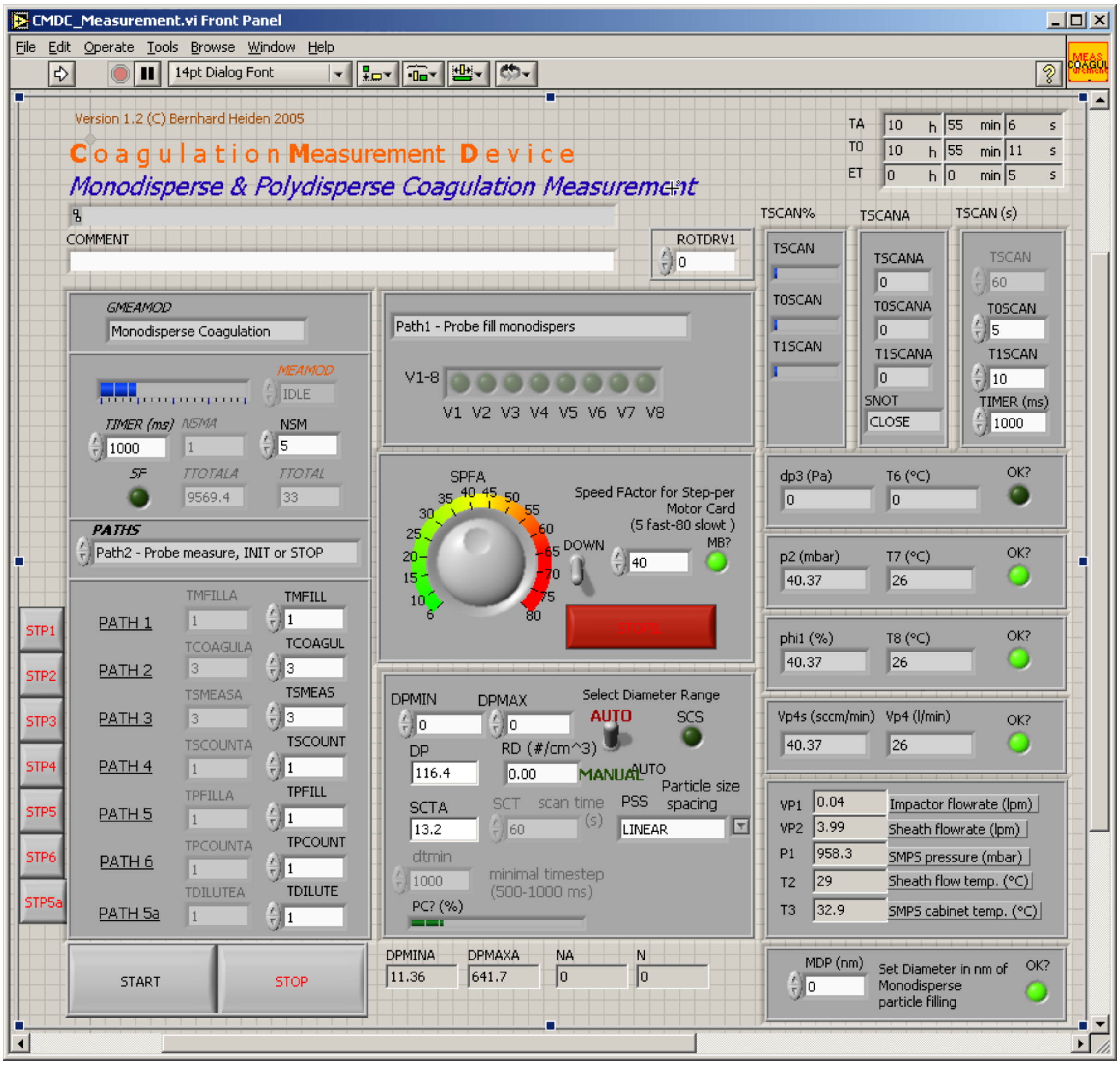

Figure 25 Application window of the CMD-Program: "CMDC_Measurement.vi"; this is the central window controlling all measurements

impactor. When the flow rate is small the impaction is low and hence the maximum diameter is high.

DP: Is the actual set diameter of the CMD software at the SMPS, it is determined corresponding to the time plan and the settings for DPMIN/DMAX and PSS.

RD: Is the actual read particle size concentration of the CPC [#/cm^3]

SCT/SCTA: Scanning time beginning from the setting of DPMIN at the SMPS classifier and actual time

PSS: Particle Size Spacing mode: LINEAR/LOGARITHMIC; Depending on the mode the particle diameter difference Δd_p between scanning intervals is calculated in the manner of equal distances for the LOGARITHMIC scales or for LINEAR size spacing in the linear scale.

dtmin: Equal to timer on the right setting (deactivated) (ms).

PC?%: Percentage of success for the actual scanning process.

DPMINA/DPMAXA: Actual setting of the minimum/maximum diameter read from the SMPS in nanometer.

N/NA: The number of N different particle size scans determined by the user setting and the actual number of the scanning diameter.

T0/TA/ET: Starting time, Difference time and actual time

TSCAN/TSCANA: Calculated and actual total time for measuring path 3 set by the scanning times T0SCAN and T1SCAN.

T0SCAN/T0SCANA: *Scanning start time* and actual scanning start time. For this time interval the path for the measurement path 3 is set waiting for the aerosol to flow into the SMPS. After this time, the scanning can begin.

T1SCAN/T1SCANA: Time set for scanning mode and corresponding actual time at the SMPS.

TIMER (ms): Sets the timing interval for the logging of the measurement data in the protocol file. It is restricted to approximately 3s for all sensors in operation.

SNOT intern notifier (see above I.1.14.1.3, p.70). Variable indicating the states of the SCAN Modus.

TSCAN/TSCAN0/TSCAN1: Progress indicators of each scanning mode.

The LEDS on the right side denote the correct operation of the sensors. They can be partly turned off to increase measurement time interval TIMER in the variable SM (Figure 50).

dp3(Pa)/ T6(°C): Actual sensor values for the differential pressure sensor ASP1400 dp3 and the temperature measurement on this sensor. T_6 represents not the ambient temperature.

p2(mbar)/T7(°C): Actual NI-DAQ measurement of the pressure and the temperature in the settler.

phi1(%)/T8(°C): Actual relative humidity measurement phi_1 and the corresponding temperature measurement on the sensor T_8. These values can also be read on the digital display of the attached microcontroller evaluation kit EK-H2.

Vp4s(sccm/min)/Vp4(l/min): Standard flow measurement with the flow sensor ASF1430. The corresponding actual flow rate V_{p4} [l/min] is calculated by means of the measurements p_2 and T_7, the standard state T_s=20 [°C] ,p_s=1013 [mbar] and the ideal gas law.

The following measurement values are read from the SMPS classifier microcontroller:

VP1: SMPS impactor flow rate [l/min]

VP2: SMPS sheath flow rate [l/min]

P1: SMPS pressure [mbar]

T2 : SMPS sheath flow temperature [°C]

T3: SMPS cabinet temperature [°C]

MDP(nm): Monodisperse particle diameter which is set for monodisperse filling of the CMD. The OK LED indicates that the command is sent successfully to the SMPS.

START: The start button starts the measurement series after setting all variables above.

STOP: This button is used to leave this program and go back to the main menu.

Fundamental considerations

I.1.15 Reactor characterization

The settler proposed is a *constant concentration reactor*. This is a reactor whose ideal concentration is constant. This can be explained by its operation. In the measurement mode the sample flow volume is vacuumed off the settler while simultaneously pumping it out. With this method

- mixing of the batch volume with ambient air
- dilution
- pressure and temperature change can be avoided.

Under the *ideal condition* of no coagulation deposition or settling of particles the mass m and the number concentration N is constant, explaining the constant concentration reactor (see Table 9).

The constant concentration reactor is comparable with a *discontinuous stirred tank reactor* (dCSTR)[68] (Moser 1988) with constant volume process. The concentration profile is a function of time and not of space. The reaction is the coagulation, deposition or settling of

[68] This is a batch reactor with a stirrer. First the reactor is filled discontinuously after the reaction it is emptied.

particles. The variable volume allows for a constant concentration which is comparable with a constant volume process for incompressible fluids, without reaction.

Under real conditions either deposition, coagulation or both will occur,[69] which is shown in Table 9.

Table 9 Classification of important ideal physical states relevant for the CMD

	Constant concentration	*Deposition*	*Coagulation*	*Coagulation & Deposition*
dN/dt	0	0	<>0	<>0
dm/dt	0	<>0	0	<>0

The number concentration gradient dN/dt can be measured with the CMD. For the mass, gradient dm/dt, e.g. a TEOM[70], or a filter measurement is necessary[71].

Determining the decay in mass and number concentrations allows for distinguishing between deposition and coagulation as a function of measurement mode.

An advantage of the constant concentration reactor is that the pressure variation of the thermodynamic state is minimized (T, p=constant). This conserves, probably, the state of nanoaerosols also in the case of nucleation processes, as condensation and evaporation is a function of the vapor pressure, and hence of the thermodynamic state. Therefore it is expected that liquid aerosols can also be investigated.

With defined state transitions e.g. warming, additional insight in particle growth mechanisms is gained. A constant concentration reactor, like that presented here allows for investigation of the real aerosol like behavior at constant conditions for low concentrations with *tunable measurement uncertainty*[72] in a systematic way.

I.1.16 Residence times

There are several paths in CMD each with several residence times according to the overall flow rate. This overall (sample) flow rate is factored in by the ASF flow sensor V_{P4} and the

[69] Settling can be neglected for nanoparticles except for long time ranges.

[70] Tapered element microbalance

[71] The accuracy of the mass measurement has to be very high and or the measurement time has to be very long.

[72] Depending on number concentration and the time of coagulation the coagulation measurement accuracy increases.

SMPS differential pressure measurement V_{P1}. The flow rates are decisive for the particle size distribution measurement for several reasons:

- They are limiting the process of possible measurement of coagulation
- They limit the range of measuring time, and parameter settings of the CMD, as e.g. filling time; scanning start time etc.
- They allow the correct interpretation and shifting measurement parameters especially the particle diameter of the size distribution.

The concept of residence time τ [s] is closely linked to the flow rate as can be seen of the defining equation:

$$\tau = \frac{V}{V_p} \cdot 60 \tag{0-17}$$

V_p [l/min] is the general flow rate and V [l] is the volume. By means of the residence time a statistical mean time of particles in a certain volume is described, valid for any type of reactor[73]. The SMPS sheath flow for example, is, in terms of process terminology, a recycle flow reactor. The CMD settler is, with respect to coagulation, a batch reactor, where the waiting time equals the residence time, with respect to filling a fed batch reactor.

Following the individual residence times and their dependencies are described for the whole CMD system.

I.1.16.1 Overall residence time for measurement

I.1.16.1.1 Standard SMPS system

The residence times for the standard SMPS measurement with the AIMS (Aerosol Instrument Manager Software)[74] software is given in Table 10. There is a short connector tube between the SMPS monodisperse output and the CPC. This tube leads to the residence time τ_0, which is "included" as a standard factor **td** in the AIMS software, together with the residence time of the CPC (τ_6)[75]. When a longer connector tube is used, there has to be a correction made to this factor, according to the equations given in chapter I.1.17.1 p.87.

Table 10 Residence times for the standard SMPS system

Residence time	*Path*
τ_0	DMA out→CPC in

[73] e.g.: batch reactor, fed batch reactor, recycle flow reactor and tube reactor

[74] original software for the SMPS system from TSI (www.tsi.com)

[75] See also in the subsequent chapter I.1.16.3 p.83 and I.1.16.4 p.86

τ_3	DMA in → DMA out
τ_6	CPC in → CPC

A second standard factor **tf** [s] is also calculated for each measurement[76], which is identical with the residence time τ_3 defined in (0-21). As τ_3 is dependant on the sheath flow and the sample flow rate it is very important to have a calibrated sample flow (e.g. with the bubble flow meter "Gilibrator 2" in the standard SMPS measurement. This is even more important as the integrated differential pressure flow measurement for the sample flow (V_{p1} [l/min]) shows a drift with time. Pollution leads to a different differential pressure, and hence a different flow rate. In the case of the measurement of cigarette smoke, the impactor had been polluted after the measurement of one cigarette with a 0.5 [mm] long "wire" approximately 1 [mm] in diameter, leading to a significant change in flow rate.

The wrong size distribution finally leads to a wrong particle diameter. A correction can be made afterwards according to (0-21), if the "real" sample and sheath flow is known.

Some remark is given to the use of the AIMS software. The parameters that are put in for the sample flow are decisive for the following size distribution calculation[77]. It has to be taken care to take the actual sample flow values of the SMPS display or, for example, flow rates measured with the bubble flow meter. Otherwise the peak of the size distribution will be shifted. This is even more important as the SMPS sample flow measurements is sensitive to pollution.

I.1.16.1.2 CMD system

The most important residence times for the CMD system are given in Table 11.

Table 11 Residence times for the CMD system and the starting and endpoints for the related paths. These are part of different main paths listed in Table 7.

Residence time	*Path*	*Main paths*	*Formula*
τ_1	Settler bottom→ SMPS in	3	V_1/V_{p4}
τ_2	SMPS in→ DMA in	3,1,2	V_2/V_{p4}
τ_3	DMA in → DMA out	3,1,2	$V_3/(V_{p2}+V_{p4})$

[76] This quantity is calculated automatically in the AIMS Software and can not be change by the user

[77] There is no possibility for the AIMS software to get measurement results from the SMPS as the data connection is only between computer and the serial interface of the CPC. The CPC itself is connected with the SMPS classifier by a data cable transmitting the signal for the DMA high voltage to be set.

τ_4	DMA out→CPC in	3,2	V_4/V_{p4}
$\tau_5 = \tau_{1+} \tau_{2+} \tau_4$	Settler bottom→ DMA in & DMA out→CPC in	3	$(V_1+V_2+V_4)/V_{p4}$
τ_6	CPC in → CPC	3,4,6,2	1.48 [s]
τ_7, τ_{70}	Settler top→ Settler bottom	5a,5b,1	V_7/V_{p4}
$\tau_8 \approx t_{FILL}$	Ambient air→Settler bottom	5a,5b	V_8/V_{p4}
τ_9	Settler bottom→CPC in	4	V_9/V_{p4}
τ_{10}	Ambient air/probe in →SMPS in	1,2	V_{10}/V_{p4}
τ_{11}	DMA out→settler bottom	1	V_{11}/V_{p4}
τ_{12}	Ambient air/probe in→CPC in	6	V_{12}/V_{p4}

I.1.16.2 Settler

There are three operating modes for the settler:

1. Filling
2. Waiting for Coagulation and deposition
3. Measurement

According to these modes different residence times are of importance.

The minimal *filling time* t_{FILL} (τ_8 [min]) for the settler is, at first approximation, the same as t_{total} in Figure 27[78], as this is the residence time for the settler in the fed batch operation mode. It is defined as:

$$\tau_8 = \frac{V_8}{V_{p4}} \cdot 60 \qquad (0\text{-}18)$$

V_8 [l] is the volume from the path between aerosol inlet including the total volume of the settler V_{70} [l], and V_{p4} [l/min] the filling flow rate, adjusted with the needle valve DRV1. Due to the separate needle valve DRV1 the flow rate can be higher than for the measurement mode, and so the minimum filling time is lower. The upper flow rate is limited to the maximum possible under the pressure in the settler. At a flow rate of 2.4 [l/min], the settler begins to shrink, and no safe operating mode is possible.

In Figure 26 the minimum filling time as a function of the flow rate V_{p4} and the number of rotations ROTDRV1 of the needle valve DRV1 is shown. The relation between V_{p4} and ROTDRV1 was gained experimentally (Bakk 2005)[79]. Having one setting of the needle valve the flow rate can be gained from the blue curve. Drawing a line to the blue curve then straight down to the pink curve yields the corresponding minimum filling time on the left y-axis, for

[78] Assuming constant flow rate for filling and measurement mode

[79] p. 89

complete filling of the settler. Due to incomplete mixing of the gas in the settler this time should be longer in any case.

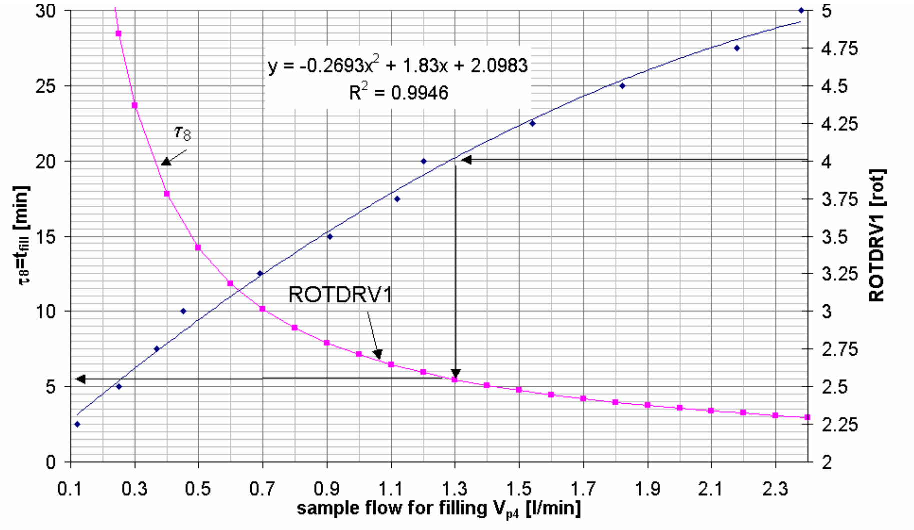

Figure 26 Minimum filling time for the settler τ_8. The total settler volume was assumed with V_{70}=7.05 [l], the volume for the settler and the gas path before was V_8=7.11[l].On the right side the number of rotations, counted from the closed valve, of the needle valve DRV1 is related to the filling flow and hence to the minimum filling time τ_8 (see text for more details)

Waiting for Coagulation is determined by the waiting time t_{WAIT} in the software. This depends on the kind of experiments planned, and is important with regard to the expected results. This parameter is best planned by a prior rough estimation of particle concentration decay.

For *Measurement* operating mode the residence or total time t_{total}, of possible measurements with one probe in the settler, is given by (0-19) and Figure 27, where V_7 [l] is the effective volume of the settler, and V_{p4} [l/min] is the sample flow rate.

$$t_{total} = \frac{V_7}{V_{p4}} \qquad (0\text{-}19)$$

The maximum measurement time t_{MEAS} for a number of NSM single measurements with the CMD is:

$$t_{MEAS} = \frac{1}{NSM} \cdot \frac{V_7}{V_{p4}} \cdot 60 \qquad (0\text{-}20)$$

Equation (0-20) is depicted in Figure 27 for application and Figure 49 in the appendix for a broader time range. When the sample flow rate V_{p4} and the number of measurements is fixed then the total measurement time t_{total} of all single measurements can be seen in Figure 27 on the left side, and the maximum measurement time of one measurement run on the right side.

For example, for the sample flow rate V_{p4}=0.3 [l/min] and 8 measurements the total measurement time t_{total} ~23 [min] and each single measurement is ~170 [s] long.

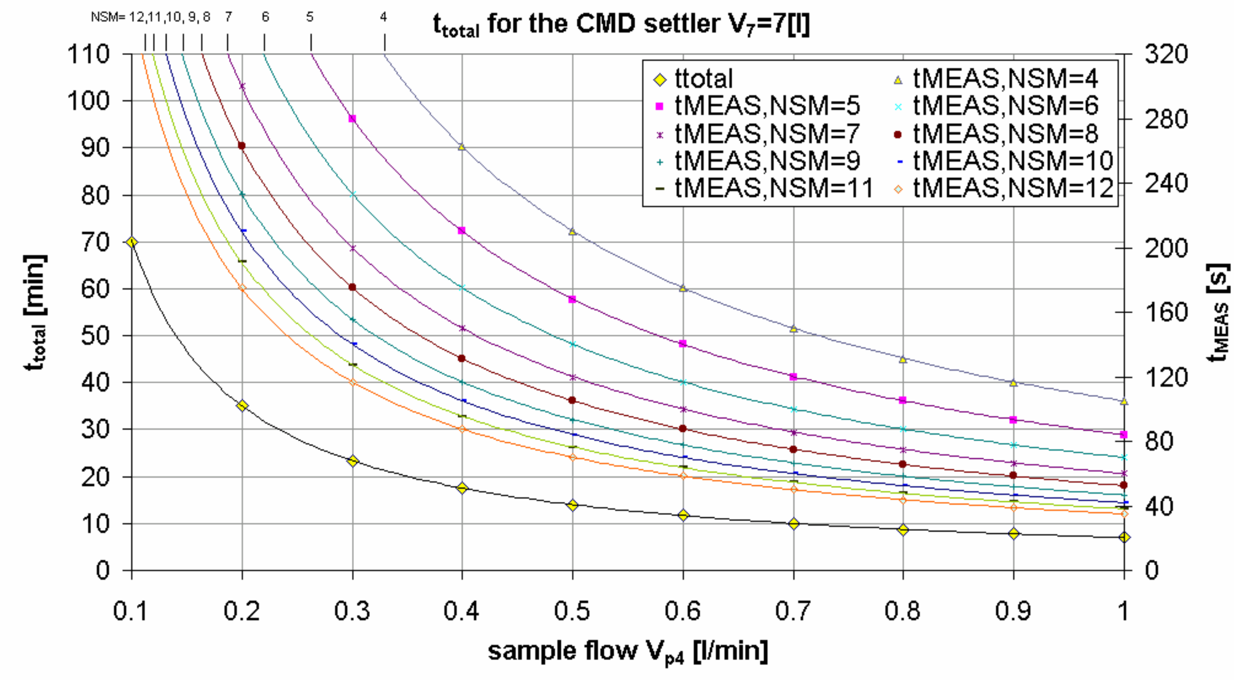

Figure 27 Total measurement time possible when emptying the settler as a function of the sample flow Vp_4 and the number of the measurements (NSM) on the right y-axis; The total measurement time as a function of Vp_4 can be read on the left y-axis (calculation see equation (0-20)).

I.1.16.3 DMA

The sheath flow in the SMPS DMA is a recycle flow and hence enhances the sample flow. The residence time τ_3 from the voltage setting to the way out of the reactor is determined by:

$$\tau_3 = \frac{V_3}{V_{p1} \cdot \left(1 + \frac{1}{\zeta}\right)} \cdot 60 \tag{0-21}$$

$$\frac{V_{p1}}{V_{p2}} = \zeta \tag{0-22}$$

$$V_3 = L_{DMA} \cdot \left(r_{a\_DMA}^2 - r_{i\_DMA}^2\right) \cdot \pi \cdot 1000 \tag{0-23}$$

V_3 is the total gas volume of the DMA according to (0-23) and Table 12, V_{p1} (equivalent to V_{p4}) is the sample flow, V_{p2} the sheath flow of the SMPS and ζ is the *sample to sheath flow volume ratio* of the DMA.

Table 12 Parameters of the SMPS DMA relevant for the residence time calculation (see text)

Name	*Symbol*	*Dimension*	*Value*
DMA Model	~	~	3081
DMA Inner Radius	r_{i_DMA}	[m]	0.00937
DMA Outer Radius	r_{o_DMA}	[m]	0.01961

Name	*Symbol*	*Dimension*	*Value*
DMA Characteristic Length	L_{DMA}	[m]	0.44369
DMA air volume	V_3	[l]	0.41365

In Figure 28 equation (0-21) is depicted for the sample flow rate V_{p1} on the x-axis, the DMA residence time τ_3 on the y-axis and with the sheath flow rate V_{p2} as parameter. To gain a good dilution of the sample flow with clean sheath air flow a ratio of 1/10 is recommended for V_{p1}/V_{p2}. Hence, with a low sample and sheath flow rate, the residence time increases drastically. Therefore, for reducing the total residence times (measurement time) this ratio should be reduced, especially as the sample flow is low.

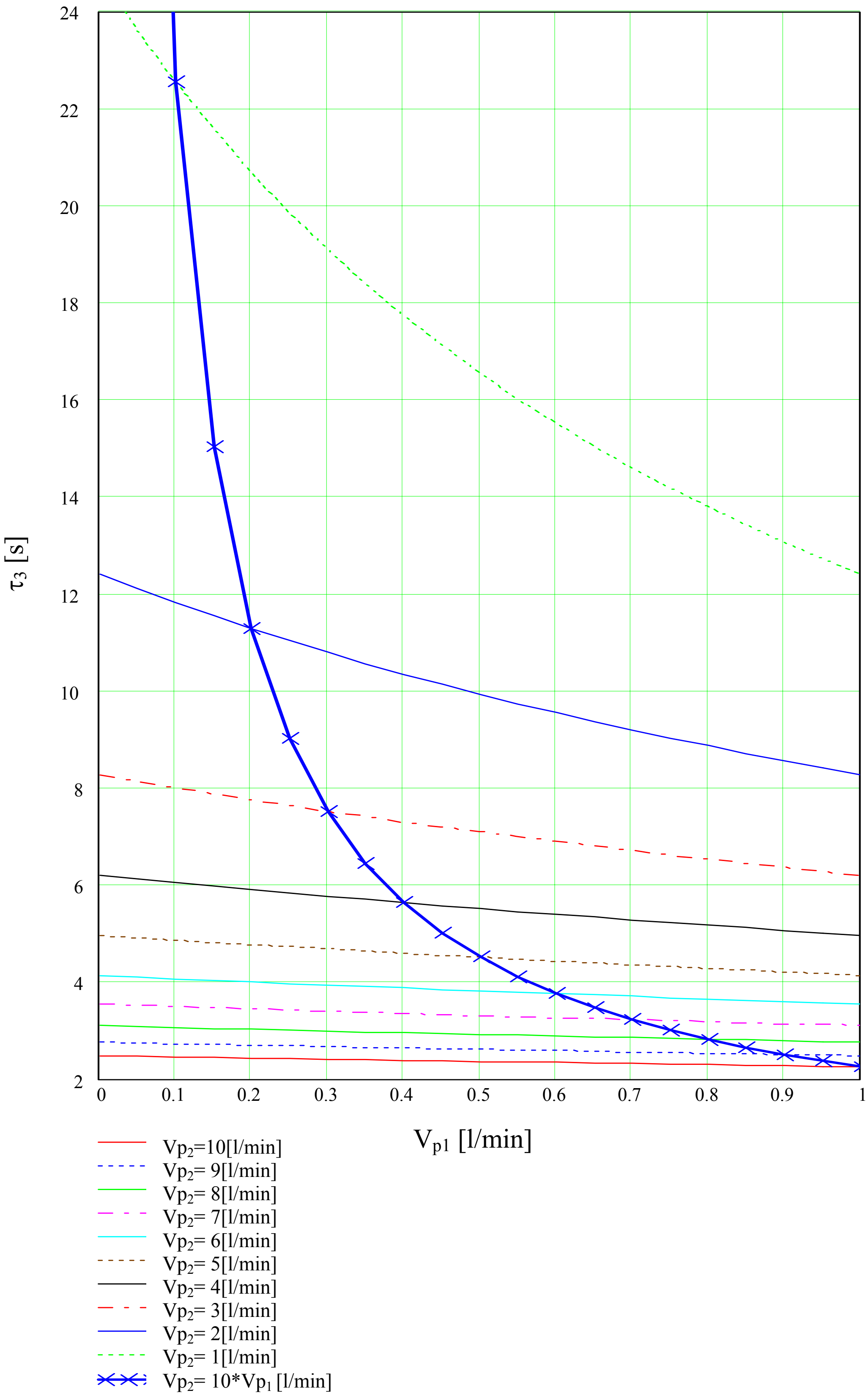

Figure 28 Residence time τ_3 for the SMPS DMA as a function of the sample flow Vp_1 and the sheath flow Vp_2. As a recommendation from TSI the ratio of sheath flow to sample flow should be at least ten. The residence time for this ratio is shown with the thick blue line.

I.1.16.4 CPC

The residence time of the CPC and the tubing as a function of the sample flow V_{P2} can be seen in Figure 29 and Table 13. There is a constant residence time τ_6 in the CPC as the volume flow is constant 1[l/min]. The *total residence time* rd *of the standard path SMPS>CPC* including the residence time of the CPC was calculated with the AIMS software. Then, rd' was calculated according to Table 13. For this purpose, the constant volume V_{0S}' and the residence time τ_6 had to be fixed. Out of this, the standard residence time of the tubing τ_{0S} and τ_{0S}' can be calculated.

The actual standard tubing between "DMA out" and "CPC in", relevant for path 3, has a volume of approximately V_0=0.0075 [l][80]. Together with the sample flow $V_{P4,}$ the residence time τ_0 results:

$$\tau_0 = \frac{V_0}{V_{P4}} \cdot 60 \tag{0-24}$$

The actual standard tubing between "Settler bottom" and "CPC in", relevant for path 4, has a volume of approximately V_0=0.1[l]. Together with the sample flow V_{p4} the residence time τ_9 results:

$$\tau_9 = \frac{V_9}{V_{P4}} \cdot 60 \tag{0-25}$$

The residence time τ_6 of the CPC alone is the same for the SMPS standard and the CMD measurement, whereas the path is longer.

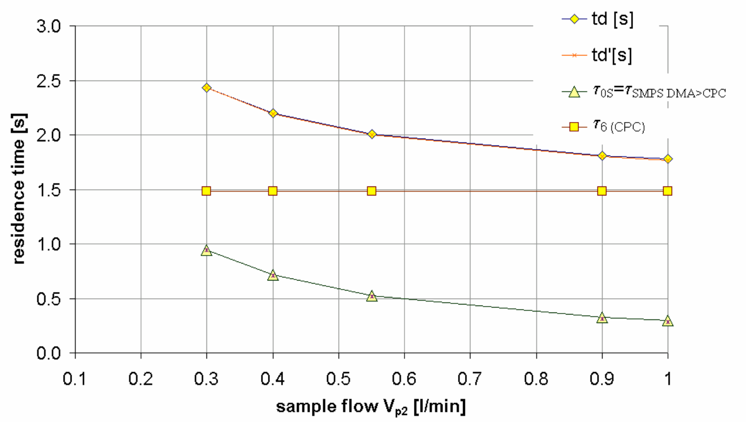

Figure 29 Residence time for the CPC3010 and the standard SMPS tubing as a function of the sample flow V_{p1} (description see text).

[80] The volume is depending only on the length and diameter of the connecting tube.

Table 13 Data according to Figure 29

V_{p2} [l/min]	td [s]	τ_{0S} [s]	td' [s]	$\tau_{0S'}$ [s]
1	1.779	0.296	1.767	0.284
0.9	1.810	0.327	1.799	0.316
0.55	2.007	0.524	2.000	0.516
0.4	2.198	0.714	2.193	0.710
0.3	2.430	0.947	2.430	0.947

V_{0S}'	[l]	**0.00473**	$td'=V_{0S}'/V_{p2}*60+\tau_6$
τ_6	[s]	**1.4835**	$\tau_{0S}=\tau_6-td$
V_{p6}	[l/min]	0.0247244	$\tau_{0S}'=V_{0S}'/V_{p2}*60$

The residence times for the path "(SMPS) DMA out→CPC" for the actual standard SMPS measurement ($\tau_0+\tau_6$) and the CMD measurements ($\tau_4+\tau_6$) are depicted in Figure 30.

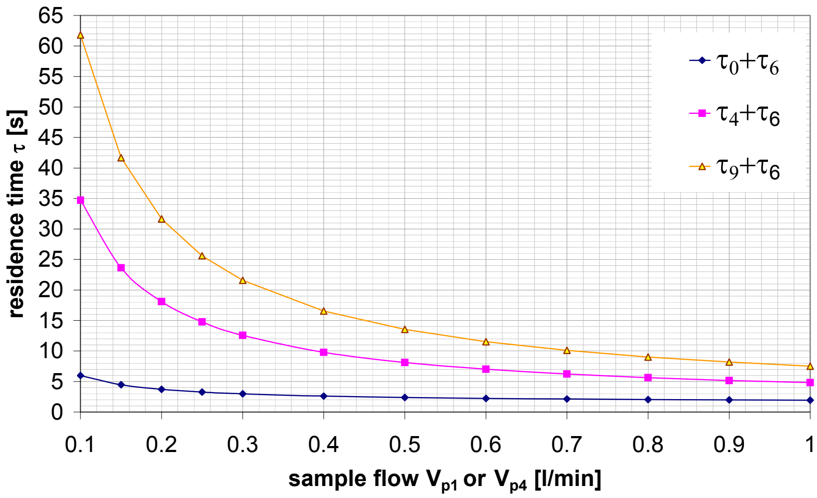

Figure 30 Residence times for the standard SMPS system $\tau_0+\tau_6$ and the CMD system $\tau_4+\tau_6$ or $\tau_9+\tau_6$ as a function of the sample flow Vp_1 or Vp_4

I.1.17 Dilution

Dilution of the aerosol flow occurs in several cases of the measurement process. First, in the bypass filter of the CPC and second in the settler when the settler is not filled long enough.

I.1.17.1 Dilution in the CPC

In the CPC an inherent dilution of the sampling line takes place. The CPC inlet consists of a needle valve DRV3, a clean air filter RLF2 and a T connector for the sampling line. The CPC case inlet is regulated to a constant volume flow of V_{p6}=1 [l/min]. As a consequence, the sample flow V_{p1} is always diluted, except in the case that the sample flow is 1 [l/min]. This means that the particle concentration has to be recalculated according to dilution. Under the assumption of no losses due to mixing equation (0-26), this gives the differential particle balance. The particle concentration dN0 is the measured particle concentration of the CPC in the time interval t+Δt. The particle concentration of the filtered air is dN00. This term is assumed to be 0.

$$dN0 = dN \cdot \frac{V_{p1}}{V_{p6}} + dN00 \cdot \left(1 - \frac{V_{p1}}{V_{p6}}\right) \tag{0-26}$$

Then the effective particle concentration before dilution is:

$$dN = \frac{dN0}{V_{p1}} \cdot V_{p6} \tag{0-27}$$

I.1.17.2 Dilution due to incomplete filling

The residence time for the filling of the CPC is quite large especially when the filling flow rate is low and the total volume is filled in (compare Figure 26). When the filling time t_{FILL} is lower than the residence time τ_8, then a mixing with the settler aerosol takes place. To determine the incomplete mixing, future experiments could be done, by measuring the aerosol mixing concentration as a function of incomplete filling time. This function would also reveal the time necessary for asymptotic filling of the settler in such a way that the settler concentration equals the probe concentration. Without further information about this fact, a safety factor **sff** for the filling time, e.g. sff=2 is useful:

$$t_{FILL'} = t_{FILL} \cdot sff \tag{0-28}$$

I.1.18 Impaction, deposition and other effects

Inertial impaction is a function of several parameters like the gas velocity the size of the particles and the geometry. There are several aspects regarding impaction and deposition important for the CMD.

1. Impaction can pollute the measurement equipment. This can lead to damage of the sensors, or distorted measurement values. Therefore an impactor before the inlet of the CMD is recommended.
2. Concerning the magnetic valves, a small diameter leads to high velocities. Together with the geometry, impaction is most probably at higher sample flow rates. They should be avoided for this reason. Electrical ball point valves would be more effective in avoiding impaction, but they are costly (4 times higher prices).

3. The used PVC pipes are not ideally suited for tubing as they can cause higher deposition rates. Antistatic tubes might give better results concerning deposition, although the effect has not been shown to be significant in the experiments.
4. The flexible tubing has the disadvantage of a possible difference in flow resistance. Metal pipes on the other hand, would have the disadvantage of a high thermal conductivity, which might lead to condensation or phase transitions.
5. The thermophoretic effect could be used to avoid particle deposition, by heating the wall temperature some degree above the gas temperature.
6. As the valves are heated in operation the thermophoretic effect can be expected as a function of valve and gas flow temperature.
7. The settler is not resistant to UV radiation. That means experiments can only be made in the "darkness" of the black NBR-Settler. For investigation of UV and sunlight radiation a transparent and UV-resistant settler type should be used. Experiments of this type were made by Husar (Friedlander 2000; Husar 1971) showing significant coagulation due to smog with organic precursors.
8. Solvents of the settler diffusing could have an influence on both particle coagulation and particle concentration counting.
9. The CMD settler can also be optionally operated as a continuous stirred tank reactor (CSTR)[81](Moser 1988)[82]. In this case, the settler is mixed by the stirrer and the particle size concentration measurement, e.g. path 2 is done with valves V7/V8 open. The optional valve VM3 is switched to "probe in" (Figure 9). This system has a residence time depending on the actual settler volume and the sample flow V_{p4}.

[81] This reactor performance has a constant output concentration depending on the residence time and the initial concentration.

[82] p. 113

Measurements of the coagulation coefficient with the CMD

In this chapter, the experimental measurement of the coagulation coefficient K with the CMD is exemplified. By means of process automation a number of tasks can be performed, founded on the theory derived in the first chapter and the built CMD and its control as explained in the second chapter. Several applications are shown as first experimental tests of the CMD and the founding theory.

First, the determination of the coagulation coefficient of *monodisperse aerosols*[83] is shown. A soot aerosol was used produced by the CAST[84] particle generator. For this purpose a polydisperse aerosol[85] produced by the CAST was separated with the DMA into a monodisperse aerosol and then subsequent size distribution measurements were done.

Second, the determination of the coagulation coefficient of polydisperse aerosols is shown, first by the sequential size distribution measurement of an incense aerosol, then by the number distribution measurements by two different concepts[86]. By measurement of the concentration, while emptying the whole settler, and discontinuously diluting and measuring the aerosol size concentration over a free specified time interval.

Finally, in all these cases the time dependant concentrations lead to the determination of the coagulation coefficient K.

Monodisperse aerosols

The CAST, having the advantage of producing a reproducible number size distribution, was used for a series of monodisperse measurements. For this purpose, the geometric mean

---

[83] A monodisperse aerosol is an aerosol with only one particle diameter. In reality this is an aerosol with a narrow size distribution (e.g. small standard deviation), whereas a polydisperse aerosol has a wide size distribution (e.g. large standard deviation).

[84] Soot particle generator for production of defined particle number concentrations from Matter-Engineering www.matter-engineering.com

[85] As combustion generated aerosols are polydisperse in general.

[86] Especially two different CMD operations: "Polydisperse Coagulation I" and –"II".

diameter of the size distribution can be set with the CAST. There were two types of measurements made. One with the CAST setting of d_{pg}=85 [nm] and one with d_{pg}=160 [nm]. The first one produced an unimodal (see Table 14) the second a bimodal polydisperse size distribution.

Table 14 *Monomodal size distribution measured with the standard SMPS system and setting the CAST diameter to d_p=85 [nm].*

Symbol	*Description*	*Value*	*Unit*
d_{pg}	Geometric mean diameter	76.1	[nm]
σ_g	Geometric standard deviation	1.60	~
N_∞	Total concentration	1.04E+07	[#/cm^3]
	Impactor type(cm)	0.071	[cm]
V_{p2}	Sheath flow	4	[lpm]
V_{p1}	Aerosol flow	0.4	[lpm]

To generate a reproductive number size distributions the burner of the CAST was in operation for at least half an hour. The subsequent aerosol was then stable for the rest of the measurements[87]. For producing large amounts of aerosols, it was necessary to vacuum off the exhaust gas continuously[88]. First, measurements with the AIMS Software were made then compared with the subsequent monodisperse CMD measurements with the same CAST setting.

A first method of getting the monodisperse coagulation coefficient is shown in the following for the CAST particle diameter setting of 160 [nm]. Before the CMD measurements, the size distribution of the CAST had to be stabilized for more than half an hour. All the residence times are given in Table 15 according to definitions of Table 11. The corresponding size distributions, measured with the CMD operation “Monodisperse Coagulation”, are depicted in Figure 31 and Figure 32 for dN for different perspectives with and without logarithmic scale of the y-axis. The size distribution of measured particle concentration dN is plotted against the particle diameter. There was a bimodal size distribution although a monomodal one had been expected, possibly caused by pollution of the burner nozzle or the instability of large soot aerosols in the CAST. Also measurements with the aerosol one day later shown in Figure 32 were made.

[87] It is not possible to produce exactly the same number size distributions on different days.

[88] Some pollution of the exhaust gas with the ambient air occurred, as the system was not hermetically separated from the laboratory.

Table 15 Residence times for the CAST experiments #65 & #67; τ_I is the time d_p is shifted to concentration because of residence time between DMA and CPC; τ_{II} is the time the raw data are shifted to the beginning of measurement mode; V_{p2} is the sheath, V_{p2} is the sample flow and NSMA is the number of each single size distribution measurement.

V_{p2} [l/min]	V_{p4} [l/min]	NSMA	τ_5 [s]	τ_4 [s]	τ_3 [s]	τ_2 [s]	τ_1 [s]	τ_0 [s]	τ_I [s]	τ_{II} [s]
4	0.3579	#1	29.8	9.8	5.70	3.9	16.0	5.0	35.5	15.51
4	0.3551	#2	30.0	9.9	5.70	4.0	16.2	5.0	35.7	15.59
4	0.3551	#3	30.0	9.9	5.70	4.0	16.2	5.0	35.7	15.59
4	0.3551	#5	30.0	9.9	5.70	4.0	16.2	5.0	35.7	15.59
4	0.3551	#7	30.0	9.9	5.70	4.0	16.2	5.0	35.7	15.59
4	0.2031	#8	52.5	17.3	5.90	6.9	28.3	8.8	58.4	23.19
4	0.2031	#9	52.5	17.3	5.90	6.9	28.3	8.8	58.4	23.19

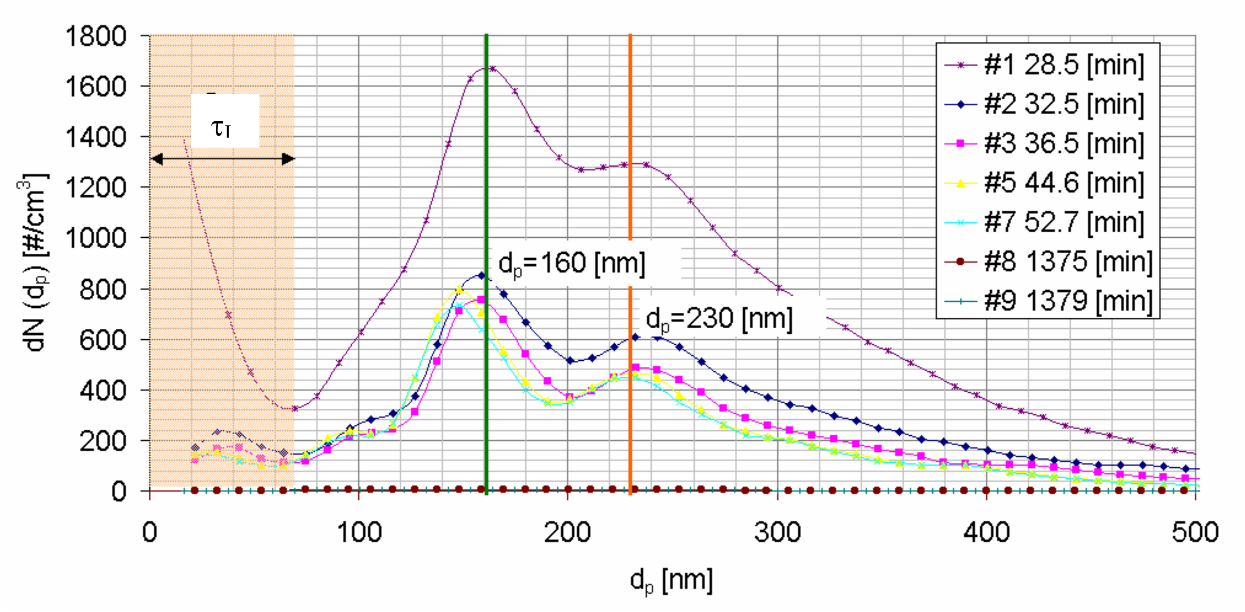

Figure 31 Monodisperse CMD measurement of the CAST setting d_{pg}=160 [nm]; τ_I is the residence time before the aerosol flow enters the measurement site of the SMPS Classifier (experiment #65).

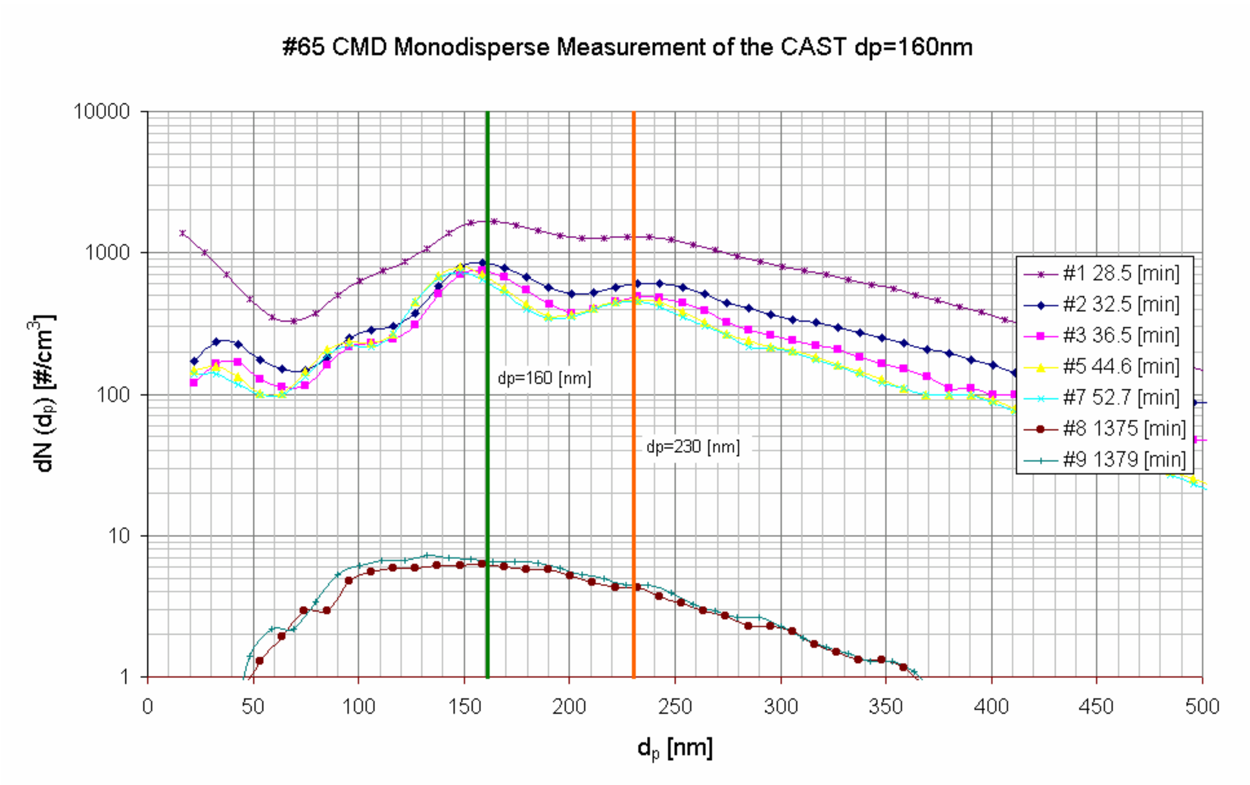

Figure 32 Monodisperse CMD measurement of the CAST setting d_{pg}=160 [nm]

The resulting total particle concentrations are shown in Table 16 and Figure 33. The initial measurement #1 has probably shifted to high concentrations due to the starting condition of the measurement. The second measurement reveals that there are quite high particle losses or dilution. Later I discovered that these losses were mainly due to the nonreturn valve where only 11% passed.

Table 16 Particle concentrations of run #65& #67

	t_{total}(min)	t(min)	N_∞ (#/cm^3)	%	
Bimodal polydisperse CAST distribution	~	~	6.88E+06	100	~
Measured monodisperse cutout	~	~	**2.24E+05**	3.3%	**100%**
#1	40	0	6.80E+04	~	30.4%
#2	44	4.0	2.42E+04	~	11%
#3	48	8.0	1.89E+04	~	8%
#5	56	16.1	1.84E+04	~	8%
#7	64	24.2	1.74E+04	~	8%
#8	1375	1335.2	1.99E+02	~	0.1%
#9	1379	1339.2	2.24E+02	~	0.1%

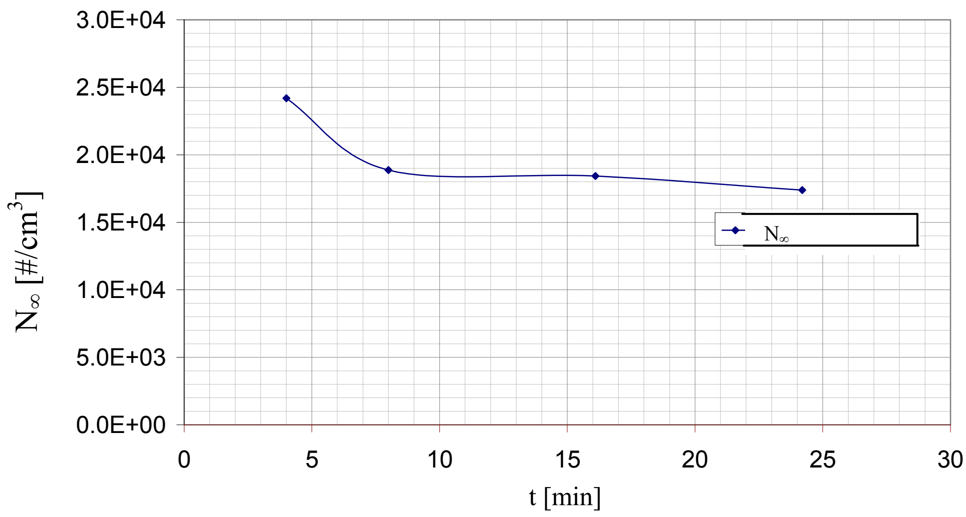

Figure 33 Total particle concentrations N_∞ of run #65

I.1.19 Control measurement

At the end of the measurement, the total concentration of the aerosol was measured. The results with the AIMS measurement and the standard SMPS system setup are depicted in Figure 34. The distribution was clearly bimodal. Three measurements #1-3 in a series gave reproducible results. As it is seen from the picture, there is some indication that the normal distribution is somewhat distorted, leading to a bimodal distribution. This might be the case due to pollution of the CAST dilution system, as it was the last measurement on this day.

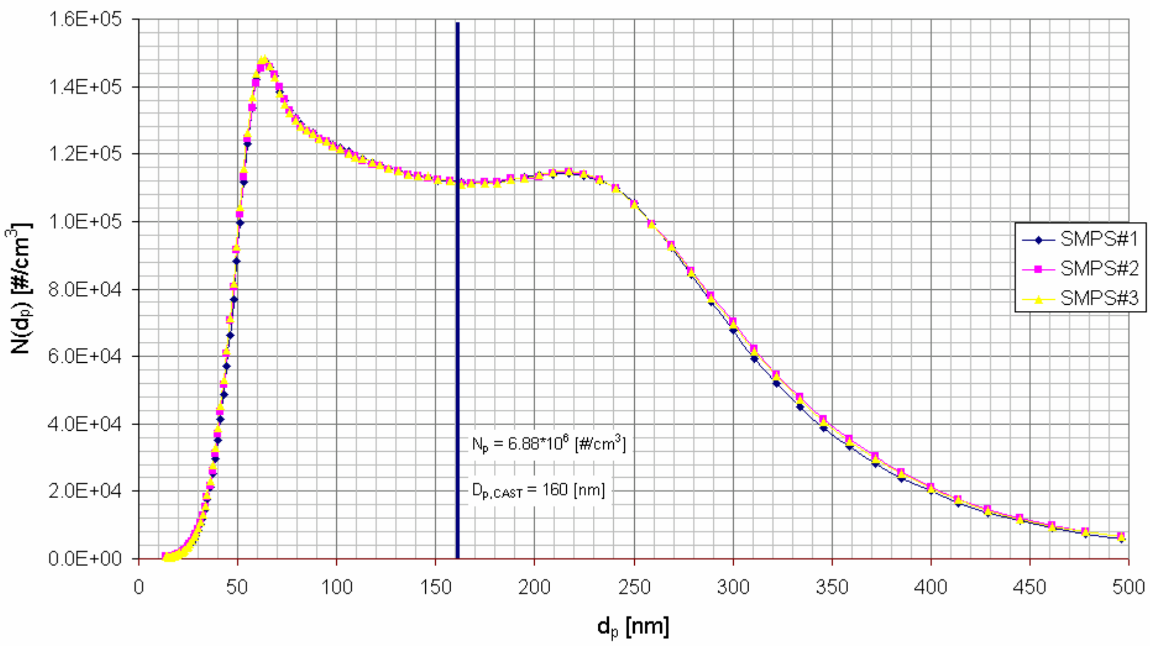

Figure 34 Control measurement of the CAST measurement with the standard SMPS system for experiment #65

One day later there was another measurement made with the same probe, which had remained during this time in the settler. In the meantime also transport of the CMD to the laboratory had taken place. According to Figure 35 the distribution had reached background level. The peak of the lognormal size distribution was in the same region as the original aerosol, which indicates that everything had been deposited in the meantime.

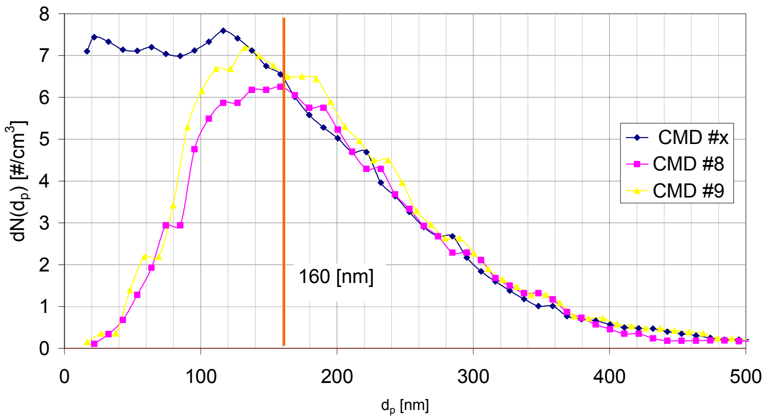

Figure 35 CMD measurement one day after the soot measurements of experiment #65 with the same aerosol enclosed (experiment #67); the numbers #x refer to the usual different first measurement and #8-9 to the single measurement run of the monodisperse measurements (see Table 16); Dilution with ambient air had occurred .

I.1.20 Results: Smoluchowski coagulation plot

The Smoluchowski coagulation plot is given in Figure 36, the corresponding characteristic values in Table 17. The first two measurement points are regarded to overestimate the particle concentration due to a rest particle concentration in the tubing from primary sampling. The concentrations of the last sampling points yield a straight line in the Smoluchowski plot getting an apparent coagulation coefficient of K_a=46.49*10^{-10} [cm^3] which is in the same order of magnitude of the K_a values of Rooker and Davies (Rooker and Davies 1979).

Table 17 Results for the parameters of the initial concentration N_0, the apparent coagulation coefficient K_a which is approximately the same as the coagulation coefficient K and Pearson's regression coefficient r^2 of the monodisperse soot measurement (experiment #65); L was not determined because only one data set for K_a existed

N_0 [#/cm^3]	L [1/s]	K_a [cm^3/(#*s)]	r^2 [~]
2.24E+05	~	4.649*10^{-9}	0.9363

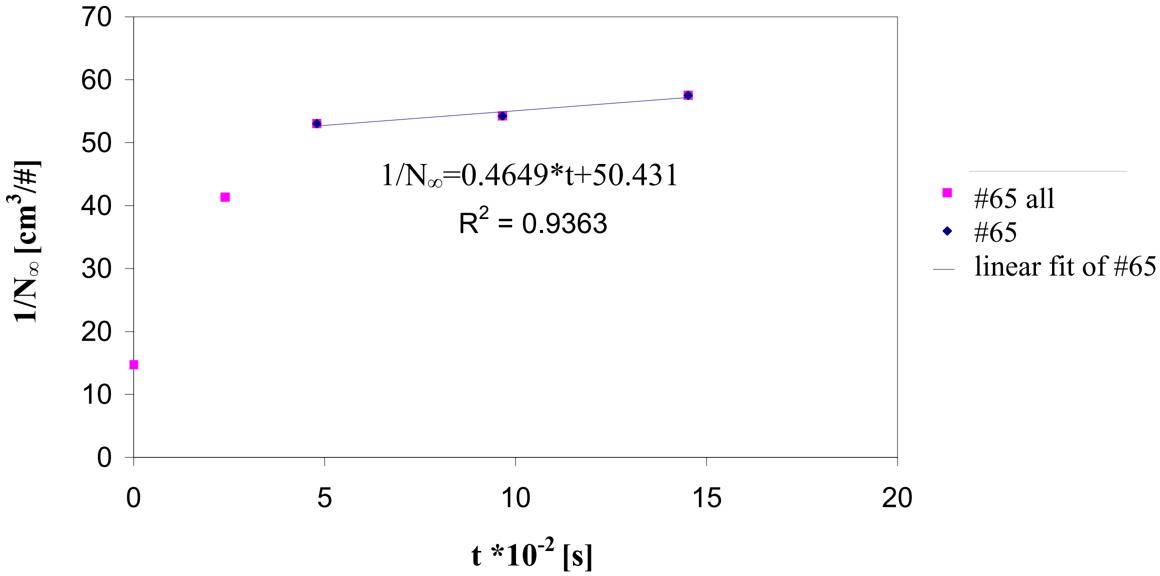

*Figure 36 Smoluchowski coagulation plot for monodisperse soot measurements with the CAST; $K_a=4.649*10^{-9}$ [cm^3/(#*s)] (experiment #65).*

Polydisperse aerosols

There were performed two principal types of measurements of the coagulation coefficient. First considering the size distribution measurement, second the particle concentration only.

I.1.21 Measurement of the coagulation coefficient of polydisperse aersols by means of a size distribution measurements - Incense Measurements

One measurement run of the coagulation coefficient of a polydisperse incense aerosol was made for approximately 140 [min], by means of sequential sized distribution measurement. The parameters of the measurement are given in Table 18. In Figure 37 and Figure 38 different views of the results of the complete measurement run is given. The operation "Polydisperse Coagulation" consists of subsequent particle number distribution measurements. The evolution in particle concentration for different size classes is given in Figure 37, for the whole particle size distribution in Figure 38.

Table 18 Parameters important for CMD operation „Polydisperse Coagulation" and the incense measurements in this mode.

Name	*Value*	*Unit*	*Description*
SPFA	8	~	Speed factor
V_{p7}	0.339	l/min	Settler flow
V_{p4}	0.310	l/min	Measured sample flow
α	0.029	~	Leakage ratio
V_{p2}	2.992	l/min	Measured sheath flow
V_{p1}	0.354	l/min	Measured sample flow

τ_6	1.48	s	Residence time CPC
V_3	0.41365	l	Volume inside the SMPS DMA
ζ	0.10365	~	Sample to sheath flow volume ratio of the DMA
τ_3	7.52	s	Residence time DMA
V_4	0.05540	l	Volume of air in the path between SMPS and CPC for the CMD
τ_4	10.72	s	Residence time settler DMA in
V_1	0.0956	l	Volume of air in the path between Settler and SMPS in
V_2	0.0235	l	Volume of air inside the SMPS between input and DMA
τ_1	18.50	s	Residence time related to V_1
τ_2	4.55	s	Residence time related to V_2
τ_I	20	s	Time d_p is shifted to concentration because of residence time between DMA and CPC
τ_{II}	23	s	Time the raw data are shifted to the beginning of measurement mode
dilution	2.9	~	Dilution with respect to the raw data
t_{total}	1242	s	Time for emptying settler

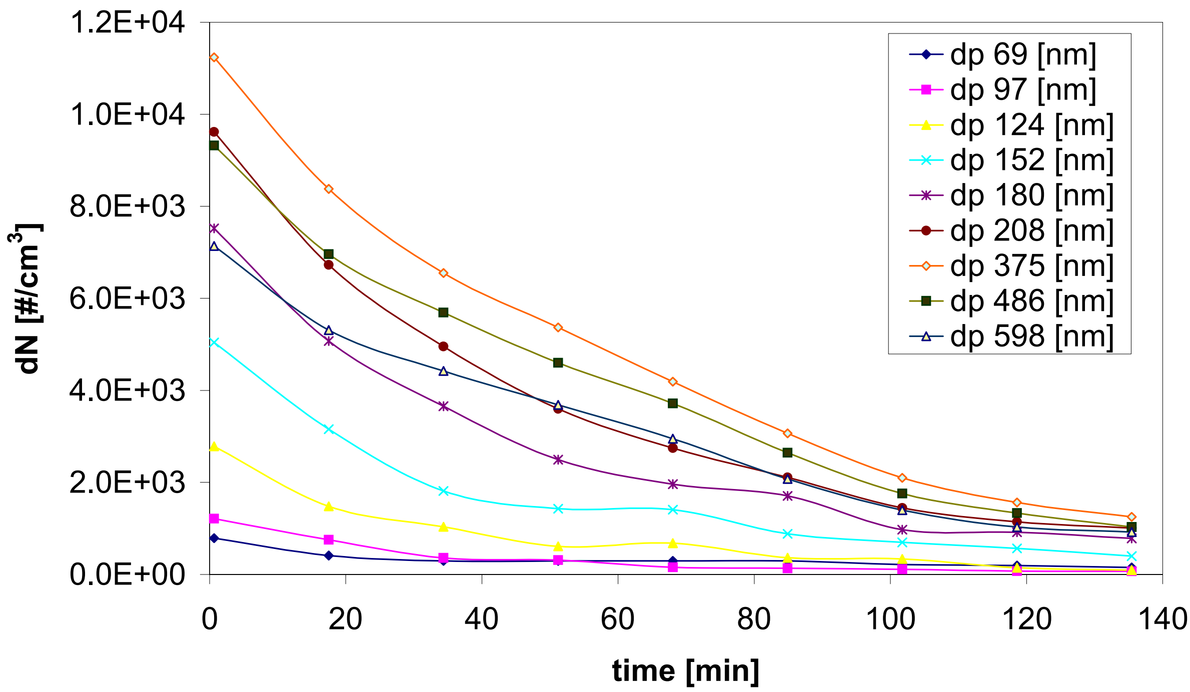

Figure 37 Evolution of the sized distribution of different particle sizes over time measured with the CMD for incense and nine sequential runs NSMA=1..9 in the CMD operation "Polydisperse Coagulation". dN is the particle size measured with the CPC plus the correction for the dilution and d_p is the mobility particle diameter in nm (This is a different view of Figure 38).

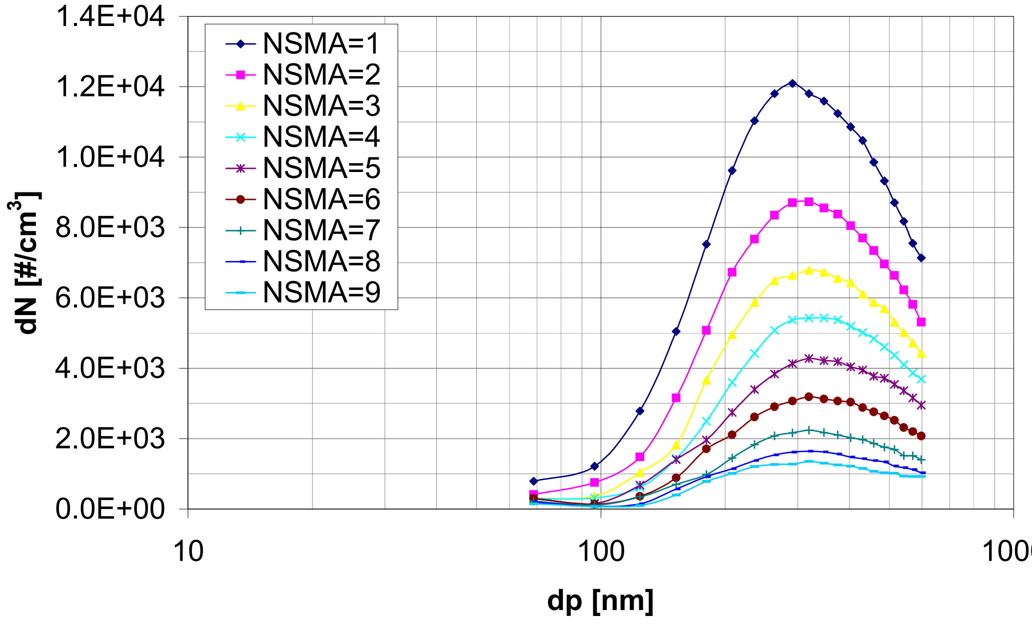

Figure 38 Sized distributions measured with the CMD for the incense measurements for nine sequential runs NSMA=1..9 in the CMD operation "Polydisperse Coagulation". dN is the particle size measured with the CPC plus the correction for the dilution and d_p is the mobility particle diameter in nm.

In Figure 39 the calculated total concentrations from the fit with the logarithmic normal distribution are given. The measured size distribution shows, on the left side, a good correspondence with the logarithmic normal distribution. On the right side, the slope of the measured distribution is less steep than that shown for the fitted distribution and the measured data are cut off[89] going to large diameters. For a more accurate determination of the sized distribution and relating parameters a different fit would have to be taken, whereas the logarithmic size distribution is a good first approximation.

The correction for the relative volume of the settler has also been done Figure 39. It shows that for long coagulation times t_{COAGUL} it has nearly no influence on the concentration. This is, in general, the case when $t_{COAGUL} >> t_{MEAS}$, where t_{MEAS} is the measurement time of a single run[90].

[89] The cutting off could have been avoided by choosing longer time intervals for size distribution measurements in the set up of the operation "Polydisperse Coagulation".

[90] NSMAi, i=1.. NSM, NSM is number of single measurement runs.

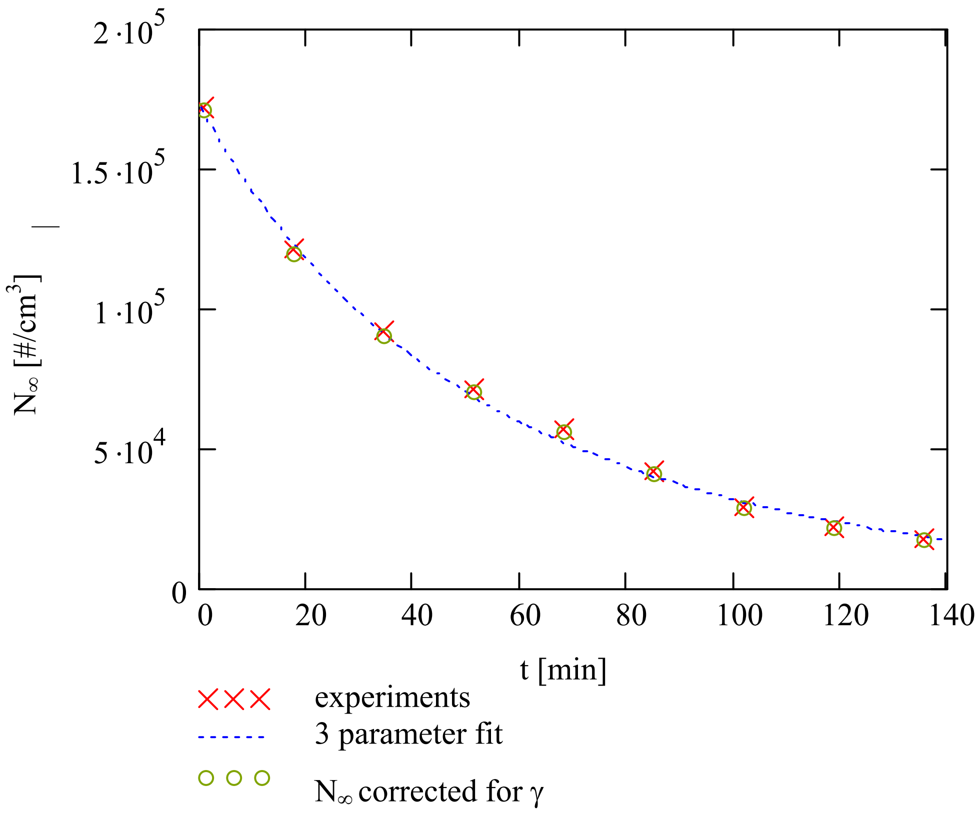

Figure 39 Particle concentration decay of the incense measurements. The experimental values (crosses) are corrected for the particle concentration according to the position of the settler (circles). A three parameter fit of equation (0-47) and N_∞, K and L is depicted with a dotted line.

In Figure 18, the parameters of the incense measurements are given for the resulting logarithmic normal distribution parameters. The resulting size distribution N_∞ is also shown in Figure 39 together with the correction for the position of the settler γ and the three parameter fit of equation (0-47).

Table 19 Parameters for the incense experiments and the 9 measurements NSMA=1..9; γ relates to the position of the settler (0=start position), t to the total time of the measurement relating to the median diameter of the relevant data sets for NSMA$_i$ (i=1..9). Parameters N_∞, d_{pg} and σ_g fitted for the logarithmic normal distribution. The values for the mean total particle concentration N_∞ over time are also depicted in Figure 39.

Symbol	*Unit*	*NSMA=1*	*NSMA=2*	*NSMA=3*	*NSMA=4*	*NSMA=5*	*NSMA=6*	*NSMA=7*	*NSMA=8*	*NSMA=9*
γ	~	4.3%	12.5%	20.7%	28.9%	37.1%	45.3%	53.6%	61.8%	70.0%
t	[min]	0.65	17.5	34.35	51.2	68.05	84.9	101.75	118.6	135.45
N_∞	[#/cm^3]	1.72E+05	1.21E+05	9.14E+04	7.12E+04	5.68E+04	4.20E+04	2.91E+04	2.19E+04	1.78E+04
$1/N_\infty$	[cm^3/#]	5.82E-06	8.26E-06	1.09E-05	1.40E-05	1.76E-05	2.38E-05	3.43E-05	4.57E-05	5.61E-05
d_{pg}	[nm]	277.3	286.4	295.8	300.6	299.3	297.4	293.4	292.7	292.3
σ_g	~	1.58	1.56	1.54	1.54	1.54	1.54	1.56	1.55	1.54

The fitted parameters together with the regression coefficient are given in Table 20.

Table 20 *Results for the parameters* N_0, K, L and Pearson's regression coefficient r^2, *of the incense measurement (experiment #107)*

N_0 [#/cm^3]	L [1/s]	K [cm^3/(#*s)]	r^2 [~]
1.719E+5	2.37E-4	3.404E-8	0.998

I.1.22 Measurement of the coagulation coefficient of polydisperse aersols by means of a number distribution measurement

For the measurement of the coagulation coefficient K of polydisperse aerosols by means of a particle number measurement with the CMD, the complex operations "Polydisperse Coagulation I" and "–II" were used (see section 0). The theory derived in section I.1.7 is then applied.

I.1.22.1 Polydisperse Coagulation I (Method 4)

The fast coagulation method serves as control for the coagulation measurement. By means of a least mean square analysis of equation (0-61) for three parameters, N_0, L_0 and K these parameters can be fitted to the experimental data. For the complex operation "Polydisperse coagulation I" the settler is emptied once for each measurement within the time $t_{total} \cong$ 68 [min]. The results for the raw measurement data are depicted in Figure 40.

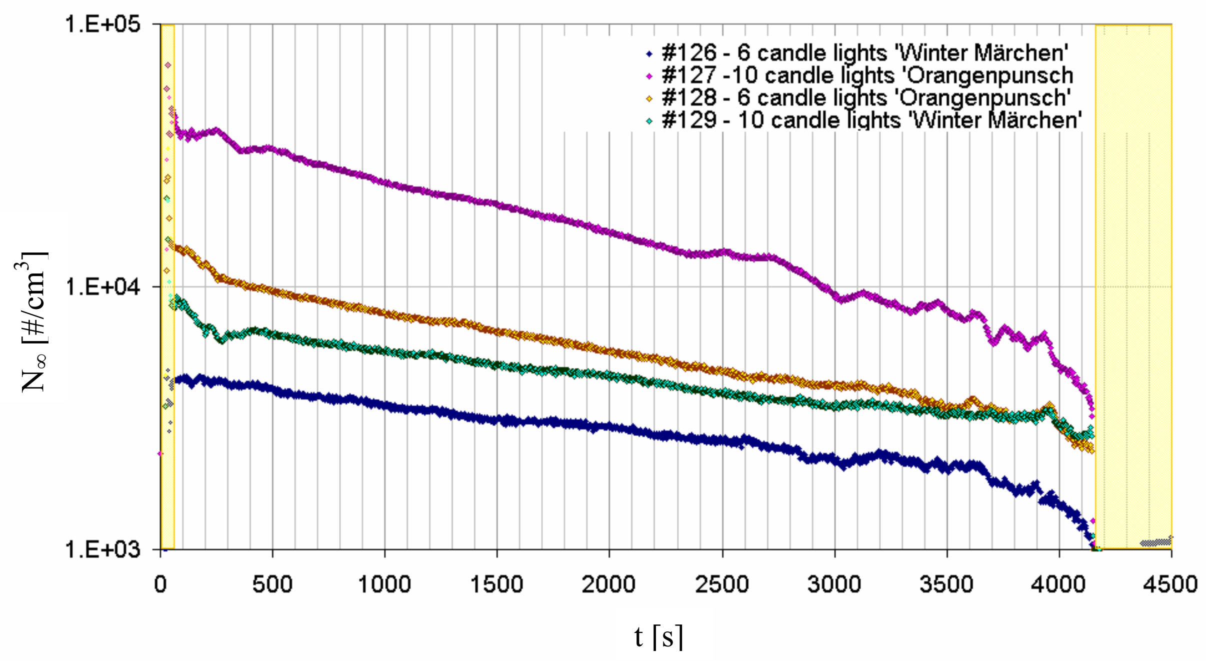

Figure 40 Raw data for experiments #126-#129: Test for operation "Polydisperse Coagulation I" for determination of the coagulation constant, for two different types of candle lights and two different concentrations; The candle light with the flavor "Orangenpunsch" produce higher particle concentrations N_∞ than the candle lights with the flavor "Winter Märchen".

For these measurements two different test aerosols with different concentrations were taken. The flavor "Orangenpunsch" (OP) and "Wintermärchen" (WM) were used with 10 and 6 candles respectively, resulting in higher particle concentrations approximately proportional to the number of candles. The yellow areas depict the delay due to the residence time $\tau_9+\tau_6$ the aerosol takes from the settler to the CPC measurement (compare section I.1.16.4 and I.1.17.1). As the volume flow was quite low, there was an inherent dilution due to the settler bypass filter. The total dilution ratio was approximately 10 according to the settler velocity (SPFA=26 compare Figure 11), the dilution ratio according to the measured flow V_{p4} only was 7.25, which is effectively the clean air dilution. The rest of the dilution is due to the leakage flow.

The results of the recalculated original concentration in the settler, together with the least mean squares fit, calculated in Mathcad® is depicted in Figure 41. The corresponding data values are shown in Table 22 and Table 21 for the AIMS and CMD measurement respectively. The coagulation coefficient K cannot be clearly assigned to the different types of aerosols although the regression coefficient is nearly 1 for every measurement, indicating the applicability of equation (0-61). In addition, the wall diffusion frequency L_0 is also underlying a change, due to the fitting procedure. For $\gamma \rightarrow 1$ the volume is also decreasing nonlinear. This effect was not further taken into account in equation (0-61) because it was assumed to be small. Although fluctuation in the volume might explain deviations seen in the measurements (Figure 40 and Figure 41).

Table 21 Results for the experiments #126-#129; On the left side, the results of the AIMS measurement for d_{pg}, σ_g and N_0 are given. They were repeated several times. On the right side, the results of the coagulation experiments for the coagulation coefficients K and the parameters L_0, N_0 and the regression coefficients r^2 are given. In the last row the ambient air measurements are given, which are a diluted mixture of both particle sources.

			AIMS			CMD							
Experiment	Flavor	Candles	Mean geometric diameter	Geometric standard deviation	Total concentration	Initial particle concentration	Wall diffusion frequency	Mean wall diffusion frequency		Coagulation coefficient	Mean coagulationa coefficient		Pearson's regression coefficient
#	type	#	d_{pg}	σ_g	N_0	N_0	L_0	L_{0m}		K	K_m		r^2
			nm	~	#/cm³	#/cm³	1/s	1/s		cm³/s	cm³/s		~
127	OP	10	85.1	1.73	4.98E+04	4.17E+04	9.39E-05			**1.37E-08**			0.995
128	OP	6	~	~	~	1.29E+04	2.10E-05	5.75E-05	**3.99E-05**	**4.854E-08**	3.11E-08	**3.98E-08**	0.990
129	WM	10	97.9	1.71	1.54E+04	7.62E+03	8.51E-06			**4.565E-08**			0.979
126	WM	6	~	~	~	4.50E+03	3.60E-05	2.23E-05		**5.13E-08**	4.85E-08		0.994
Ambient air			94.8	1.72	1.46E+04	~	~	~		~	~	~	~

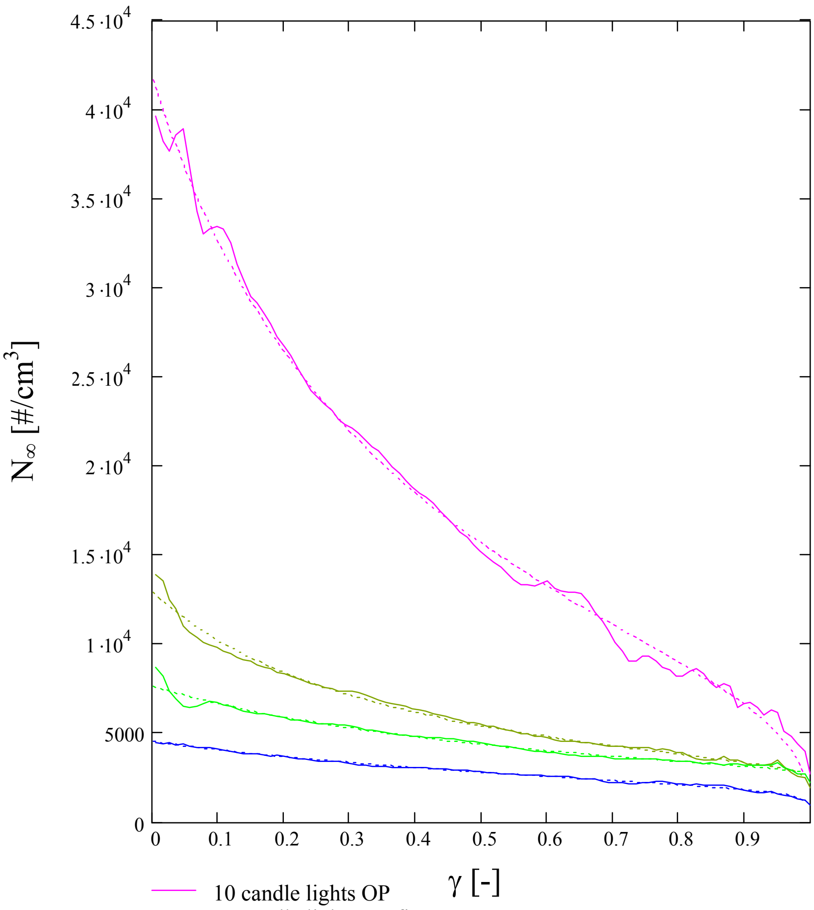

Figure 41 Fitted results for experiments #126-#129; Test for operation "Polydisperse Coagulation I" for determination of the coagulation constant, for two different types of candles and two different concentrations; The candles with the flavor "Orangenpunsch"(OP) produced higher particle concentrations N_∞ than the candles with the flavor "Winter Märchen"(WM). On the y-axis, the particle number concentration is depicted, on the x-axis, the dimensionless total time t_{total}. Straight lines depict the concentration corrected experimental data and dotted lines depict the experimental data fitted with equation (0-61).

Table 22 Base parameters for the experiment #126-#129 described in the text

Name	*Value*	*Unit*	*Description*
SPFA	26	~	Speed factor in the Labview software
V_{p7}	0.1	l/min	Settler flow
V_{p4}	0.138	l/min	Measured sample flow
$\tau_9+\tau_6$	61	s	Residence time settler→CPC, path 4
dilution	10	~	Dilution with respect to the raw data
t_{total}	4211	s	Time for emptying settler

I.1.22.2 Polydisperse Coagulation II (Method 3)

For determination of the coagulation coefficient K it is straight forward to apply the complex operation “Polydisperse Coagulation II” of section I.1.13.1.2 for the measurement together with the method derived in section 0 for evaluation.

Several experiments were performed in this sequence. The particle sources were again candles with different flavors and numbers (see Table 21). In Figure 42 the Smoluchowski plot of one typical experiment is depicted. The variable NSMA depicts the number of experimental runs, beginning with 0. After filling the probe into the settler, the valve VM2 is switched manually to the clean air filter RLF1. For the dilution process the number of rotations of DRV1 (variable ROTDRV1) was set to 2.25[91]. Then the probe was measured for 900 [s]. In the next step the settler was moved back into its starting position while diluting the aerosol. This process was repeated several times (compare Figure 21).

In Figure 42 the reciprocal particle concentration on the y-axis is drawn over the time along the x-axis. The different experimental runs NSMA are shown as parameters, where NSMA=0 is the first experiment. From the linear fit of the measurement values, the section with the y-axis gives the apparent coagulation coefficient.

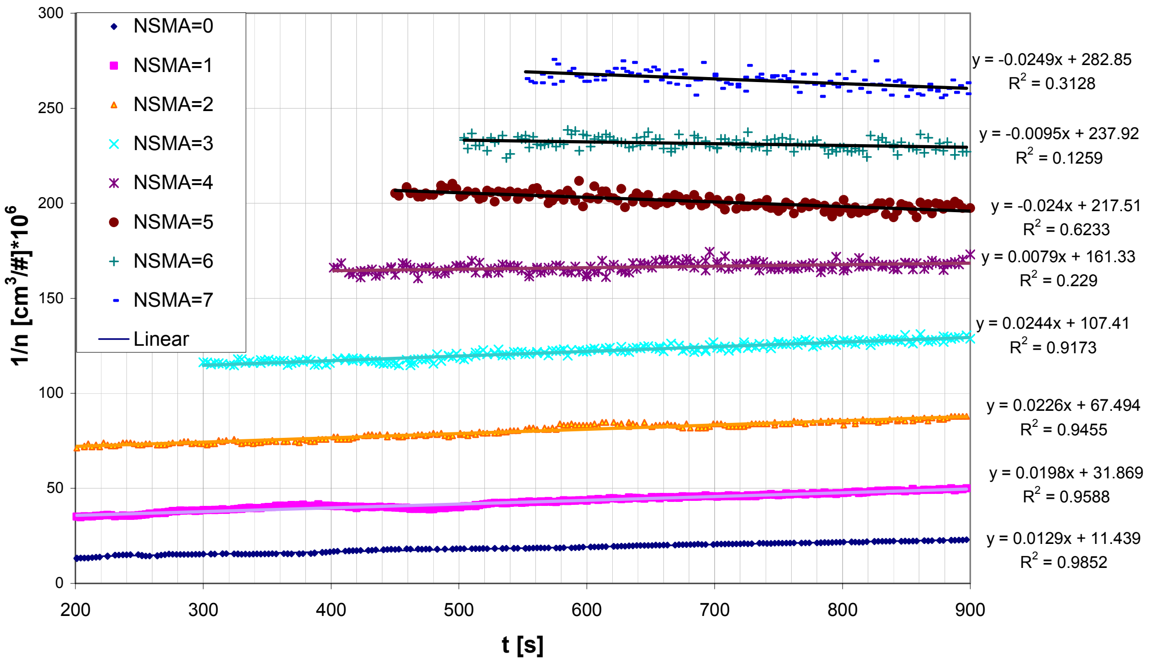

Figure 42 Smoluchowski plot of experiment #119; The particle source were – 4 candles with the flavor OP

[91] The setting of the manual needle valve DRV1 determines both the filling flow and the dilution flow of the settler. The lower the number of rotations the lower is the dilution.

A negative slope means that the particle concentration is increasing instead of decreasing, which can be explained by the fact that the dilution process fills the settler with particle free air. While measuring, particles on the wall are resuspended or injected from the ambient air leakage, increasing the measured particle concentration.

With increasing dilution the initial measured particle concentration is fluctuating while the regression coefficient is decreasing, this is the reason for cutting off the measurements at increasingly later time's Figure 42.

According to the theory of Rooker and Davies and the solution of (0-42) the apparent coagulation coefficient K_a can then be gained as slope of the yielded straight lines. E.g. the coagulation coefficient for the first measurement (NSMA=0) would then be $K_a=1.29*10^{-8}$ $[cm^3/(\#*s)]$. The equivalent value K_{ac}[92] of the CMD method derived in section I.1.7.5 tabulated for the same experiment #119 in Table 23 is $K_{ac}= 0.77*10^{-8}$ $[cm^3/(\#*s)]$. The second value is hence 40% lower indicating that the theory of Rooker and Davis is not fully applicable for the CMD.

In Figure 43 a typical measurement of the velocity is shown. The velocity is fairly constant, and most of the measurements values are even within ±0.5% m.v.(measurement value), although the measurement of the flow sensor is ±1% m.v. The constant flow measurement indicates that the concentration fluctuations are due to an inhomogenity of the aerosol rather then that of sample flow.

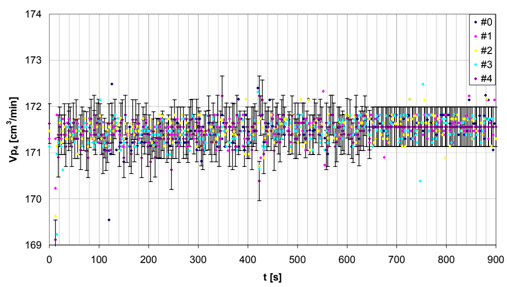

Figure 43 Volume flow Vp_4 for all measurements of experiment #121; The particle source were 4 candle lights with the flavor WM;

[92] Apparent coagulation coefficient for the constant concentration reactor.

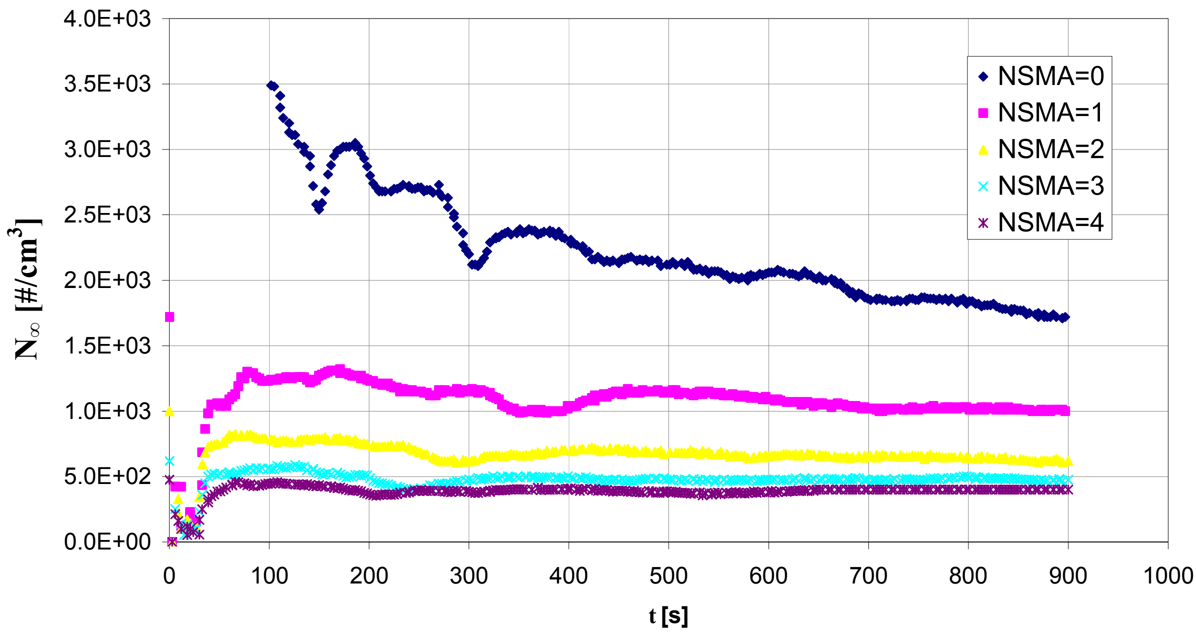

Figure 44 Number concentration N_∞ measured with the operation "Polydisperse Coagulation II" and experiment #121.The particle sources were 4 candles with the flavor WM; The residence time is not subtracted from the measurement time.

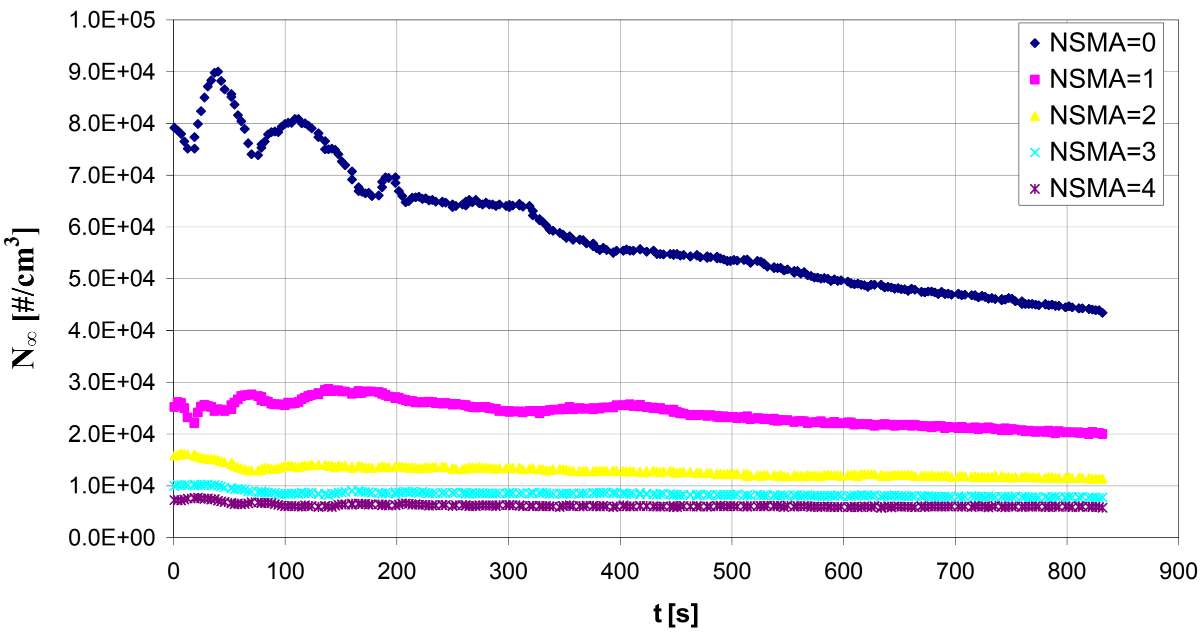

Figure 45 Number concentration N_∞ measured with the operation "Polydisperse Coagulation II" and experiment #119. The particle sources were 4 candles with the flavor OP; the residence time is already subtracted from the measurement time.

In Figure 44 and Figure 45 experiments #121 and #119 are depicted for the measured particle concentration and the operation “Polydisperse Coagulation II”. As the initial concentration N_0 was quite low, the consequent dilution leads to a drastic concentration decrease in such a manner that the concentration decrease after the third measurement was quite low. In addition the fluctuation in the beginning of the measurements indicates that the dilution process causes turbulences that dominate the beginning of the measurement. Therefore it is difficult to determine the initial slope of the concentration with this method, and hence the coagulation coefficient exactly.

The problem of the dilution would be solved best by a mass flow controller, instead of DRV1, with changing volume flow for each consequent concentration measurement. Turbulence of the flow concentration could be avoided by waiting a critical time, until the filled air volume has calmed down that has to be gained experimentally. Generally higher particle concentrations should give more accurate results, as the observed particle concentration reduction is higher.

The resulting apparent coagulation coefficients K_{ac} should give straight lines in Figure 46 with positive slope depicted for a series of measurements. Each set of points represents one measurement in operation “Polydisperse coagulation II”. The section with the y-axis gives the coagulation coefficient K the slope the particle wall diffusion frequency L_0.

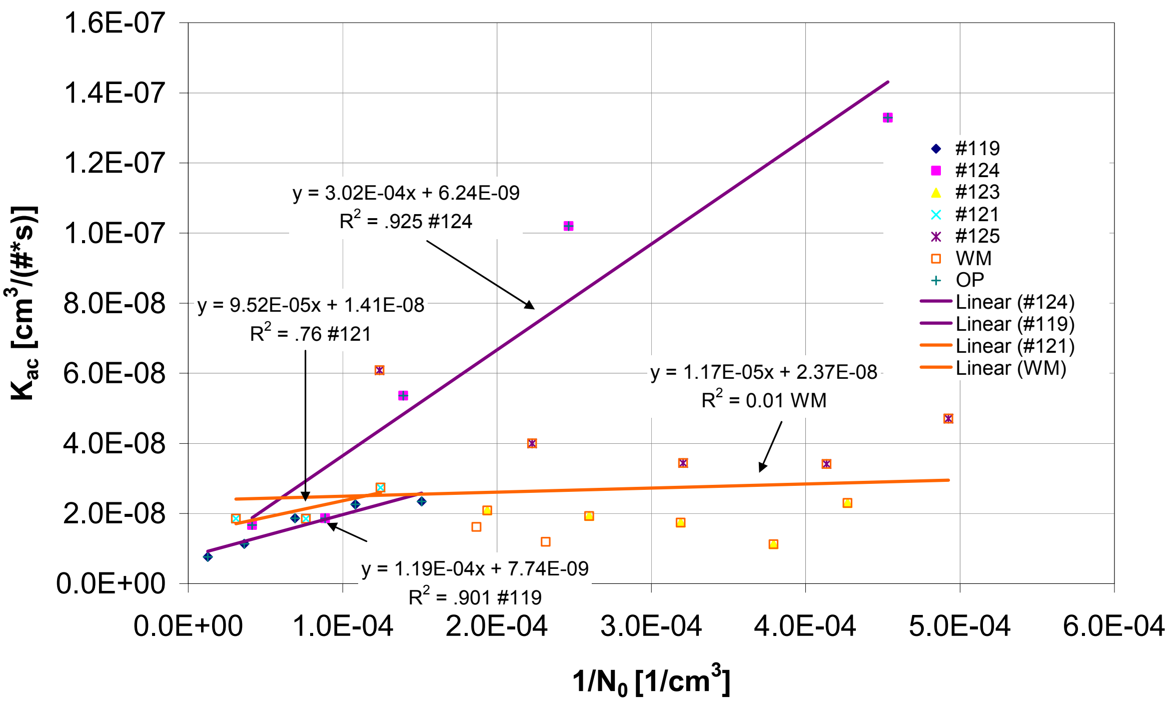

Figure 46 Summary of the measurements for the operation „Polydisperse Coagulation II“

The corresponding values to Figure 46 are shown in Table 23. The sign # denotes the number of the experiment, flavor and number of candles denotes the kind of particle source. The first r^2 denotes the *linear regression coefficient* of the concentration values according to the single step measurements NSMA=i (i=1…NSM) and the resulting $K_{ac.}$ Only concentrations starting at γ=0 and $N_\infty=N_0$ after the residence time have been regarded. The second *linear regression coefficient* r^2 denotes the correlation between K_{ac} and $1/N_0$ according to Figure 46, where the blue values have not been used for regression. L_0 is the wall diffusion frequency and K_m is the final mean coagulation coefficient as a function of particle source.

Table 23 Results of the coagulation coefficients calculation with the graphical method for polydisperse aerosols produced by 4 and 6 candle lights with the flavor OP and WM for the CMD operation "Polydisperse Coagulation II. Details are described in the text.

Experiment	Flavor	Candles	Initial particle concentration				Pearson's regression coefficient	Wall diffusion frequency	Coagulation coefficient	Pearson's regression coefficient	Mean coagulation coefficient
#	Type	#	N_0 #/cm³	Δt	K_{ac} cm³/(#*s)	$1/N_0$	r^2	L_0 1/s	K cm³/(#*s)	r^2 ~	K_m cm³/(#*s)
#119	OP	4	7.91E+04	1.65E+03	7.66E-09	1.26E-05	0.92	**1.61E-04**	**5.93E-09**	**0.98**	**6.91E-09**
			2.76E+04	3.19E+03	1.14E-08	3.63E-05	0.80				
			1.45E+04	3.70E+03	1.87E-08	6.91E-05	0.84				
			9.24E+03	4.79E+03	2.26E-08	1.08E-04	0.72				
			6.61E+03	6.44E+03	2.35E-08	1.51E-04	0.48				
#124	OP	6	2.42E+04	2.48E+03	1.67E-08	4.14E-05	0.93	**3.02E-04**	**7.89E-09**	**0.92**	
			1.13E+04	4.75E+03	1.87E-08	8.86E-05	0.66				
			7.18E+03	2.60E+03	5.36E-08	1.39E-04	0.89				
			4.06E+03	2.42E+03	1.02E-07	2.46E-04	0.97				
			2.21E+03	3.41E+03	1.33E-07	4.53E-04	0.77				
#123	WM	4	5.16E+03	9.27E+03	2.09E-08	1.94E-04	0.80	-8.73E-06	**2.11E-08**	0.03	
			3.85E+03	1.35E+04	1.93E-08	2.60E-04	0.51				
			3.13E+03	1.84E+04	1.74E-08	3.19E-04	0.21				
			2.64E+03	3.38E+04	1.12E-08	3.79E-04	0.09				
			2.34E+03	1.86E+04	2.30E-08	4.27E-04	0.28				
#121	WM	4	3.24E+04	1.67E+03	1.85E-08	3.09E-05	0.83	9.52E-05	**1.41E-08**	0.76	**1.41E-08**
			1.31E+04	4.13E+03	1.85E-08	7.63E-05	0.65				
			8.03E+03	4.55E+03	2.74E-08	1.25E-04	0.58				
			5.35E+03	1.16E+04	1.61E-08	1.87E-04	0.10				
			4.32E+03	1.94E+04	1.19E-08	2.32E-04	0.07				
#125	WM	6	8.07E+03	2.04E+03	6.09E-08	1.24E-04	0.67	-3.88E-05	**5.55E-08**	0.26	
			4.49E+03	5.57E+03	4.00E-08	2.23E-04	0.78				
			3.12E+03	9.32E+03	3.44E-08	3.21E-04	0.55				
			2.42E+03	1.21E+04	3.41E-08	4.13E-04	0.55				
			2.03E+03	1.05E+04	4.71E-08	4.93E-04	0.64				

For the particle source OP, a coagulation coefficient of K_m=6.91*10^{-9} [cm^3/(#*s)] results. For the particle source WM, the total particle concentration was generally lower, leading to a low correlation coefficient r^2. The resulting values for L_0 showed partly negative valued indicating erroneous results. One reason might have been resuspension of particles. The value of the best measurement gave the result of K_m=1.41*10^{-8} [cm^3/(#*s)].

Conclusions

Theory of coagulation and diffusion

A measurement system for measuring the coagulation coefficient has been built and compared with data from the literature and evaluated for different methods from an expanded particle theory of particle loss due to deposition and coagulation. By means of this theory, the characteristic quantities of the initial concentration N_∞, the diffusion frequency L and the particle coagulation coefficient K can be determined. In this work, for the first time, 4 methods are introduced beginning with the theory from Rooker and Davies (Rooker and Davies 1979) (1) for different time scales and different reactor types according to Table 24 and chapter 0. The second method (2) generalizes this theory and is applicable for detailed calculation and long time observation of the aerosol concentration. Method (3) is the analogous method for short times, taking into account that the reactor is of constant concentration type. The last method (4) is the generalized form applicable for the constant concentration reactor and for long time observation.

Table 24 Methods for determination of the coagulation coefficient K with the theory of loss by coagulation and deposition; CV denotes the constant volume and CC the constant concentration reactor;

Method	*Restrictions*	*Characteristic equation*	*Reactor type*
(1)	$t \rightarrow 0$	(0-46)	CV
(2)	t: 0..∞ (general method)	(0-47)	CV
(3)	$\gamma \rightarrow 0$	(0-64);(0-67)	CC
(4)	γ: 0..∞ (general method)	(0-61)	CC

A better applicability of method (2) & (4) then (1) & (3) is given for higher particle concentrations, due to higher accuracy and physical limitations (reactor size, settler velocity). In general higher particle concentrations or a larger settler volume enhance the evaluation of the coagulation coefficient K compared to the diffusion frequency L.

For the special case when the measurement time, t_{MEAS}, is large compared to the coagulation time, t_{COAGUL}, method (4) reduces to the method (2). In general, for $t_{MEAS} >> t_{COAGUL}$ and for large volumes, the constant concentration reactor can be approximated with the constant volume reactor.

Coagulation Measurement Device (CMD)

A coagulation coefficient measurement device (CMD) has been built on the basis of various data acquisition hardware and integrated with the LABVIEW Software as described in chapter 0. In Table 25, the advantages and the disadvantages of the built CMD are summarized.

In general, the advantage of a CMD for coagulation measurement is that it can be applied for different kinds of aerosols and different types of reactions as coagulation, diffusion deposition & nucleation when the thermodynamic state, p,V and T can be kept constant with regard to the particle concentration without aerosol reaction as e.g. coagulation[93]. Furthermore it is applicable to a variety of measurement sites and measurements can be performed quasi in situ avoiding transport and ageing effects of the sampled aerosol. An advantage of the constant concentration reactor over the tube reactor is the simplicity and flexibility of construction which allows for a smaller dimension with comparable functionality.

A general disadvantage of the CMD is the pollution due to deposition. For the built CMD, the settler has to be cleaned manually, which is time consuming. When cleaned the leakage flow has to be determined again empirically. This problem increases as the accuracy of coagulation measurement is higher for higher particle concentrations and hence higher pollution. Further general disadvantages are, that complex tasks difficult to oversee have to be done[94], even though a high grade of automation has been done (e.g. complex operations in section I.1.13.1) also there is a longer time requirement for the constant concentration reactor (CC) compared to the tube reactor (Heiden and Sturm 2005).

A main advantage of the built CMD application is that different reactor types are applicable (CC, variable constant volume reactor (CV)). Another advantage is that the measuring is done in the dispersed aerosol until the aerosols pass the CPC (condensation particle counter). This makes possible alternate measurement of the same aerosol with other measuring devices. With different settler materials, different wall deposition and the influence of radiation (e.g. transparent material) etc. can be measured. The volume of the settler can be varied by different settler dimensions (e.g. outer and inner diameter). A standard bellow also reduces costs, due to mass production. The applied bellow avoids particle deposition due to

---

[93] This is an advantage over the widely applied constant volume batch reactor in the case of a small volume compared to the sampled volume.

[94] E.g. setting of the manual needle valve DRV1; setting of the parameters of the software;

electrostatic charge by means of antistatic equipment, but it is not resistant to UV radiation. Further advantages are that there is an expandable software platform and expandable data acquisition hardware and that the reactor is, in total, a flexible, basic research reactor for the transition regime. Theory evaluation becomes interesting for expanding the CMD to temperature regulation and mixing for investigating turbulence–diffusion compared to convection-diffusion effects of coagulation.

Disadvantages of the built CMD are that is has a quite small volume, resulting in a high surface to volume ratio, hence, higher deposition, and also that the volume of the settler is difficult to measure exactly. The leakage flow is difficult to determine and can change due to maintenance operations like cleaning or replacing the settler bellow. It is difficult to trim because of the low net aerosol flow. As the settler flow is determined by the exact stepper motor control, a constant settler flow and a constant CPC flow allows for a simplified net dilution calculation of the particle aerosol concentration, thus compensating for the leakage flow. Further disadvantages of minor importance are that the applied flexible bending leads to possible variations in flow resistance, the valves are heated during operation, leakage of the bellow is difficult to perceive directly and that there is higher diffusion in the tubes for the CMD-system compared to the SMPS-system due to higher residence times and longer tube lengths.

Table 25 Advantages and disadvantages of the CMD with constant concentration reactor for the general and the special case relating to the build CMD

Type	*Advantage*	*Disadvantage*
General	* Different kinds of aerosol * Different types of reaction: Coagulation, diffusion, deposition & nucleation * Constant thermodynamic state compared to constant volume reactor * Any location, in situ * Smaller dimension, simpler and more flexible then tube reactor	* Pollution * Laborious, complex tasks * Low concentrations, low accuracy * Longer time requirement then tube reactor
Application	* Several reactor types applicable * Expandable for measurement devices * Other settler materials available * Other settler sizes * Standard bellow (antistatic) * One control platform * Flexible and research reactor * Temperature regulation * Mixing * Settler flow exact due to stepper motor	* Small volume * Higher diffusion due to high surface to volume ratio * Volume measurement * Leakage flow, valves, settler * Flexible bending * Higher diffusion to longer paths & residence times * Not resistant to UV radiation * Leakage detection * Cleaning * Valve heating

Coagulation coefficient

In Figure 47 the results for the coagulation coefficients measured and calculated in chapter 0 are summarized. The mean coagulation coefficient K for method 2 & 4 is $3.69*10^{-9}$ [cm^3/(#*s)], the mean coagulation coefficient K for method 1 & 3 is $6.89*10^{-9}$ [cm^3/(#*s)]. The mean value for L is $1.27*10^{-4}$ [1/s].

Method 2[95] & 4 yield approximately 5 times higher coagulation coefficients then method 1 & 3, calculated for the mean coagulation coefficients. The cause for the difference might be that the assumed time of linear approximation especially for higher concentrations is taken too short, that there is a difference due to different aerosol sources, that each aerosol mixture behaves stochastically different or some other reason.

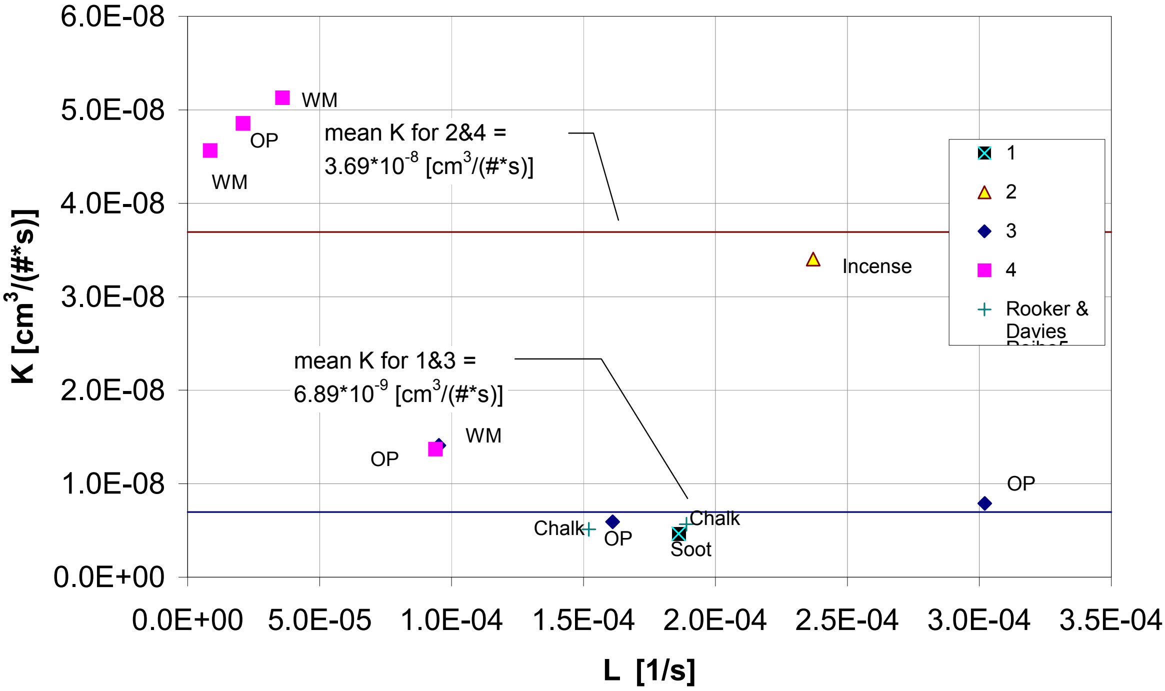

Figure 47 Coagulation coefficients K and wall diffusion frequencies L for the four different methods 1-4 of Table 24 as parameter; The mean coagulation coefficient for similar methods 1&3 and 2&4 are shown as straight lines. For the measurement point for method 1 L is unknown, hence, the mean value of the experiments of method 3 was taken. There were taken the following aerosol sources denoted at each point: soot, candles flavor WM & OP, incense and chalk for the experiments of Rooker and Davies (Rooker and Davies 1979).

Compared with the experiments of Rooker and Davies (Rooker and Davies 1979) there is a good accordance with the results gained with methods 1&3 for the mean values of K and L. The experiments of Rooker and Davies show, as the CMD experiments, a wide variation in K values ranging from $5.97*10^{-8}$ [cm^3/(#*s)] to $4.97*10^{-9}$ [cm^3/(#*s)] yielding a factor of approximately 6 from minimum to maximum, which is quite in the range of the measurements of this work performed with all different methods. The good accordance of the mean value of the wall diffusion frequency L for method 1 & 3 can be explained by comparable reactor dimensions of the settler and the experiments of Rooker and Davies[96], where the surface to volume ratios were 4 to 5 times lower then for the CMD experiments, were higher values of L are indicating a higher particle loss due to deposition. On the other hand, the Knudsen numbers were 0.32 for the CMD experiments and between 6 and 13 for Rooker and Davies. This indicates that there is a discrepancy between the theoretical[97] and the experimental coagulation coefficient for the Knudsen number in the transition regime.

Outlook

There are still a number of open questions for the CMD. Future research of the coagulation coefficient measurement with the CMD will have to examine following questions:

- What is the extent of dilution due to leakage, and does it have significant influence? Is there a need to expand the theory of loss and coagulation for leakage? How can leakage be avoided and or be detected and corrected systematically and automated?
- What effects have long duration experiments on the accuracy with regard to pollution and maintenance?
- What are the coagulation coefficients K of aerosols of different sources?
- Is there a significant dependency of the deposition frequency as a function of operation mode and sample flow rates?
- What are the causes for the measured fluctuating coagulation coefficient K and can a clear distinction between aerosol sources and K be made?
- What influence have different wall materials and/or sizes of the settler and can there be done a model investigation of wall deposition in closed rooms as e.g. in tunnels?
- What is the dependency of particle structure and can integral structure properties like the fractal dimension D_f be measured in accordance with detailed structure measurements e.g. with scanning electron microscopy (SEM)?
- What is the experimental relation between monodisperse and polydisperse coagulation?

---

[95] Numbers of method are according to Table 24.

[96] Balloon sizes of diameter 19 and 24 cm.

[97] Equation (0-27).

Literature

1. **Bakk, E. S. (2005). "Prüfroutinen für den einwandfreien Normalbetrieb der Koagulationsmessung mit dem Aerosol Koagulationsmessgerät." Diploma Thesis: *Prüfroutinen für den einwandfreien Normalbetrieb der Koagulationsmessung mit dem Aerosol Koagulationsmessgerät*, Institut für Thermodynamik und Verbrennungskraftmaschinen, Technische Universität Graz.**

2. **Brugger, B. (2005). "Fail-Safe Analysis of the Coagulation Measurement Device (CMD)." Diploma Thesis: *Fail-Safe Analysis of the Coagulation Measurement Device (CMD)*, Institut für Thermodynamik und Verbrennungskraftmaschinen, Technische Universität Graz.**

3. **Dymond, J. and Smith, E. B. (1980). The Virial Coefficients of Pure Gases and Mixtures, Oxford University Press, New York.**

4. **Friedlander, S. K. (2000). Smoke, Dust, and Haze, Oxford University Press, New York.**

5. **Fuchs, N. A. (1989). The Mechanics of Aerosols, Dover Publications, Inc., New York.**

6. **Heiden, B. and Sturm, P. J. (2005). "Development of a Coagulation Coefficient Measurement Device (CMD)." Conference: "Sustainability for Humanity & Environment in the extended connection field science - economy - policy", Timisoara, Romania, Vol. 1, 75-78.**

7. **Hinds, W. C. (1999). Aerosol Technology: properties, behavior, and measurement of airborne particles, John Wiley & Sons, Inc., New York.**

8. **Husar, R. B. (1971). "Coagulation of Knudsen Aerosols." Ph.D. thesis, Department of Mechanical Engineering, University of Minnesota.**

9. **Ivanišin, M., Bischof, O. F., Zerrath, A., Krinke, T., and Heiden, B. (2005). "Abgaspartikelmessmethoden und Auswirkung der Abgasnachbehandlung auf die Partikelanzahlemissionen." CTI Fachkonferenz Diesel-Partikel-Filter, Stuttgart.**

10. **Jamal, R. and Hagestedt, A. (2001). Labview Das Grundlagenbuch, Addison-Wesley, München.**

11. **Jullien, R. and Botet, R. (1987). Aggregation and Fractal Aggregates, World Scientific Publishing Co, Singapore.**

12. **Kostoglou, M. and Konstandopoulos, A. G. (2001). "Evolution of aggregate size and fractal dimension during Brownian coagulation." Aerosol Science, 32, 1399-1420.**

13. **Mandelbrot, B. B. (1987). Die fraktale Geometrie der Natur, Birkhäuser Verlag, Basel.**

14. **Moser, A. (1988). Bioprocess Technology - Kinetics and Reactors, Springer, New York.**

15. **National Instruments (2003). Labview Bascis I - Kurssoftware Version 7.0, National Instruments, Salzburg-Bergheim, Austria.**

16. **National Instruments (2004). Labview Bascis II - Development Course Software Manual Version 7.0, National Instruments, Austin, Texas.**

17. **Oertel, H. (2001). Prandtl-Führer durch die Strömungslehre, Friedrich Vieweg & Sohn Verlagsgesellschaft mbH, Wiesbaden.**

18. **Pflügl, M. and Rentz, A. (2000). Stoffaustausch (Skriptum), Institut für Grundlagen der Verfahrenstechnik und Anlagentechnik, Technische Universität Graz, Graz.**

19. **Rooker, S. J. and Davies, C. N. (1979). "Measurement of the coagulation rate of a high Knudsen number aerosol with allowance for wall losses." Journal of Aerosol Science, 10, 139-150.**

20. **Rudyak, V. Y. and Krasnolutskii, S. L. (2001). "Kinetic description of nanoparticle diffusion in rarefied gas." Doklady Physics, 46(12), 897-899.**

21. **Rudyak, V. Y. and Krasnolutskii, S. L. (2002). "Diffusion of nanoparticles in a rarefied gas." Technical Physics, 47(7), 807-813.**

22. **Schnell, M., Cheung, C. S., and Leung, C. W. (2004). "Coagulation of diesel particles in an enclosed chamber." Journal of Aerosol Science, 35(10), 1289-1293.**

23. **Smoluchowski, M. (1917). "Versuch einer mathematischen Theorie der Koagulationskinetik kolloidaler Lösungen." Zeitschrift für physikalische Chemie, 92, 129-168.**

24. **Soldov, A. and Ochkov, V. (2005). Differential Models - An introduction with Mathcad, Springer Verlag, Berlin.**

25. **Zahoransky, R., Feld, H.-J., Dittmann, R., Samenfink, W., and Laile, E. (2000). "Das optische Dispersionsquotienten-Verfahren für die on-line/in-situ Partikelanalyse." Beitrag in der Festschrift: Prof. Dr. Ing. Dr. h.c. Sigmar Wittig Rektor der Universität Karlsruhe zum 60. Geburtstag, Wizard Zahoransky KG, erschienen am Institut für Thermische Strömungsmaschinen Universität Karlsruhe (T.H.).**

FIGURES

Figure 1 Corrected settling factor c_{sf} for fractal particles as a function of the settling velocity c_s for spherical particles. Decreasing fractal dimension D_f and decreasing particle size d_p leads to a decreasing settling velocity. The value D_f=1.78 is the value for Brownian coagulation in the three dimensional space often applied for soot particles (Jullien and Botet 1987) p.88. 27

Figure 2 Solution of the Smoluchowski equation for different initial concentration and a constant coagulation coefficient K=54*10 [cm^3/s]. 30

Figure 3 Solution of the Smoluchowski equation for a different concentration decrease α and the corresponding actual as the initial particle concentration N and N_0; Different coagulation times t are used as a parameter. The coagulation coefficient is constant K= 54*10^{-10} [cm^3/s]. 31

Figure 4 Principal surface, volume and particle concentration relation of the settler 33

Figure 5 Solution of the logistic equation for the constant concentration reactor for different initial concentrations N_0 and a constant emptying time t_{total} =75 [min] and the constants L_0=1.89*10^{-4} [1/s] and =56.7*10^{-10}[cm^3/s] according to equation (0-61) 39

Figure 6 Graphical method to determine the apparent coagulation coefficient K_{ac} according to equation (0-67). The method is described in the text. 41

Figure 7 Basic Setup of the CMD 46

Figure 8 Flow chart of the standard SMPS system 47

Figure 9 Flow chart of the CMD system 48

Figure 10 Settler in the end switch positions 51

Figure 11 Flow rates Vp_4 of the flow sensor ASF 1430 for different times of emptying and filling the settler; The parameter SPFA denotes the speed factor of the stepper motor in the LABVIEW software. It is proportional to the stepper motor steps per time unit. 52

Figure 12 Settler flow rates as a function of the total time for pressing out the complete settler volume; Vp_4 is according to the measurement in Figure

11; The measured flow together with the calculated leakage flow Vp_7 (see text) is shown with the blue dotted line and shows a good accordance with the volume flow Q calculated from the settler geometry according to equation (0-4). 53
Figure 13 Calculation of the total effective settler volume according to the measurement in Figure 11 and equation (0-5). 54
Figure 14 Scheme of the settler flow Vp_7 the leakage flow Vp_L and the measured flow Vp_4 for the mass balance 55
Figure 15 Pressure difference measurements for the sensor ASP 1400 for different times of emptying and filling the settler. 57
Figure 16 Volume flow Vp_4 at T_4=20°C as a function of different settler temperatures T_7 and the total measurement time t_{total}. The ambient temperature T_2 is also 20°C........ 61
Figure 17 δ in % at T_4=20°C as a function of different settler temperatures T_7 and the total measurement time t_{total} . The ambient temperature T_2 is also 20°C. 61
Figure 18 Labview implementation of the paths of the CMD........ 64
Figure 19 Labview implementation of the operations of the CMD 65
Figure 20 The complex operations “Monodisperse Coagulation” and “Polydisperse Coagulation” 66
Figure 21 Complex operations Polydisperse Coagulation I and II........ 67
Figure 22 Decision chart for the simple operations of the CMD denoted with bold letters. 68
Figure 23 Main application window of the CMD-Program: „CMDC_Menu.vi“ 71
Figure 24 Application window of the CMD-Program: „CMDC_Initialization.vi“........ 72
Figure 25 Application window of the CMD-Program:”CMDC_Measurement.vi”; this is the central window controlling all measurements........ 75
Figure 26 Minimum filling time for the settler τ_8. The total settler volume was assumed with V_{70}=7.05 [l], the volume for the settler and the gas path before was V_8=7.11[l].On the right side the number of rotations, counted from the closed valve, of the needle valve DRV1 is related to the filling flow and hence to the minimum filling time τ_8 (see text for more details)........ 82
Figure 27 Total measurement time possible when emptying the settler as a function of the sample flow Vp_4 and the number of the measurements (NSM) on the

right y-axis; The total measurement time as a function of Vp_4 can be read on the left y-axis (calculation see equation (0-20)). 83

Figure 28 Residence time τ_3 for the SMPS DMA as a function of the sample flow Vp_1 and the sheath flow Vp_2. As a recommendation from TSI the ratio of sheath flow to sample flow should be at least ten. The residence time for this ratio is shown with the thick blue line. 85

Figure 29 Residence time for the CPC3010 and the standard SMPS tubing as a function of the sample flow V_{p1} (description see text). 86

Figure 30 Residence times for the standard SMPS system $\tau_0+\tau_6$ and the CMD system $\tau_4+\tau_6$ or $\tau_9+\tau_6$ as a function of the sample flow Vp_1 or Vp_4 87

Figure 31 Monodisperse CMD measurement of the CAST setting d_{pg}=160 [nm]; τ_I is the residence time before the aerosol flow enters the measurement site of the SMPS Classifier (experiment #65). 93

Figure 32 Monodisperse CMD measurement of the CAST setting d_{pg}=160 [nm] 94

Figure 33 Total particle concentrations N_∞ of run #65 95

Figure 34 Control measurement of the CAST measurement with the standard SMPS system for experiment #65 95

Figure 35 CMD measurement one day after the soot measurements of experiment #65 with the same aerosol enclosed (experiment #67); the numbers #x refer to the usual different first measurement and #8-9 to the single measurement run of the monodisperse measurements (see Table 16); Dilution with ambient air had occurred 96

Figure 36 Smoluchowski coagulation plot for monodisperse soot measurements with the CAST; $K_a=4.649*10^{-9}$ [cm^3/(#*s)] (experiment #65). 97

Figure 37 Evolution of the sized distribution of different particle sizes over time measured with the CMD for incense and nine sequential runs NSMA=1..9 in the CMD operation "Polydisperse Coagulation". dN is the particle size measured with the CPC plus the correction for the dilution and d_p is the mobility particle diameter in nm (This is a different view of Figure 38)................. 98

Figure 38 Sized distributions measured with the CMD for the incense measurements for nine sequential runs NSMA=1..9 in the CMD operation "Polydisperse Coagulation". dN is the particle size measured with the CPC plus the correction for the dilution and d_p is the mobility particle diameter in nm. 99

Figure 39 Particle concentration decay of the incense measurements. The experimental values (crosses) are corrected for the particle concentration according to the position of the settler (circles). A three parameter fit of equation (0-47) and N_∞, K and L is depicted with a dotted line. 100
Figure 40 Raw data for experiments #126-#129: Test for operation “Polydisperse Coagulation I” for determination of the coagulation constant, for two different types of candle lights and two different concentrations; The candle light with the flavor ”Orangenpunsch” produce higher particle concentrations N_∞ than the candle lights with the flavor “Winter Märchen”. 102
Figure 41 Fitted results for experiments #126-#129; Test for operation “Polydisperse Coagulation I” for determination of the coagulation constant, for two different types of candles and two different concentrations; The candles with the flavor ”Orangenpunsch”(OP) produced higher particle concentrations N_∞ than the candles with the flavor “Winter Märchen”(WM). On the y-axis, the particle number concentration is depicted, on the x-axis, the dimensionless total time t_{total}. Straight lines depict the concentration corrected experimental data and dotted lines depict the experimental data fitted with equation (0-61). 104
Figure 42 Smoluchowski plot of experiment #119; The particle source were – 4 candles with the flavor OP 105
Figure 43 Volume flow Vp_4 for all measurements of experiment #121; The particle source were 4 candle lights with the flavor WM; 106
Figure 44 Number concentration N_∞ measured with the operation “Polydisperse Coagulation II” and experiment #121.The particle sources were 4 candles with the flavor WM; The residence time is not subtracted from the measurement time. 107
Figure 45 Number concentration N_∞ measured with the operation “Polydisperse Coagulation II” and experiment #119. The particle sources were 4 candles with the flavor OP; the residence time is already subtracted from the measurement time. 107
Figure 46 Summary of the measurements for the operation „Polydisperse Coagulation II“.. 108

Figure 47 Coagulation coefficients K and wall diffusion frequencies L for the four different methods 1-4 of Table 24 as parameter; The mean coagulation coefficient for similar methods 1&3 and 2&4 are shown as straight lines. For the measurement point for method 1 L is unknown, hence, the mean value of the experiments of method 3 was taken. There were taken the following aerosol sources denoted at each point: soot, candles flavor WM & OP, incense and chalk for the experiments of Rooker and Davies (Rooker and Davies 1979). 114
Figure 48 CMD flow chart with possible valve positions 135
Figure 49 Total measurement time possible when emptying the settler as a function of the sample flow Vp_4 and the number of the measurements (NSM) on the right y-axis; The total measurement time as a function of Vp_4 can be read on the left y-axis (this Figure is similar to Figure 27 but also lower sample flow rates can be seen) 136
Figure 50 Detailed front panel of the main measurement program: CMDC_Menu.vi 141
Figure 51 Program Hierarchy CMDC_Menu.vi branch CMDC_Measurement.vi 141
Figure 52 Program Hierarchy CMDC_Menu.vi branch CMDC_Initialization.vi........ 142
Figure 53 Program hierarchy for SMPS_SCAN_CPCCXX.vi and SM_RUNC.vi; Both programs are implicitly sub vi's of CMDC_Measurement.vi and therefore not shown in Figure 51. 142
Figure 54 Standard application "SM4xDRV.EXE" from Hasotec for the stepper motor control. Has to be started and closed before running the LABVIEW program to load the driver for the Hasotec driver card into PC-memory. 145

TABLES

Table 1 Methods of the determination of the coagulation coefficient K; CV denotes the constant volume and CC the constant concentration reactor; 34
Table 2 Main settler parameters 50
Table 3 t_{total}=time for one run of the effective flow rate experiments; α=leakage ratio; Vp_4=sample flow rate; Vp_7=settler flow rate; dp_3=differential pressure settler; T_7=temperature settler, mean T_{7m}=298.3 [K]; mean p_{2m}=.9819 [bar]; $\rho_4=\rho_7$=1.147 [kg/m^3] orange values are extrapolated;.................. 56
Table 4 Parameters of equation (0-14) to determine the settler flow Vp_7 and the sample flow Vp_4 from pressure difference $dp_3=\Delta p$ of Figure 15. 58
Table 5 Vp_4 at T_4=20°C as a function of the settler temperature T_7 and the total measurement time t_{total} and Vp_7=const according to Table 3 62
Table 6 δ in % at T_4=20°C as a function of T_7 and the total measurement time t_{total};Vp_7 is const according to Table 3.. 62
Table 7 CMD paths: green=filling or cleaning; orange=settler measuring; blue=like standard SMPS measuring 63
Table 8 Operations of the CMD 65
Table 9 Classification of important ideal physical states relevant for the CMD 78
Table 10 Residence times for the standard SMPS system 79
Table 11 Residence times for the CMD system and the starting and endpoints for the related paths. These are part of different main paths listed in Table 7. 80
Table 12 Parameters of the SMPS DMA relevant for the residence time calculation (see text) 83
Table 13 Data according to Figure 29 87
Table 14 Monomodal size distribution measured with the standard SMPS system and setting the CAST diameter to d_p=85 [nm]. 92
Table 15 Residence times for the CAST experiments #65 & #67; τ_I is the time d_p is shifted to concentration because of residence time between DMA and CPC;$\tau_{I\ I}$ is the time the raw data are shifted to the beginning of

measurement mode; V_{p2} is the sheath, V_{p2} is the sample flow and NSMA is the number of each single size distribution measurement....................................... 93

Table 16 Particle concentrations of run #65& #67 94

Table 17 Results for the parameters of the initial concentration N_0, the apparent coagulation coefficient K_a which is approximately the same as the coagulation coefficient K and Pearson's regression coefficient r^2 of the monodisperse soot measurement (experiment #65); L was not determined because only one data set for K_a existed 96

Table 18 Parameters important for CMD operation „Polydisperse Coagulation“ and the incense measurements in this mode. 97

Table 19 Parameters for the incense experiments and the 9 measurements NSMA=1..9; γ relates to the position of the settler (0=start position), t to the total time of the measurement relating to the median diameter of the relevant data sets for $NSMA_i$ (i=1..9). Parameters N_∞ , d_{pg} and σ_g fitted for the logarithmic normal distribution. The values for the mean total particle concentration N_∞ over time are also depicted in Figure 39................................... 100

Table 20 Results for the parameters N_0, K, L and Pearson's regression coefficient r^2, of the incense measurement (experiment #107).. 101

Table 21 Results for the experiments #126-#129; On the left side, the results of the AIMS measurement for d_{pg}, σ_g and N_0 are given. They were repeated several times. On the right side, the results of the coagulation experiments for the coagulation coefficients K and the parameters $L_{0,}$, N_0 and the regression coefficients r^2 are given. In the last row the ambient air measurements are given, which are a diluted mixture of both particle sources. 103

Table 22 Base parameters for the experiment #126-#129 described in the text 104

Table 23 Results of the coagulation coefficients calculation with the graphical method for polydisperse aerosols produced by 4 and 6 candle lights with the flavor OP and WM for the CMD operation “Polydisperse Coagulation II. Details are described in the text.. 109

Table 24 Methods for determination of the coagulation coefficient K with the theory of loss by coagulation and deposition; CV denotes the constant volume and CC the constant concentration reactor; 111

Table 25 Advantages and disadvantages of the CMD with constant concentration reactor for the general and the special case relating to the build CMD 113
Table 26 Length and volume of the connecting tubes in the CMD 133
Table 27 Detailed residence time paths.. 134
Table 28 Hierarchy of the Main vi's and Sub vi's together with the icons of the Labview 7.1 software for the CMD according to Figure 51-Figure 53 143
Table 29 All software variables in the Labview 7.1 implementation for the CMD of the vi's shown in the hierarchy in Figure 51-Figure 53. 146
Table 30 Device and corresponding programs, icons in Labview the variable names and their unit of all vi's used for the CMD 152

INDEX

AIMS 15, 18, 79, 80, 86, 95
apparent coagulation coefficient 16, 34, 35, 36, 40, 96
apparent particle concentration 59
bubble flow meter 16, 49, 56, 80
CAST 91, 92, 94, 95
CMD system 47, 80
coagulation coefficient 21, 25, 29, 30, 31, 32, 33, 34, 36, 40, 43, 67, 71
coagulation kernel 21, 26, 29
collision diameter 29
collision frequency function 26
complex operation 63, 65, 66, 67, 68, 73
concentration decrease 31
conctraction number 57
constant concentration reactor 36, 39, 45, 49, 77, 78, 112
Cunningham correction factor 28, 29
differential pressure correction factor 57
fed batch reactor 79
film theory 32
flow sensor 49, 51, 52, 54, 60, 72, 76, 78
flowrate correction factor 60
fractal aggregates 23
fractal dimension 23, 24, 26
general dynamics equation 25, 32
growth 21, 25, 26, 33, 42, 78
Knudsen number 28
laws of growth 21
leakage flow 53, 54
leakage ratio 19, 54
lognormal size distribution 22, 24, 25, 96, 137
mean free path 28, 29, 41
operation concept 64, 70
particle transfer coefficient 33, 37
particle wall diffusion frequency 16, 33, 37
path concept 63
primary particle 23, 41, 43
residence time 21, 45, 64, 68, 78, 79, 80, 85
sample flow 49, 53, 54, 55, 56, 57, 77, 82, 85, 87
sample to sheath flow volume ratio 83
settler 13, 50
settler flow 52
settler system 45, 49
settling velocity 15, 26
simple operation 67
standard SMPS system 18, 45, 46, 47, 64, 68, 79, 95
standard state 59
Stokes law 26
surface to volume ratio 28, 50
total particle concentration 24, 25
total time 52, 53, 54, 56, 76, 82
total time ratio 19, 36

two film theory 32
valve system 49
volume to surface ratio 13, 50

Appendix A

Detailed specifications

Tubes

Table 26 Length and volume of the connecting tubes in the CMD

Type	*Source*	*Destination*	d_i *[mm]*	d_a *[mm]*	*L [cm]*	*V [l]*	*Name*
CMD	SMPS mono out	V3R	6	9	79	0.0223	
CMD	V4A	V3A	6	9	15	0.0042	
CMD	V6A	Pump intake	6	9	36	0.0102	
CMD	V2R	SMPS in	9	11	57	0.0363	
CMD	V2P	V3P	6	9	24.5	0.0069	
CMD	V1P	V5R	6	9	54	0.0153	
CMD	V6R	CPC out	6	9	76	0.0215	
CMD	V4P	V5P	6	9	25	0.0071	
CMD	V4R	VM1	6	9	22	0.0062	
CMD	V7A	Settler bottom	6	9	20	0.0057	
CMD	V5A	V7P	6	9	100	0.0283	
CMD	V1R	VM2	6	9	47	0.0133	
CMD	VM2	Ambient air/ probe in	6	9	0	0.0000	
CMD	V1A	ASF	6	9	16	0.0045	
CMD	ASF	V2A	6	9	12	0.0034	
CMD	ASF	ASF	6	~	8	0.0023	
CMD	VM1	RSV	6	9	77	0.0218	
CMD	RSV	RSV	6	~	7	0.0020	
CMD	RSV	CPC tube	6	9	0	0.0000	
CMD	CPC tube	CPC in	6	9	0	0.0000	
CMD	V8P	Settler top	6	9	26	0.0074	
CMD	V8A	DRV1	6	9	56	0.0158	
CMD	DRV1	V6P	6	9	132	0.0373	
CMD/SMPS	SMPS in	SMPS poly out	6	~	47	0.0133	
CMD/SMPS	SMPS poly out	DMA in	6	~	36	0.0102	
CMD/SMPS	DMA out	SMPS mono out	6	~	3	0.0008	
SMPS	SMPS mono out	CPC tube	6	~	23.5	0.0066	
CMD	Ambient air	Settler top	~	~	~	7.1113	V_8
CMD/SMPS	DMA in	DMA out	~	~	44.4	0.4136	V_3
CMD	Settler top	Settler bottom	144	204	46	7.049	V_{70}
CMD/SMPS	SMPS in	DMA in	6	~	83.0	0.0235	V_2
CMD/SMPS	CPC in	CPC	~	~	~	0.0247	V_6
CMD	Settler bottom	SMPS in	~	~	267	0.0956	V_1
CMD	DMA out	CPC in	~	~	193	0.0554	V_4

Type	*Source*	*Destination*	d_i *[mm]*	d_a *[mm]*	*L [cm]*	*V [l]*	*Name*
SMPS	DMA out	CPC in	~	~	26.5	0.0075	V_0
CMD	Settler	CPC in	~	~	460	0.1745	V_5
CMD	Settler	CPC in	~	~	~	0.1005	V_9
CMD	Probe in/ambient air	SMPS in	~	~	~	0.0597	V_{10}
CMD	DMA out	Settler bottom	~	~	~	0.0684	V_{11}
CMD	Probe in/ambient air	CPC in	~	~	~	0.0646	V_{12}

Detailed residence times

Table 27 Detailed residence time paths

Residence time	*Path*	*Detail*
τ_0	DMA out→CPC in	DMA out→SMPS poly out →CPC tube→CPC in
τ_1	Settler bottom→ SMPS in	Settler bottom→V7A→V7P→V5A→V5R→V1P →V1A→ASF→V2A→V2R→SMPS in
τ_2	SMPS in→ DMA in	SMPS in →SMPS poly out→DMA in
τ_3	DMA in → DMA out	DMA in → DMA out
τ_4	DMA out→CPC in	DMA out→SMPS mono out→V3R→V3A →V4A→V4R→VM1→RSV→CPC tube→CPC in
$\tau_5 = \tau_1 + \tau_2 + \tau_4$	Settler bottom→ DMA in & DMA out→CPC in	Settler bottom→V7A→V7P→V5A→V5R→V1P →V1A→ASF→V2A→V2R→SMPS in →SMPS poly out→DMA in & DMA out→SMPS mono out→V3R→V3A→V4A →V4R→VM1→RSV→CPC tube→CPC in
τ_6	CPC in → CPC	CPC in → CPC
τ_7	Settler top→ Settler bottom	Settler top→ Settler bottom
$\tau_8 \approx t_{FILL}$	Ambient air/probe in →Settler top	Ambient air/probe in(→RLF1)→VM2→V1R→V1P→V5R →V5A→V7P→V7A→Settler bottom→Settler top
τ_9	Settler bottom→CPC in	Settler bottom→V7A→V7P→V5A→V5R→V1P →V1A→ASF→V2A→V2P→V3P→V3A→V4A →V4R→VM1→RSV→CPC tube→CPC in
τ_{10}	Ambient air/probe in →SMPS in	Ambient air/probe in(→RLF1)→VM2→V1R →V1A→ASF→V2A→V2R→SMPS in
τ_{11}	DMA out→settler bottom	DMA out→V3R→V3A→V4A→V4P→V5P →V5A→V7P→V7A→settler bottom
τ_{12}	Ambient air/probe in→CPC in	Ambient air/probe in(→RLF1)→VM2→V1R →V1A→ASF→V2A→V2P→V3P→V3A →V4A→V4R→VM1→RSV→CPC tube→CPC in

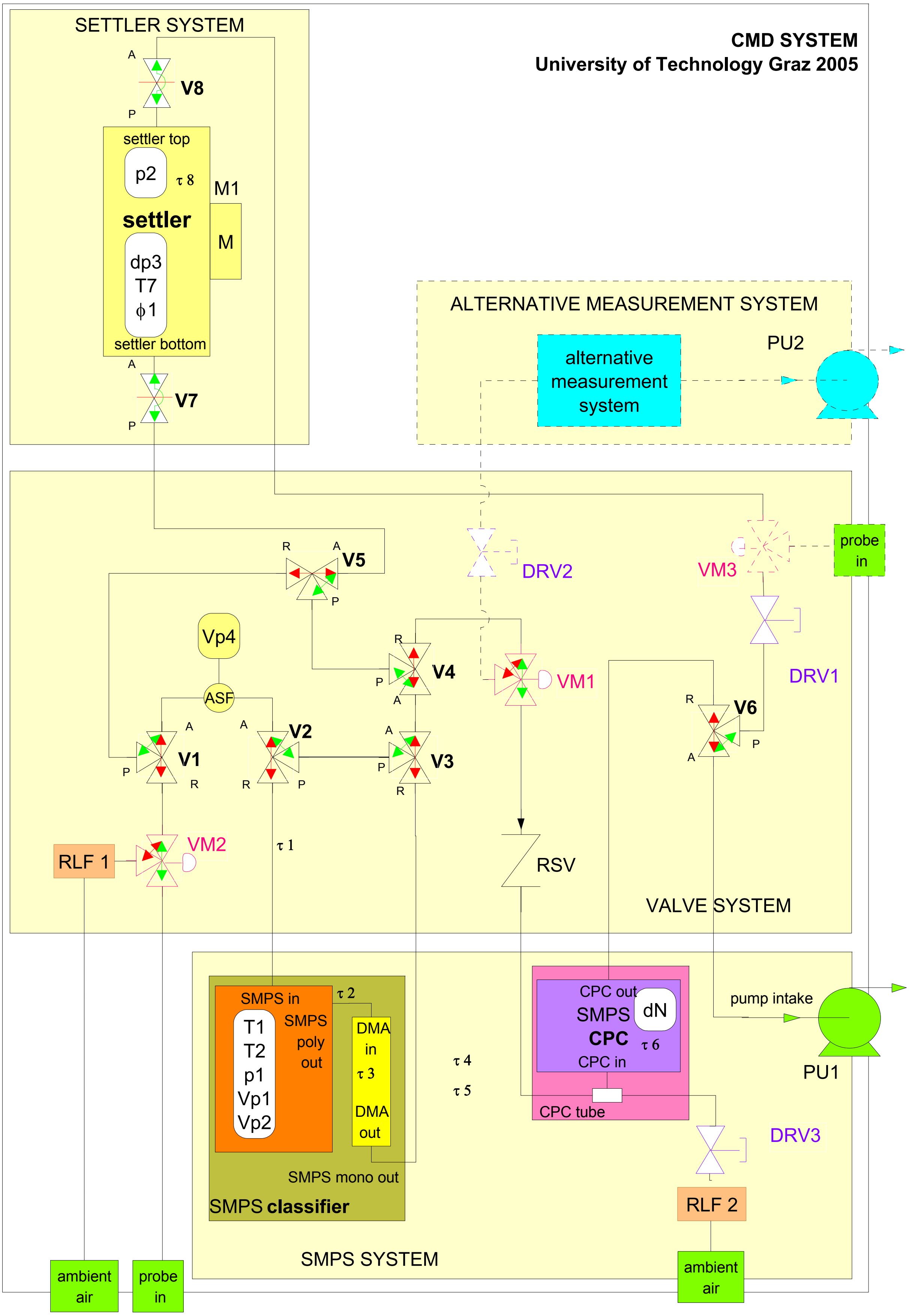

Figure 48 CMD flow chart with possible valve positions

Settler

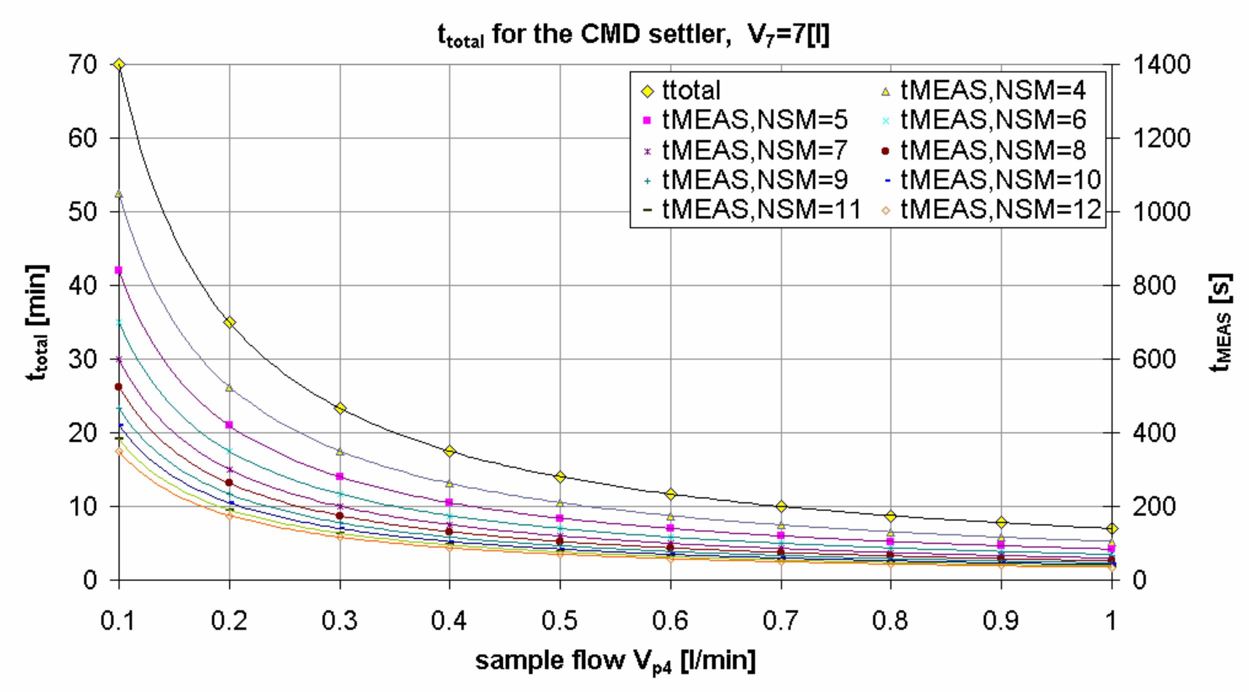

Figure 49 Total measurement time possible when emptying the settler as a function of the sample flow Vp_4 and the number of the measurements (NSM) on the right y-axis; The total measurement time as a function of Vp_4 can be read on the left y-axis (this Figure is similar to Figure 27 but also lower sample flow rates can be seen)

Appendix B

Visual Basic (VB) programs determining the lognormal size distribution

```
Sub Distribution_()
'Calculation of the logarithmic normal distribution dN/dlog(dp)
'and the dN distribution
'(C) B.Heiden 7.10.2005
'Const name1 = "VTG"  'name of sheet where distribution is calculated
Pi = WorksheetFunction.Pi()
Dim r1, r2, r3, r As Range
'Workbooks("Partikelverteilungen.xls").Activate
Worksheets("Parameter").Activate
dp1 = Cells(2, 2)
DN1 = Cells(3, 2)
typed = Cells(4, 2)
name1 = Cells(5, 2)
' Add a new sheet or overwrite the old
y = True
For i = 1 To ActiveWorkbook.Sheets.Count
   x = ActiveWorkbook.Sheets(i).Name
   If (name1 = x) Then y = False
Next
If y Then
   Set VTG = Worksheets.Add
   VTG.Name = name1
End If
' READ in the basis distribution
' Number of lines in Table
n = Range(dp1).Count
Worksheets(name1).Activate
Cells(1, 1) = "dp"
Range(Names(dp1)).Copy
Worksheets(name1).Paste (Cells(2, 1))
Cells(1, 2) = "dN/dlog(Dp)"
Cells(1, 7) = "dN(dp)"
Range(Names(DN1)).Copy
If typed = 1 Then Worksheets(name1).Paste (Cells(2, 2))
If typed = 2 Then Worksheets(name1).Paste (Cells(2, 7))
'---------------------------------------------------------------
'---------------------------------------------------------------
Nges = 0
dpg = 0
xq = 0
deltadp = 0
'---------------------------------------------------------------
For i = 2 To n
   dpm1 = Cells(i - 1, 1)
```

```
    dp = Cells(i, 1)
    dp1 = Cells(i + 1, 1)
    'Mean difference
    Select Case i
        Case 2
        deltadp = (dp1 - dp)
        Case n
        deltadp = (dp - dpm1)
        Case Else
        deltadp = (dp1 - dpm1) / 2
    End Select
    xq = xq + (dp * _
            WorksheetFunction.Ln(10)) / (deltadp)
Next i
xq = xq / (n - 1)
'-----------------------------------------------------------------------
For i = 2 To n + 1
    dp = Cells(i, 1)
    Select Case typed
        Case 1
            ' Calculate dN from dNdlogDp
            dNdlogDp = Cells(i, 2)
            dN = dNdlogDp / xq
            Cells(i, 7) = dN
        Case 2
            ' Calculate dNdlogdDp from dN
            dN = Cells(i, 7)
            dNdlogDp = dN * xq
            Cells(i, 2) = dNdlogDp
    End Select
Next i
'------------------------------------------------------------------------
For i = 2 To n
    dp = Cells(i, 1)
    dp1 = Cells(i + 1, 1)
    dNdlogDp = Cells(i, 2)
    dNdlogDp1 = Cells(i + 1, 2)
    'Mean diameter
    dpm = (dp + dp1) / 2
    'Mean logarithmic diameter
    Cells(1, 3) = "dpm_ln"
    dpm_ln = (dp1 - dp) / _
            WorksheetFunction.Ln(dp1 / dp)
    Cells(i, 3) = dpm_ln
    'Mean dN/dlog(dp)
    dNdlogDp_ln = (dNdlogDp1 - dNdlogDp) / _
            WorksheetFunction.Ln(dNdlogDp1 / dNdlogDp)
    lndp1dp = WorksheetFunction.Ln(dp1 / dp)
    mdN = dNdlogDp_ln * lndp1dp
    Nges = Nges + mdN
    Cells(1, 4) = "mdN"
    Cells(i, 4) = mdN
    dpgi = mdN * WorksheetFunction.Ln(dpm_ln)
    dpg = dpg + dpgi
Next
'Total particle concentration [#/cm^3]
Nges = Nges / 2.3
'Mean diameter
dpg = Exp(dpg / (Nges * 2.3))
sigma = 0
```

```
For i = 2 To n
   mdN = Cells(i, 4)
   dpm_ln = Cells(i, 3)
   sigmai = mdN * (WorksheetFunction.Ln(dpm_ln) - WorksheetFunction.Ln(dpg)) ^ 2
   Cells(1, 5) = "sigmai"
   Cells(i, 5) = sigmai
   sigma = sigmai + sigma
Next
'Standard deviation
lnsigma = (sigma / (Nges * 2.3 - 1)) ^ 0.5
sigma = Exp(lnsigma)
'Calculated logarithmic normal lognormal distribution
For i = 2 To n
   dpm_ln = Cells(i, 3)
   dNdlogDp_calc = Nges * 2.3 / (2 * Pi) ^ 0.5 / _
   Log(sigma) * Exp(-((Log(dpm_ln / dpg)) ^ 2 / 2 / (lnsigma ^ 2)))
   Cells(1, 6) = "dNdlogDp_calc"
   Cells(i, 6) = dNdlogDp_calc
Next
' Writing and formatting of statistical results
MsgBox ("Nges: " & Nges & " dpg: " & dpg & " sigma: " & sigma & " xq: " & xq)
Cells(1, 9).NumberFormat = "0.00E+00"
Cells(2, 9).NumberFormat = "0.0"
Cells(3, 9).NumberFormat = "0.00"
Cells(4, 9).NumberFormat = "0.00"
Cells(1, 8) = "Nges"
Cells(2, 8) = "dpg"
Cells(3, 8) = "sigmag"
Cells(4, 8) = "xq"
Cells(1, 9) = Nges
Cells(2, 9) = dpg
Cells(3, 9) = sigma
Cells(4, 9) = xq
'-----------------------------------------------------------------------------------------
'Make diagramm
'-----------------------------------------------------------------------------------------
   Worksheets(name1).Activate
   r1 = "A1:B" & n & ",F1:F" & n
   r2 = "A2:B" & n
   'Set r = Union(r1, r2)
   With Charts.Add
      .ChartWizard Source:=Worksheets(name1).Range("A1:B" & n & ",F1:F" & n), _
       gallery:=xlXYScatter, Title:="Lognormalverteilung", _
       Format:=2, PlotBy:=xlColumns, _
       CategoryTitle:="Dp (nm)", valuetitle:="dN/dlog(Dp) [#/cm^3]"
   End With
   ActiveChart.Location Where:=xlLocationAsObject, Name:=name1
   ActiveChart.ChartType = xlXYScatterSmoothNoMarkers
   ActiveChart.SetSourceData Source:=Sheets(name1).Range("A1:B105,F1:F105"), _
         PlotBy:=xlColumns
   Call Diagrammformat_
End Sub

Sub Diagrammformat_()
' logarithmic scalin
   With ActiveChart.Axes(xlCategory)
         .MinimumScale = 10
         .ScaleType = xlLogarithmic
   End With
 'grid net
```

```
    With ActiveChart.Axes(xlPrimary)
        .HasMajorGridlines = True
        .HasMinorGridlines = True
    End With
    ActiveChart.Axes(xlSecondary).HasMajorGridlines = True
    ActiveChart.Axes(xlCategory).MinorGridlines.Border.ColorIndex = 15
    ActiveChart.Axes(xlCategory).MajorGridlines.Border.ColorIndex = 48
    ActiveChart.Axes(xlValue).MajorGridlines.Border.ColorIndex = 15
' diagram aerea
    ActiveChart.PlotArea.Select
    Selection.Interior.ColorIndex = xlNone
' format of data rows
    ActiveChart.SeriesCollection(1).Select
    Selection.Border.LineStyle = xlNone
    With Selection
        .MarkerBackgroundColorIndex = xlAutomatic
        .MarkerForegroundColorIndex = xlAutomatic
        .MarkerStyle = xlDiamond
        .MarkerSize = 2
    End With
    ActiveChart.PlotArea.Select
 End Sub
```

Appendix C

Labview 7.1 software implementation of the CMD

Detailed main front panel

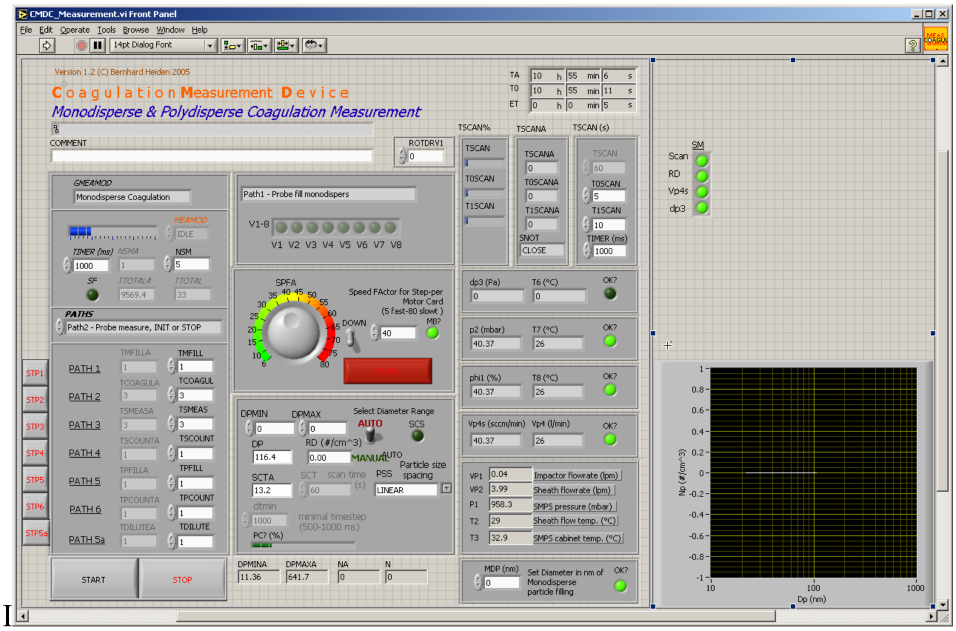

Figure 50 Detailed front panel of the main measurement program: CMDC_Menu.vi

Software hierarchy

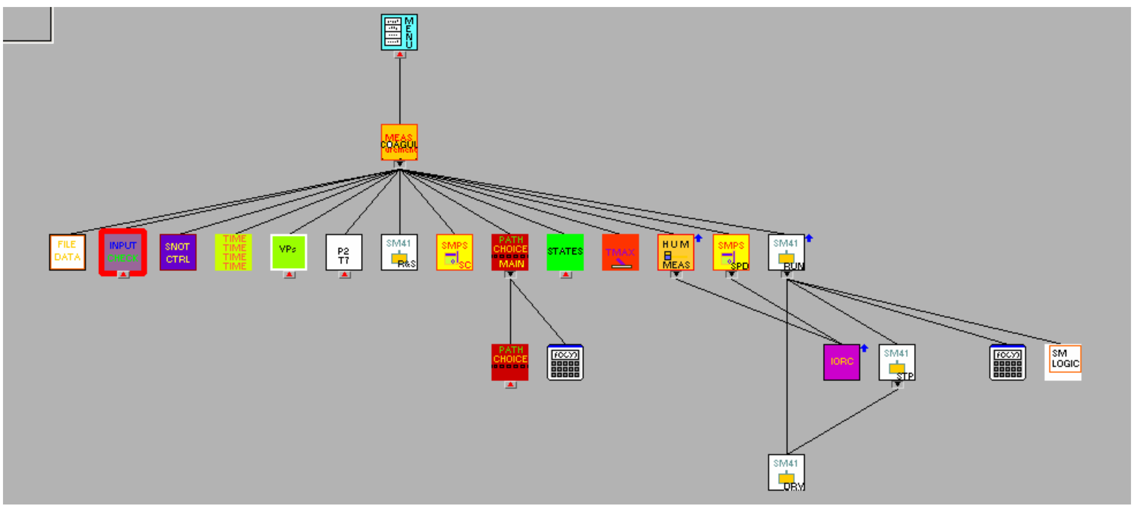

Figure 51 Program Hierarchy CMDC_Menu.vi branch CMDC_Measurement.vi

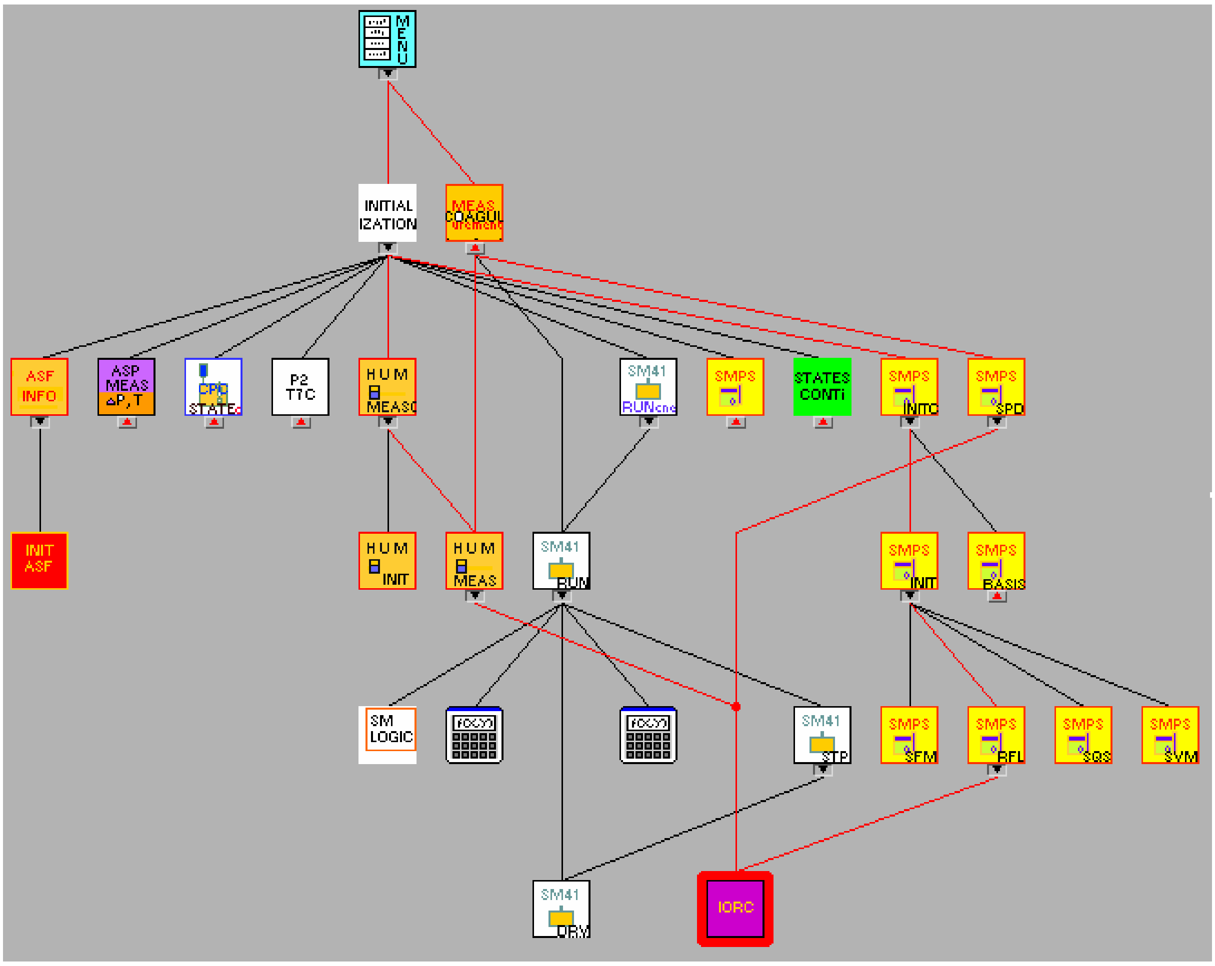

Figure 52 Program Hierarchy CMDC_Menu.vi branch CMDC_Initialization.vi

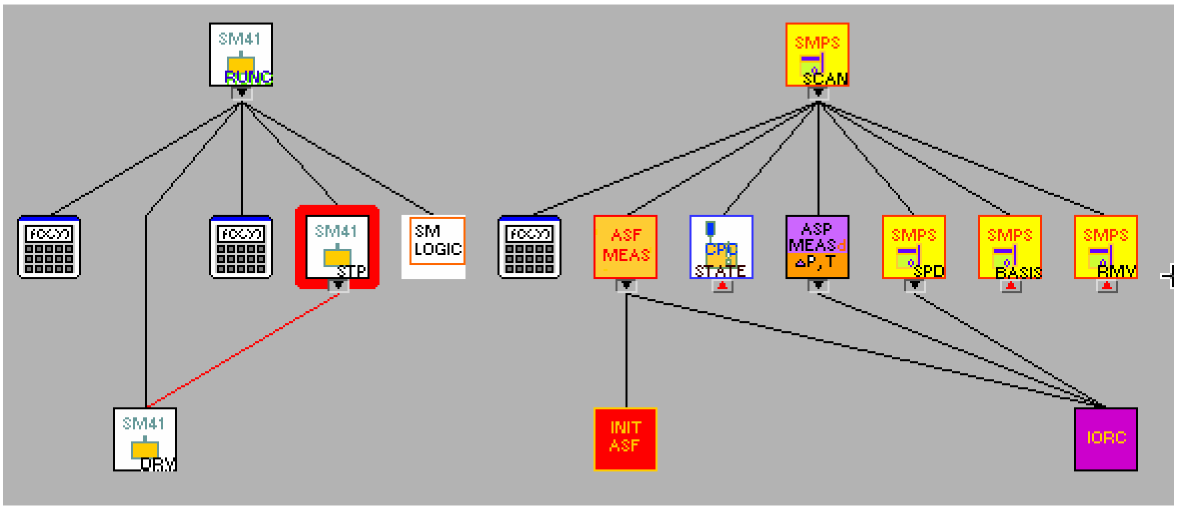

Figure 53 Program hierarchy for SMPS_SCAN_CPCCXX.vi and SM_RUNC.vi; Both programs are implicitly sub vi's of CMDC_Measurement.vi and therefore not shown in Figure 51.

Table 28 Hierarchy of the Main vi's and Sub vi's together with the icons of the Labview 7.1 software for the CMD according to Figure 51-Figure 53

Device	Main vi	Main vi Icon	Sub vi	Sub vi Icon
ASF				
	ASF_INFOC	ASF INFO	ASF_INIT	INIT ASF
	ASF_MEAS	ASF MEAS	ASF_INIT	INIT ASF
	ASF_MEAS	ASF MEAS	IORC	IORC
ASP				
	ASP_MEASD	ASP MEAS ΔP,T	IORC	IORC
CMD				
	CMDC_Measurement	MEAS COAGUL	SMPS_SPD	SMPS SPD
	CMDC_Measurement	MEAS COAGUL	SM_RUN	SM41 RUN
	CMDC_Initialization	INITIAL IZATION	ASF_INFOC	ASF INFO
	CMDC_Measurement	MEAS COAGUL	P2T7	P2 T7
	CMDC_Initialization	INITIAL IZATION	HUM_MEASC	HUM MEASC
	CMDC_Measurement	MEAS COAGUL	HUM_MEAS	HUM MEAS
	CMDC_Menu	MENU	CMDC_Measurement	MEAS COAGUL
	CMDC_Menu	MENU	CMDC_Initialization	INITIAL IZATION
	CMDC_Measurement	MEAS COAGUL	SM_RUNC	SM41 RUNC
	CMDC_Measurement	MEAS COAGUL	STATES	STATES
	CMDC_Initialization	INITIAL IZATION	STATESC	STATES CONTI
	CMDC_Measurement	MEAS COAGUL	CMDC_SNOTCTRL	SNOT CTRL
	CMDC_Measurement	MEAS COAGUL	CMDC_INPTCHK	INPUT CHECK
	CMDC_Measurement	MEAS COAGUL	CMDC_FD	FILE DATA
	CMDC_Measurement	MEAS COAGUL	CMDC_TIME	TIME TIME TIME TIME
	CMDC_Measurement	MEAS COAGUL	CMDC_VPs	VPs
	CMDC_Measurement	MEAS COAGUL	SM_RS	SM41 R&S
	CMDC_Measurement	MEAS COAGUL	SMPS_SCXX	SMPS SC
	CMDC_Measurement	MEAS COAGUL	MAIN PATH CHOICE	PATH CHOICE MAIN
	MAIN PATH CHOICE	PATH CHOICE MAIN	PATH CHOICE	PATH CHOICE

Device	Main vi	Main vi Icon	Sub vi	Sub vi Icon
	CMDC_Measurement	MEAS COAGUL	TMAXSW	TMAX
	CMDC_Initialization	INITIAL IZATION	ASP_MEASC	ASP MEAS ΔP,T
	CMDC_Initialization	INITIAL IZATION	CPC_STATEC	CPC STATEc
	CMDC_Initialization	INITIAL IZATION	P2T7C	P2 T7C
	CMDC_Initialization	INITIAL IZATION	SMPS_BASISC	SMPS
	CMDC_Initialization	INITIAL IZATION	SM_RUNCNE	SM41 RUNcne
	CMDC_Initialization	INITIAL IZATION	SMPS_INITC	SMPS INITC
	CMDC_Measurement	MEAS COAGUL	SMPS_SCANC_CPCCX	SMPS SCAN
HUM				
	HUM_MEASC	HUM MEASC	HUM_INIT	HUM INIT
	HUM_MEAS	HUM MEAS	IORC	IORC
	HUM_MEASC	HUM MEASC	HUM_MEAS	HUM MEAS
SMOT				
	SM_RUN	SM41 RUN	SM_DRV	SM41 DRV
	SM_RUN	SM41 RUN	SM_STP	SM41 STP
	SM_RUN	SM41 RUN	SM_LOGIC	SM LOGIC
	SM_RUNCNE	SM41 RUNcne	SM_RUN	SM41 RUN
	SM_STP	SM41 STP	SM_DRV	SM41 DRV
	SM_RUNC	SM41 RUNC	SM_STP	SM41 STP
	SM_RUNC	SM41 RUNC	SM_LOGIC	SM LOGIC
	SM_RUNC	SM41 RUNC	SM_DRV	SM41 DRV
SMPS				
	SMPS_INITC	SMPS INITC	SMPS_INIT	SMPS INIT
	SMPS_SCANC_CPCCX	SMPS SCAN	SMPS_RMV	SMPS RMV
	SMPS_INITC	SMPS INITC	SMPS_BASIS	SMPS BASIS
	SMPS_INIT	SMPS INIT	SMPS_SFM	SMPS SFM
	SMPS_INIT	SMPS INIT	SMPS_SVM	SMPS SVM

Device	Main vi	Main vi Icon	Sub vi	Sub vi Icon
	SMPS_SCANC_CPCCX		CPC_STATE	
	SMPS_SCANC_CPCCX		ASF_MEAS	
	SMPS_INIT		SMPS_SQS	
	SMPS_INIT		SMPS_RFL	
	SMPS_SCANC_CPCCX		ASP_MEASD	
	SMPS_SCANC_CPCCX		SMPS_SPD	
	SMPS_SCANC_CPCCX		SMPS_BASIS	
	SMPS_SPD		IORC	
	SMPS_RFL		IORC	

CMD stepper motor control

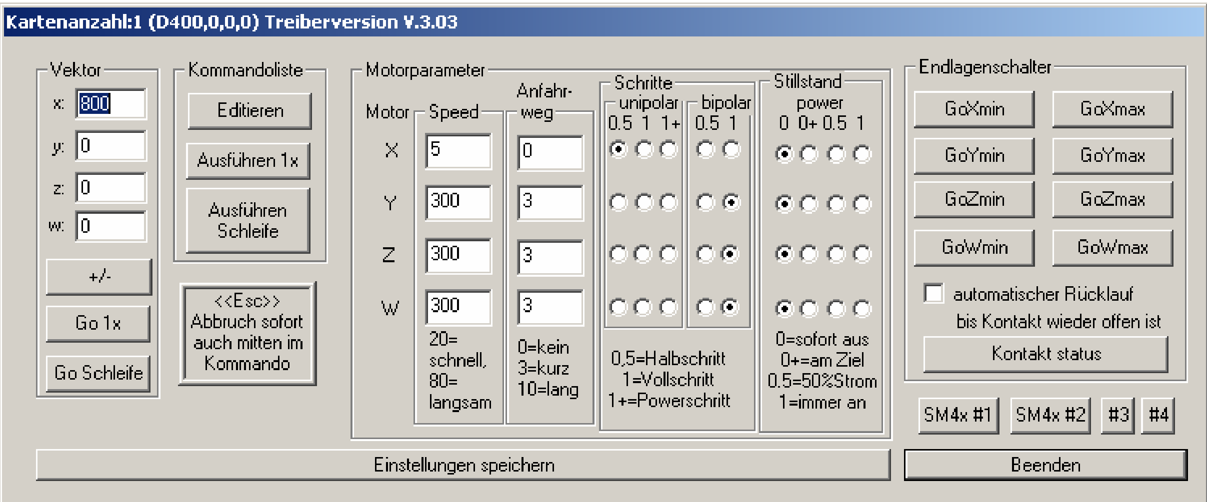

Figure 54 Standard application "SM4xDRV.EXE" from Hasotec for the stepper motor control. Has to be started and closed before running the LABVIEW program to load the driver for the Hasotec driver card into PC-memory.

Software variables in the Labview 7.1 implementation

Table 29 All software variables in the Labview 7.1 implementation for the CMD of the vi's shown in the hierarchy in Figure 51-Figure 53.

Name	Description	Unit
ASF	Cluster for Vp4s (sccm/min), OK? (bool)	-
ASP	Cluster for dp3 (Pa); T6 (°C), OK? (bool)	Pa, °C, bool
BFS	Bypass Flow Status is OK? (Yes/No)	bool
BKSTP?	Is true for back stepping	bool
BOT	Bypass blower On Time	h
bxout	Output parameter SMCard SM41 (HASOTECH)	-
BYPASS-FLOW	Bypass flow stable yes/no	bool
C M D C	Cluster for command buttons	-
CBSTLP	Count of back step loops	-
CC	Cumulative Counts since the last measurement from the CPC	-
COMMENT	COMMENT for the documentation of the measurement	text
CONTR	Continuous or stepwise run of stepper motor (true/false)	bool
COT	Classifier On Time	h
CPATH	Input/Output cluster for path i=1..6;NSM, SF, TTOTALA, TTOTAL, PATHS, TMFILL, TMFILLA, TCOAGUL, TCOAGULA, TSMEAS, TSMEASA, TSCOUNT, TSCOUNTA, TPFILL, TPFILLA, TPCOUNT, TPCOUNTA, TDILUTE, TDILUTEA	-, s
CT	Cumulative Time of the last measurement from the CPC	s
cxin	Input parameter1 SMCard SM41 (HASOTECH)	-
cxout	Output parameter1 SMCard SM41 (HASOTECH)	-
D1	Intermediate result	bool
D2	Intermediate result	bool
DAORST?	Title or values are written	bool
DATA	Output string of one line	-
Delta t	Time since start of the measurement	s
DeltaDp	Diameter difference in nm for scanning intervals	nm
DIASET	Cluster for monodisperse filling: MDP, OK?	nm, bool
DP	Diameter of Particle	nm
DP Time	Time for scan	-
dp1	Pressure drop impactor (cm H2O)	cm H2O
dp2	Pressure drop across the bypass orifice	mm H2O
dp3	Differential pressure of ASP1400 (CMD settler)	Pa

Name	*Description*	*Unit*
dp3_unit	Unit of dp3	-
DPMAX	Diameter of Particle MAXimum that could be measured with SMPS	nm
DPMAXA	Actual DPMAX of SMPS	nm
DPMIN	Diameter of Particle MINimum that could be measured with SMPS	nm
DPMINA	Actual DPMIN of SMPS	nm
dtmin	Minimal time step (500-1000 ms) needed for setting minimal time interval	ms
DVRN	Duplicate of Visa Resource Name	-
dxin	Input parameter2 SMCard SM41 (HASOTECH)	-
dxout	Output parameter2 SMCard SM41(HASOTECH)	-
EMB	Electrical MoBility from SMPS	$cm^2/(V*s)$
error in	Error in cluster	-
error out	Error out cluster	-
FF	Factor Flow for ASF1430	-
FILE	Output FILE name	-
FT	Factor for Temperature of the ASF sensor	-
FVS	Firmware version of the SMPS	-
GMEAMOD	Operations type	-
HIGH-VOLTAGE	HIGH VOLTAGE OK yes/no	bool
HUM	Cluster for humidity measurement; phi1(%), T8 (°C)	%,°C
HVS	High Voltage Status stable? (Yes/No)	bool
IL	Inner Loop count	-
INIT	Initial flag	bool
INIT OK	Humidity init vi OK?	bool
LOOPA	Actual loop number	-
MB?	Stepper motor (Card) Busy?	bool
MEAS OK	Humidity sub vi measurement OK?	bool
MEASC OK	Humidity main vi measurement OK?	bool
MNA	Model Name (SMPS)	-
MOTOR	Motor Type (0-3) =Std	-
MSW	Milliseconds to wait	ms
N	Number of scan intervals	-
N&NA	N & NA	-
NA	Number of actual SMPS scans	-

Name	*Description*	*Unit*
NLOOP	Number of loops	-
NROT	N motor ROTations	-
NROT>NTIME	NROT>NTIME?	bool
NSCAN	Cluster for NSCAN, N0SCAN, N1SCAN	-
NSCANA	Cluster for NSCANA, N0SCANA, N1SCANA	-
NSDIST	Flow chart particle concentration versus diameter (raw data)	-
NSM	Number of single measurements	-
NSMA	Actual NSM	-
NSMT	NSM	-
nthM	Actual nth measurement of the monodisperse measurement: Coagulation & Measurement together	-
NTIME	Inner Loop was repeated N-TIMEs	-
Ntot	Total particle counts since last measurement	#
OK?	Status whether command OK? (Yes/No)	bool
P1	Absolute pressure (SMPS sensor)	mbar
P2	Absolute pressure sensor CMD (settler)	mbar
P2T7	P2T7 Cluster; p2 (mbar); T7 (°C); OK?	mbar, °C
PATH Array	Array of paths that are sequentially use for the actual operation	-
Path cluster	Cluster for path settings: Path, V1-8	-
PATHS	Name of path	-
PB	Port Bytes at serial port	-
PB1	Port Bytes	-
PBS	Port Bytes Set?	-
PC?	Percent Complete?	%
phi1	Relative humidity sensor CMD	%
PSS	Particle Size Spacing (type: linear/logarithmic)	-
R0	LIQUID fill is OK? (1/0)	bool
R5	CPC is ready? (1/0)	bool
RA	Number of counts during the last (6s)	-
RB	Number of counts during the last (1s)	-
RBU	Read Buffer	-
RC	Return Count	-
RD	Actual display concentration of CPC	$\#/cm^3$
rgbx	Command code SMCard SM41 (HASOTECH)	-

Name	*Description*	*Unit*
ROTDRV1	Number of rotations of needle valve DRV1	rot
RT	Reference Temperature for ASF	°C
RTT	ReTrace Time in seconds	s
RUN	Run path or not?	bool
RV	Reads Vacuum State (0=low vacuum - there might be a problem with the filters; 1=vacuum is OK);	bool
SCS	SCan Status OK? (Yes/No)	bool
SCT	SCan Time in seconds. Scan time for one size distribution measurement	s
SCTA	Actual SCan Time	s
SDMA	Selected DMA (4-0) 4=Model 8081	-
SDP	Dp measurement OK	bool
SDR	Select particle Diameter Range: AUTO/MANUAL (1/0)	bool
SF	Measurement is running?	bool
SFM	Setting blower mode (Dual=D / Single=S)	-
SFS	Sheath Flow Status is OK (Yes/No)	bool
SGAS	Selected Gas Type(5-0)	-
SHEATH FLOW	Sheath flow stable yes/no	bool
SIMP	Selected Impactor (3-0): (2) 0.0457cm; (1) 0.0508cm; (0) 0.0710cm	-
size	Size of the path array	-
SM	Boolean array of optional measurements when false the measurement is omitted; (1)SMPS Scan, (2) RD, (3) Vp4s, (4) dp3	bool array
SMOTOR	Cluster for stepper motor control; SPFA, MB?, STOPIL	-
SMPS	Cluster for SMPS Control; DPMIN, DPMAX, DP, RD, SCT, SCTA, PSS, dtmin, PS?, SCS, SDR	-
SMPS DATA	Cluster for SMPS Data; VP1 (lpm), VP2 (lpm), P1 (mbar), T2 (°C), T3 (°C)	-
SNOT	State machine states	-
SOT	Sheath blower On Time	h
SPD	Select Particle Diameter command OK? (Yes/No)	bool
SPFA	Speed Factor for Stepper Motor Card (20 slow-80 fast)	-
SRD	Rd measurement OK	bool
Standard File?	Select standard or user defined file for data output	bool
START	START button for continuous programs	bool
STATE	Text of the actual valve state of the CMD - Pathx	-
STEA	Toggles between STatus or mEAsurement (1/0) - Status LEDS or particle number measurement	bool

Name	*Description*	*Unit*
STOP	Stop of program	-
StopBottom	Control LED for Bottom end switch	-
STOPi	Stop inner loop	bool
STOPIL	Stop inner loop for the stepper motor application to stop continuous run	bool
STOPMOTOR?	Is true if one end switch is true	bool
StopTop	Control LED for TOP end switch	-
STPR	Number of STeps Per Rotation	-
stwait	Set time to wait for time out	s
SVM	Setting Voltage Mode (A=Analog; P=Panel Control)	-
SVP	Vp measurement OK	bool
SWO	Switch off?	bool
SWOFF	Switch off when maximum time has reached	bool
T1	Cabinet temperature	°C
T2	Sheath flow temperature	°C
T3	Bypass flow temperature	°C
T4	CPC Condenser temperature	°C
T5	CPC Saturator temperature	°C
T6	ASP temperature	°C
T6_unit	Unit of T6	-
T7	CMDC temperature Pt100	°C
T8	CMD settler: Humidity temperature sensor on EK-H2	°C
TA	Actual elapsed time	s
TCLEAN	Time for STEP Cleaning of the CMD settler	s
TCLEANA	Actual time for STEP cleaning of the CMD settler	s
TCOAGUL	Time for STEP coagulation	s
TCOAGULA	Actual time for STEP coagulation	s
TFILL	Time for STEP filling the probe into the CMD settler	s
TFILLA	Actual time for STEP filling the probe into the CMD settler	s
TIME	Time cluster; TA, T0, ET	-
TIME0	Time for the beginning of the measurement series (T0)	-
TIMEA	Actual time (TA)	-
TIMER	Time interval for reading data from the hardware	ms
TMAX	Time when SWOFF is switched to true	s
TMEAS	Time for STEP Measurement with the SMPS	s

Name	*Description*	*Unit*
TMEASA	Actual time for STEP Measurement with the SMPS	s
TSCAN	Cluster for TSCAN, T0SCAN, T1SCAN, and TIMER	s, ms
TSCAN%	Cluster for TSCAN, T0SCAN, T1SCAN	%
TSCANA	Cluster for TSCANA, T0SCANA, T1SCANA, and SNOT	s, text
ttotal	Time total	s
ttotalm	Total time in milliseconds	ms
twait	Actual time for sub-vi	s
UNIT	Unit for ASF (sccm or °C)	-
UPDOWN	Up down control of the stepper motor	bool
V1	State of valve 1	bool
V1-8	Array of valves V1-8 indicating their state:0=off (closed) 1=on (opened)	bool array
V2	State of valve 2	bool
V3	State of valve 3	bool
V4	State of valve 4	bool
V5	State of valve 5	bool
V6	State of valve 6	bool
V7	State of valve 7	bool
V8	State of valve 8	bool
VBALG	Velocity of "BALG"	rpm
VMOT	Motor control velocity (from SM card) - approximately motor velocity	rpm
VOLT	DMA VOLTage	V
VP1	Sample flow rate SMPS	lpm
VP2	Sheath flow rate SMPS	lpm
VP2A	VP2	lpm
VP3	Bypass flow rate SMPS	lpm
VP4	Flow rate of the ASF Sensor	lpm
VP4H	VP4 hexadecimal code	-
VP4s	Flow rate ASF Sensor	sccm
VP4SN	Vp4 Cluster; Vp4s (sccm/min) Vp4 (l/min), OK?	-
VRN	VISA Resource Name - for the manual setting of the COM ports	-
WBU	Write BUffer	-

Devices and corresponding programs

Table 30 Device and corresponding programs, icons in Labview the variable names and their unit of all vi's used for the CMD

Device	Name of vi	Icon	Variable		Unit
ASF					
	ASF_INFOC		*Reads most setting values of the ASF1430 sensor*		
			error in	Error in cluster	-
			error out	Error out cluster	-
			FF	Factor Flow for ASF1430	-
			FT	Factor for Temperature of the ASF sensor	-
			OK?	Status whether command OK? (Yes/No)	bool
			PB	Port Bytes at serial port	-
			PB1	Port Bytes	-
			RB	Number of counts during the last (1s)	-
			RC	Return Count	-
			RT	Reference Temperature for ASF	°C
			STOP	Stop of program	-
			UNIT	Unit for ASF (sccm or °C)	-
			VRN	VISA Resource Name - for the manual setting of the COM ports	-
	ASF_INIT		*Initializes ASF sensor for measurement*		
			error in	Error in cluster	-
			error out	Error out cluster	-
			OK?	Status whether command OK? (Yes/No)	bool
			PB	Port Bytes at serial port	-
			VRN	VISA Resource Name - for the manual setting of the COM ports	-

page 1 of 26

Device	Name of vi	Icon	Variable		Unit
			WBU	Write BUffer	-
	ASF_MEAS		*Measurement of the flowrate for the ASF1430*		
			ASF	Cluster for Vp4s (sccm/min), OK? (bool)	-
			error in	Error in cluster	-
			error out	Error out cluster	-
			OK?	Status whether command OK? (Yes/No)	bool
			PB	Port Bytes at serial port	-
			RC	Return Count	-
			twait	Actual time for sub-vi	s
			VP4H	VP4 hexadecimal code	-
			VP4s	Flow rate ASF Sensor	sccm
			VRN	VISA Resource Name - for the manual setting of the COM ports	-
ASP					
	ASP_MEASC		*Measure the differential pressure and temperature with ASP1400 continuously*		
			dp3	Differential pressure of ASP1400 (CMD settler)	Pa
			dp3_unit	Unit of dp3	-
			error in	Error in cluster	-
			error out	Error out cluster	-
			OK?	Status whether command OK? (Yes/No)	bool
			STOP	Stop of program	-
			T6	ASP temperature	°C

page 2 of 26

Device	Name of vi	Icon	Variable		Unit
			T6_unit	Unit of T6	-
			TIME	Time cluster; TA, T0, ET	-
	ASP_MEASD		*Measure the differential pressure and temperature with ASP1400*		
			ASP	Cluster for dp3 (Pa); T6 (°C), OK? (bool)	Pa, °C, bool
			dp3	Differential pressure of ASP1400 (CMD settler)	Pa
			error in	Error in cluster	-
			error out	Error out cluster	-
			OK?	Status whether command OK? (Yes/No)	bool
			PB	Port Bytes at serial port	-
			RBU	Read Buffer	-
			RC	Return Count	-
			stwait	Set time to wait for time out	s
			T6	ASP temperature	°C
			twait	Actual time for sub-vi	s
			VRN	VISA Resource Name - for the manual setting of the COM ports	-
CMD					
	CMDC_FD		*Output file formatting (File Data)*		
			ASP	Cluster for dp3 (Pa); T6 (°C), OK? (bool)	Pa, °C, bool
			DAORST?	Title or values are written	bool
			DATA	Output string of one line	-
			DIASET	Cluster for monodisperse filling: MDP, OK?	nm, bool

page 3 of 26

Device	Name of vi	Icon	Variable		Unit
			DPMAXA	Actual DPMAX of SMPS	nm
			DPMINA	Actual DPMIN of SMPS	nm
			GMEAMOD	Operations type	-
			HUM	Cluster for humidity measurement; phi1(%), T8 (°C)	%,°C
			N	Number of scan intervals	-
			N&NA	N & NA	-
			NA	Number of actual SMPS scans	-
			NSMA	Actual NSM	-
			P2T7	P2T7 Cluster; p2 (mbar); T7 (°C); OK?	mbar, °C
			PATHS	Name of path	-
			ROTDRV1	Number of rotations of needle valve DRV1	rot
			SMPS	Cluster for SMPS Control; DPMIN, DPMAX, DP, RD, SCT, SCTA, PSS, dtmin, PS?, SCS, SDR	-
			SMPS DATA	Cluster for SMPS Data; VP1 (lpm), VP2 (lpm), P1 (mbar), T2 (°C), T3 (°C)	-
			SNOT	State machine states	-
			SPFA	Speed FActor for Stepper Motor Card (20 slow-80 fast)	-
			TSCANA	Cluster for TSCANA, T0SCANA, T1SCANA, and SNOT	s, text
			VP4SN	Vp4 Cluster; Vp4s (sccm/min) Vp4 (l/min), OK?	-
	CMDC_Initialization	INITIALIZATION	*CMD main program initialization and test procedures*		
			C M D C	Cluster for command buttons	-
	CMDC_INPTCHK	INPUT CHECK	*CMD sub vi for checking the input DATA an initializiing the clusters for measuring*		
			NSCAN	Cluster for NSCAN, N0SCAN, N1SCAN	-

page 4 of 26

Device	Name of vi	Icon	Variable		Unit
			NSCANA	Cluster for NSCANA, N0SCANA, N1SCANA	-
			SCT	SCan Time in seconds. Scan time for one size distribution measurement	s
			STOP	Stop of program	-
			TIMER	Time interval for reading data from the hardware	ms
			TSCAN	Cluster for TSCAN, T0SCAN, T1SCAN, and TIMER	s, ms
			TSCAN%	Cluster for TSCAN, T0SCAN, T1SCAN	%
			TSCANA	Cluster for TSCANA, T0SCANA, T1SCANA, and SNOT	s, text
	CMDC_Measurement		*CMD main programm for all measurements*		
			ASP	Cluster for dp3 (Pa); T6 (°C), OK? (bool)	Pa, °C, bool
			COMMENT	COMMENT for the documentation of the measurement	text
			CPATH	Input/Output cluster for path i=1..6;NSM, SF, TTOTALA, TTOTAL, PATHS, TMFILL, TMFILLA, TCOAGUL, TCOAGULA, TSMEAS,	-, s
			DIASET	Cluster for monodisperse filling: MDP, OK?	nm, bool
			DPMAXA	Actual DPMAX of SMPS	nm
			DPMINA	Actual DPMIN of SMPS	nm
			FILE	Output FILE name	-
			HUM	Cluster for humidity measurement; phi1(%), T8 (°C)	%,°C
			N	Number of scan intervals	-
			NA	Number of actual SMPS scans	-
			NSCAN	Cluster for NSCAN, N0SCAN, N1SCAN	-
			NSCANA	Cluster for NSCANA, N0SCANA, N1SCANA	-
			NSM	Number of single measurements	-

page 5 of 26

Device	*Name of vi*	*Icon*	*Variable*		*Unit*
			nthM	Actual nth measurement of the monodisperse measurement: Coagulation&Measurement together	-
			OK?	Status whether command OK? (Yes/No)	bool
			P2T7	P2T7 Cluster; p2 (mbar); T7 (°C); OK?	mbar, °C
			Path cluster	Cluster for path settings: Path, V1-8	-
			ROTDRV1	Number of rotations of needle valve DRV1	rot
			SM	Boolean array of optional measurements when false the measurement is omitted; (1)SMPS Scan, (2) RD, (3) Vp4s, (4) dp3	bool array
			SMOTOR	Cluster for stepper motor control; SPFA, MB?, STOPIL	-
			SMPS	Cluster for SMPS Control; DPMIN, DPMAX, DP, RD, SCT, SCTA, PSS, dtmin, PS?, SCS, SDR	-
			SMPS DATA	Cluster for SMPS Data; VP1 (lpm), VP2 (lpm), P1 (mbar), T2 (°C), T3 (°C)	-
			SNOT	State machine states	-
			START	START button for continuous programs	bool
			STATE	Text of the actual valve state of the CMD - Pathx	-
			STOP	Stop of program	-
			TCLEAN	Time for STEP Cleaning of the CMD settler	s
			TCLEANA	Actual time for STEP cleaning of the CMD settler	s
			TCOAGUL	Time for STEP coagulation	s
			TCOAGULA	Actual time for STEP coagulation	s
			TFILL	Time for STEP filling the probe into the CMD settler	s
			TFILLA	Actual time for STEP filling the probe into the CMD settler	s
			TIME	Time cluster; TA, T0, ET	-
			TMEAS	Time for STEP Measurement with the SMPS	s
			TMEASA	Actual time for STEP Measurement with the SMPS	s

page 6 of 26

Device	Name of vi	Icon	Variable		Unit
			TSCAN	Cluster for TSCAN, T0SCAN, T1SCAN, and TIMER	s, ms
			TSCAN%	Cluster for TSCAN, T0SCAN, T1SCAN	%
			TSCANA	Cluster for TSCANA, T0SCANA, T1SCANA, and SNOT	s, text
			V1-8	Array of valves V1-8 indicating their state:0=off (closed) 1=on (opened)	bool array
			VP4SN	Vp4 Cluster; Vp4s (sccm/min) Vp4 (l/min), OK?	-
	CMDC_Menu		*CMD main program*		
			C M D C	Cluster for command buttons	-
			Standard File?	Select standard or user defined file for data output	bool
	CMDC_SNOTCTRL		*CMD sub program for the choice of the SCAN mode in measuring mode*		
			LOOPA	Actual loop number	-
			NLOOP	Number of loops	-
			NSCANA	Cluster for NSCANA, N0SCANA, N1SCANA	-
			NSCANA	Cluster for NSCANA, N0SCANA, N1SCANA	-
			STOPi	Stop inner loop	bool
			TIMER	Time interval for reading data from the hardware	ms
			TSCAN%	Cluster for TSCAN, T0SCAN, T1SCAN	%
			TSCANA	Cluster for TSCANA, T0SCANA, T1SCANA, and SNOT	s, text
	CMDC_TIME		*Calculates actual and total time*		
			TIME	Time cluster; TA, T0, ET	-
			TIME0	Time for the beginning of the measurement series (T0)	-
			TIMEA	Actual time (TA)	-

page 7 of 26

Device	*Name of vi*	*Icon*	*Variable*		*Unit*
	CMDC_VPs	VPs	*Calculates the sample flow*		
			P2	Absolute pressure sensor CMD (settler)	mbar
			T7	CMDC temperature Pt100	°C
			VP4	Flow rate of the ASF Sensor	lpm
			VP4s	Flow rate ASF Sensor	sccm
	IORC	IORC	*Calculates the time and the port bytes of the serial interface*		
			DVRN	Duplicate of Visa Resource Name	-
			error in	Error in cluster	-
			error out	Error out cluster	-
			PB	Port Bytes at serial port	-
			PBS	Port Bytes Set?	-
			stwait	Set time to wait for time out	s
			twait	Actual time for sub-vi	s
			VRN	VISA Resource Name - for the manual setting of the COM ports	-
	MAIN PATH CHOICE	PATH CHOICE MAIN	*Choice of the actual path*		
			CPATH	Input/Output cluster for path i=1..6;NSM, SF, TTOTALA, TTOTAL, PATHS, TMFILL, TMFILLA, TCOAGUL, TCOAGULA, TSMEAS,	-, s
			IL	Inner Loop count	-
			NSMA	Actual NSM	-
			NSMT	NSM	-
			PATHS	Name of path	-
			RUN	Run path or not?	bool

page 8 of 26

Device	*Name of vi*	*Icon*	*Variable*		*Unit*
			SF	Measurement is running?	bool
	PATH CHOICE		*Chooses the path according to operation*		
			GMEAMOD	Operations type	-
			NSM	Number of single measurements	-
			NSMT	NSM	-
			PATH Array	Array of paths that are sequentially use for the actual operation	-
			size	Size of the path array	-
	TMAXSW		*Calculates actual time*		
			SWOFF	Switch off when maximum time has reached	bool
			TA	Actual elapsed time	s
			TIMER	Time interval for reading data from the hardware	ms
			TMAX	Time when SWOFF is switched to true	s
CPC					
	CPC_STATE		*Reads out the different states of CPC / Initializes CPC*		
			CC	Cumulative Counts since the last measurement from the CPC	-
			CT	Cumulative Time of the last measurement from the CPC	s
			error in	Error in cluster	-
			error out	Error out cluster	-
			R0	LIQUID fill is OK? (1/0)	bool
			R5	CPC is ready? (1/0)	bool
			RA	Number of counts during the last (6s)	-

page 9 of 26

Device	Name of vi	Icon	Variable		Unit
			RB	Number of counts during the last (1s)	-
			RD	Actual display concentration of CPC	#/cm^3
			RV	Reads Vacuum State (0=low vacuum - there might be a problem with the filters; 1=vacuum is OK);	bool
			SRD	Rd measurement OK	bool
			STEA	Toggles between STatus or mEAsurement (1/0) - Status LEDS or particle number measurement	bool
			T4	CPC Condenser temperature	°C
			T5	CPC Saturator temperature	°C
			ttotalm	Total time in milliseconds	ms
	CPC_STATEC		*Reads out the different states of CPC / Initializes CPC continuously*		
			CC	Cumulative Counts since the last measurement from the CPC	-
			CT	Cumulative Time of the last measurement from the CPC	s
			error in	Error in cluster	-
			error out	Error out cluster	-
			R0	LIQUID fill is OK? (1/0)	bool
			R5	CPC is ready? (1/0)	bool
			RA	Number of counts during the last (6s)	-
			RB	Number of counts during the last (1s)	-
			RD	Actual display concentration of CPC	#/cm^3
			RV	Reads Vacuum State (0=low vacuum - there might be a problem with the filters; 1=vacuum is OK);	bool
			STEA	Toggles between STatus or mEAsurement (1/0) - Status LEDS or particle number measurement	bool
			STOP	Stop of program	-

page 10 of 26

Device	Name of vi	Icon	Variable		Unit
			T4	CPC Condenser temperature	°C
			T5	CPC Saturator temperature	°C
			ttotal	Time total	s
DAQ					
	P2T7	P2 T7	*Measures the pressure and the temperature in the CMD Balg (accordeon) with the NI-DAQ SC2345*		
			OK?	Status whether command OK? (Yes/No)	bool
			P2	Absolute pressure sensor CMD (settler)	mbar
			P2T7	P2T7 Cluster; p2 (mbar); T7 (°C); OK?	mbar, °C
			T7	CMDC temperature Pt100	°C
	P2T7C	P2 T7C	*Measures the pressure and the temperature in the CMD settler with the NI-DAQ SC2345 continuously*		
			error in	Error in cluster	-
			error out	Error out cluster	-
			OK?	Status whether command OK? (Yes/No)	bool
			P2	Absolute pressure sensor CMD (settler)	mbar
			STOP	Stop of program	-
			T7	CMDC temperature Pt100	°C
HUM					
	HUM_INIT	HUM INIT	*Initializes the humitity sensor EK-H2*		
			error in	Error in cluster	-
			error out	Error out cluster	-
			OK?	Status whether command OK? (Yes/No)	bool

page 11 of 26

Device	Name of vi	Icon	Variable		Unit
			PB	Port Bytes at serial port	-
			RBU	Read Buffer	-
			RC	Return Count	-
			STOP	Stop of program	-
			VRN	VISA Resource Name - for the manual setting of the COM ports	-
	HUM_MEAS		*Measures the humidity in the CMD Balg (one sample)*		
			error in	Error in cluster	-
			error out	Error out cluster	-
			HUM	Cluster for humidity measurement; phi1(%), T8 (°C)	%,°C
			OK?	Status whether command OK? (Yes/No)	bool
			PB	Port Bytes at serial port	-
			phi1	Relative humidity sensor CMD	%
			RB	Number of counts during the last (1s)	-
			RC	Return Count	-
			stwait	Set time to wait for time out	s
			T8	CMD settler: Humidity temperature sensor on EK-H2	°C
			twait	Actual time for sub-vi	s
			VRN	VISA Resource Name - for the manual setting of the COM ports	-
	HUM_MEASC		*Measures the humidity in the CMD Balg continuously*		
			INIT OK	Humidity init vi OK?	bool
			MEAS OK	Humidity sub vi measurement OK?	bool

page 12 of 26

Device	*Name of vi*	*Icon*	*Variable*		*Unit*
			MEASC OK	Humidity main vi measurement OK?	bool
			phi1	Relative humidity sensor CMD	%
			STOP	Stop of program	-
			T8	CMD settler: Humidity temperature sensor on EK-H2	°C
			TIME	Time cluster; TA, T0, ET	-
			VRN	VISA Resource Name - for the manual setting of the COM ports	-
SMOT					
	SM_DRV		*Driver of the Stepper Motor - (code supplied from Hasotech)*		
			bxout	Output parameter SMCard SM41 (HASOTECH)	-
			cxin	Input parameter1 SMCard SM41 (HASOTECH)	-
			cxout	Output parameter1 SMCard SM41 (HASOTECH)	-
			dxin	Input parameter2 SMCard SM41 (HASOTECH)	-
			dxout	Output parameter2 SMCard SM41(HASOTECH)	-
			rgbx	Command code SMCard SM41 (HASOTECH)	-
	SM_LOGIC		*Stepper motor decision logic*		
			BKSTP?	Is true for back stepping	bool
			CONTR	Continuous or stepwise run of stepper motor (true/false)	bool
			D1	Intermediate result	bool
			D2	Intermediate result	bool
			NROT>NTIME	NROT>NTIME?	bool
			STOPMOTOR?	Is true if one end switch is true	bool

Device	Name of vi	Icon	Variable		Unit
			SWO	Switch off?	bool
	SM_RS		*Stepper motor control*		
			MB?	Stepper motor (Card) Busy?	bool
			SMOTOR	Cluster for stepper motor control; SPFA, MB?, STOPIL	-
			SPFA	Speed FActor for Stepper Motor Card (20 slow-80 fast)	-
			START	START button for continuous programs	bool
			STOP	Stop of program	-
			STOPIL	Stop inner loop for the stepper motor application to stop continuous run	bool
	SM_RUN		*Controls the run of the Stepper Motor(s) with the SM41 Card (from Hasotech)*		
			BKSTP?	Is true for back stepping	bool
			CBSTLP	Count of back step loops	-
			CONTR	Continuous or stepwise run of stepper motor (true/false)	bool
			MB?	Stepper motor (Card) Busy?	bool
			MOTOR	Motor Type (0-3) =Std	-
			NROT	N motor ROTations	-
			NTIME	Inner Loop was repeated N-TIMEs	-
			OK?	Status whether command OK? (Yes/No)	bool
			SPFA	Speed FActor for Stepper Motor Card (20 slow-80 fast)	-
			STOP	Stop of program	-
			StopBottom	Control LED for Bottom end switch	-
			STOPIL	Stop inner loop for the stepper motor application to stop continuous run	bool

page 14 of 26

Device	Name of vi	Icon	Variable		Unit
			STOPMOTOR?	Is true if one end switch is true	bool
			StopTop	Control LED for TOP end switch	-
			STPR	Number of STeps Per Rotation	-
			ttotal	Time total	s
			ttotalm	Total time in milliseconds	ms
			VBALG	Velocity of "BALG"	rpm
			VMOT	Motor control velocity (from SM card) - approximately motor velocity	rpm
	SM_RUNC		*Runs continuously the stepper motor*		
			BKSTP?	Is true for back stepping	bool
			CBSTLP	Count of back step loops	-
			CONTR	Continuous or stepwise run of stepper motor (true/false)	bool
			MB?	Stepper motor (Card) Busy?	bool
			MOTOR	Motor Type (0-3) =Std	-
			NROT	N motor ROTations	-
			NTIME	Inner Loop was repeated N-TIMEs	-
			OK?	Status whether command OK? (Yes/No)	bool
			SPFA	Speed FActor for Stepper Motor Card (20 slow-80 fast)	-
			START	START button for continuous programs	bool
			STOP	Stop of program	-
			StopBottom	Control LED for Bottom end switch	-
			STOPIL	Stop inner loop for the stepper motor application to stop continuous run	bool

Device	Name of vi	Icon	Variable		Unit
			STOPMOTOR?	Is true if one end switch is true	bool
			StopTop	Control LED for TOP end switch	-
			STPR	Number of STeps Per Rotation	-
			ttotal	Time total	s
			VBALG	Velocity of "BALG"	rpm
			VMOT	Motor control velocity (from SM card) - approximately motor velocity	rpm
	SM_RUNCNE		*Basis stepper motor control program*		
			BKSTP?	Is true for back stepping	bool
			CBSTLP	Count of back step loops	-
			CONTR	Continuous or stepwise run of stepper motor (true/false)	bool
			MB?	Stepper motor (Card) Busy?	bool
			NROT	N motor ROTations	-
			NTIME	Inner Loop was repeated N-TIMEs	-
			OK?	Status whether command OK? (Yes/No)	bool
			SPFA	Speed FActor for Stepper Motor Card (20 slow-80 fast)	-
			START	START button for continuous programs	bool
			STOP	Stop of program	-
			StopBottom	Control LED for Bottom end switch	-
			STOPIL	Stop inner loop for the stepper motor application to stop continuous run	bool
			STOPMOTOR?	Is true if one end switch is true	bool
			StopTop	Control LED for TOP end switch	-

page 16 of 26

Device	Name of vi	Icon	Variable		Unit
			STPR	Number of STeps Per Rotation	-
			ttotal	Time total	s
			VBALG	Velocity of "BALG"	rpm
			VMOT	Motor control velocity (from SM card) - approximately motor velocity	rpm
	SM_STP		*Shows whether the end switches are pressed*		
			StopBottom	Control LED for Bottom end switch	-
			StopTop	Control LED for TOP end switch	-
SMPS					
	SMPS_BASIS		*SMPS Basisdaten*		
			dp1	Pressure drop impactor (cm H2O)	cm H2O
			dp2	Pressure drop across the bypass orifice	mm H2O
			error in	Error in cluster	-
			error out	Error out cluster	-
			FVS	Firmware version of the SMPS	-
			MNA	Model Name (SMPS)	-
			P1	Absolute pressure (SMPS sensor)	mbar
			T1	Cabinet temperature	°C
			T2	Sheath flow temperature	°C
			ttotalm	Total time in milliseconds	ms
			VP1	Sample flow rate SMPS	lpm
			VP2	Sheath flow rate SMPS	lpm

page 17 of 26

Device	Name of vi	Icon	Variable		Unit
			VP3	Bypass flow rate SMPS	lpm
	SMPS_BASISC		*SMPS Basisdaten*		
			dp1	Pressure drop impactor (cm H2O)	cm H2O
			dp2	Pressure drop across the bypass orifice	mm H2O
			error in	Error in cluster	-
			error out	Error out cluster	-
			FVS	Firmware version of the SMPS	-
			MNA	Model Name (SMPS)	-
			P1	Absolute pressure (SMPS sensor)	mbar
			STOP	Stop of program	-
			T1	Cabinet temperature	°C
			T2	Sheath flow temperature	°C
			ttotalm	Total time in milliseconds	ms
			VP1	Sample flow rate SMPS	lpm
			VP2	Sheath flow rate SMPS	lpm
			VP3	Bypass flow rate SMPS	lpm
	SMPS_INIT		*Intializes SMPS for subsequent measurement*		
			BYPASS-FLOW	Bypass flow stable yes/no	bool
			error in	Error in cluster	-
			error out	Error out cluster	-
			HIGH-VOLTAGE	HIGH VOLTAGE OK yes/no	bool

page 18 of 26

Device	Name of vi	Icon	Variable		Unit
			OK?	Status whether command OK? (Yes/No)	bool
			SFM	Setting blower mode (Dual=D / Single=S)	-
			SHEATH FLOW	Sheath flow stable yes/no	bool
			STOP	Stop of program	-
			SVM	Setting Voltage Mode (A=Analog; P=Panel Control)	-
			ttotal	Time total	s
			VP2	Sheath flow rate SMPS	lpm
			VRN	VISA Resource Name - for the manual setting of the COM ports	-
	SMPS_INITC		*Intializes SMPS for subsequent measurement*		
			error in	Error in cluster	-
			error out	Error out cluster	-
			HIGH-VOLTAGE	HIGH VOLTAGE OK yes/no	bool
			OK?	Status whether command OK? (Yes/No)	bool
			SFM	Setting blower mode (Dual=D / Single=S)	-
			SHEATH FLOW	Sheath flow stable yes/no	bool
			SVM	Setting Voltage Mode (A=Analog; P=Panel Control)	-
			ttotal	Time total	s
			VP2	Sheath flow rate SMPS	lpm
			VP2A	VP2	lpm
			VRN	VISA Resource Name - for the manual setting of the COM ports	-
	SMPS_RFL		*SMPS Read FLags for stable process*		

page 19 of 26

Device	Name of vi	Icon	Variable		Unit
			BYPASS-FLOW	Bypass flow stable yes/no	bool
			error in	Error in cluster	-
			error out	Error out cluster	-
			HIGH-VOLTAGE	HIGH VOLTAGE OK yes/no	bool
			OK?	Status whether command OK? (Yes/No)	bool
			PB	Port Bytes at serial port	-
			RC	Return Count	-
			SHEATH FLOW	Sheath flow stable yes/no	bool
			twait	Actual time for sub-vi	s
			VRN	VISA Resource Name - for the manual setting of the COM ports	-
	SMPS_RMV		*Reads most measurement values of the SMPS*		
			BFS	Bypass Flow Status is OK? (Yes/No)	bool
			DP	Diameter of Particle	nm
			dp1	Pressure drop impactor (cm H2O)	cm H2O
			DPMAX	Diameter of Particle MAXimum that could be measured with SMPS	nm
			DPMIN	Diameter of Particle MINimum that could be measured with SMPS	nm
			EMB	Electrical MoBility from SMPS	cm^2/(V*s)
			error in	Error in cluster	-
			error out	Error out cluster	-
			HVS	High Voltage Status stable? (Yes/No)	bool
			P1	Absolute pressure (SMPS sensor)	mbar

page 20 of 26

Device	Name of vi	Icon	Variable		Unit
			SDMA	Selected DMA (4-0) 4=Model 8081	-
			SFM	Setting blower mode (Dual=D / Single=S)	-
			SFS	Sheath Flow Status is OK (Yes/No)	bool
			SGAS	Selected Gas Type(5-0)	-
			SIMP	Selected Impactor (3-0): (2) 0.0457cm; (1) 0.0508cm; (0) 0.0710cm	-
			SMPS DATA	Cluster for SMPS Data; VP1 (lpm), VP2 (lpm), P1 (mbar), T2 (°C), T3 (°C)	-
			SVM	Setting Voltage Mode (A=Analog; P=Panel Control)	-
			T2	Sheath flow temperature	°C
			T3	Bypass flow temperature	°C
			ttotalm	Total time in milliseconds	ms
			VOLT	DMA VOLTage	V
			VP1	Sample flow rate SMPS	lpm
			VP2	Sheath flow rate SMPS	lpm
			VP3	Bypass flow rate SMPS	lpm
	SMPS_SCANC_CPCC		Control over SMPS, CPC, ASP, ASF (sub vi for CMDC_Measurement)		
			ASF	Cluster for Vp4s (sccm/min), OK? (bool)	-
			ASP	Cluster for dp3 (Pa); T6 (°C), OK? (bool)	Pa, °C, bool
			CC	Cumulative Counts since the last measurement from the CPC	-
			CT	Cumulative Time of the last measurement from the CPC	s
			DeltaDp	Diameter difference in nm for scanning intervals	nm
			DP	Diameter of Particle	nm

Device	Name of vi	Icon	Variable		Unit
			DP	Diameter of Particle	nm
			DP Time	Time for scan	-
			DPMAX	Diameter of Particle MAXimum that could be measured with SMPS	nm
			DPMIN	Diameter of Particle MINimum that could be measured with SMPS	nm
			error in	Error in cluster	-
			error out	Error out cluster	-
			INIT	Initial flag	bool
			N	Number of scan intervals	-
			NA	Number of actual SMPS scans	-
			NSDIST	Flow chart particle concentration versus diameter (raw data)	-
			Ntot	Total particle counts since last measurement	#
			PSS	Particle Size Spacing (type: linear/logarithmic)	-
			RD	Actual display concentration of CPC	#/cm^3
			RD	Actual display concentration of CPC	#/cm^3
			SCS	SCan Status OK? (Yes/No)	bool
			SCS	SCan Status OK? (Yes/No)	bool
			SCT	SCan Time in seconds. Scan time for one size distribution measurement	s
			SCTA	Actual SCan Time	s
			SDP	Dp measurement OK	bool
			SDR	Select particle Diameter Range: AUTO/MANUAL (1/0)	bool
			SM	Boolean array of optional measurements when false the measurement is omitted; (1)SMPS Scan, (2) RD, (3) Vp4s, (4) dp3	bool array
			SMPS DATA	Cluster for SMPS Data; VP1 (lpm), VP2 (lpm), P1 (mbar), T2 (°C), T3 (°C)	-

page 22 of 26

Device	Name of vi	Icon	Variable		Unit
			SPD	Select Particle Diameter command OK? (Yes/No)	bool
			SRD	Rd measurement OK	bool
			SRD	Rd measurement OK	bool
			STOP	Stop of program	-
			STOPIL	Stop inner loop for the stepper motor application to stop continuous run	bool
			SVP	Vp measurement OK	bool
			ttotal	Time total	s
	SMPS_SCXX		*Control over SMPS, CPC, ASP, ASF*		
			ASF	Cluster for Vp4s (sccm/min), OK? (bool)	-
			ASP	Cluster for dp3 (Pa); T6 (°C), OK? (bool)	Pa, °C, bool
			DPMAXA	Actual DPMAX of SMPS	nm
			DPMINA	Actual DPMIN of SMPS	nm
			N	Number of scan intervals	-
			N&NA	N & NA	-
			NA	Number of actual SMPS scans	-
			NSDIST	Flow chart particle concentration versus diameter (raw data)	-
			SM	Boolean array of optional measurements when false the measurement is omitted; (1)SMPS Scan, (2) RD, (3) Vp4s, (4) dp3	bool array
			SMPS	Cluster for SMPS Control; DPMIN, DPMAX, DP, RD, SCT, SCTA, PSS, dtmin, PS?, SCS, SDR	-
			SMPS DATA	Cluster for SMPS Data; VP1 (lpm), VP2 (lpm), P1 (mbar), T2 (°C), T3 (°C)	-
			SNOT	State machine states	-
			STOPIL	Stop inner loop for the stepper motor application to stop continuous run	bool

page 23 of 26

Device	Name of vi	Icon	Variable		Unit
	SMPS_SFM		*SMPS Set Flow Mode --> Single or Dual Blower*		
			error in	Error in cluster	-
			error out	Error out cluster	-
			OK?	Status whether command OK? (Yes/No)	bool
			PB	Port Bytes at serial port	-
			RC	Return Count	-
			SFM	Setting blower mode (Dual=D / Single=S)	-
			STOP	Stop of program	-
			twait	Actual time for sub-vi	s
			VRN	VISA Resource Name - for the manual setting of the COM ports	-
	SMPS_SPD		*SMPS Set Particle Diameter --> needed for SMPS_SCAN*		
			DP	Diameter of Particle	nm
			OK?	Status whether command OK? (Yes/No)	bool
			PB	Port Bytes at serial port	-
			RC	Return Count	-
			stwait	Set time to wait for time out	s
			twait	Actual time for sub-vi	s
			VRN	VISA Resource Name - for the manual setting of the COM ports	-
	SMPS_SQS		*SMPS Set sheath flow rate*		
			error in	Error in cluster	-
			error out	Error out cluster	-

page 24 of 26

Device	Name of vi	Icon	Variable		Unit
			OK?	Status whether command OK? (Yes/No)	bool
			PB	Port Bytes at serial port	-
			RC	Return Count	-
			STOP	Stop of program	-
			VP2	Sheath flow rate SMPS	lpm
			VRN	VISA Resource Name - for the manual setting of the COM ports	-
	SMPS_SVM		*SMPS Set Voltage Mode --> Choice between analog and panel control*		
			error in	Error in cluster	-
			error out	Error out cluster	-
			OK?	Status whether command OK? (Yes/No)	bool
			PB	Port Bytes at serial port	-
			RC	Return Count	-
			STOP	Stop of program	-
			SVM	Setting Voltage Mode (A=Analog; P=Panel Control)	-
			VRN	VISA Resource Name - for the manual setting of the COM ports	-
VALVE					
	STATES		*States of the valves*		
			Path cluster	Cluster for path settings: Path, V1-8	-
			PATHS	Name of path	-
			STATE	Text of the actual valve state of the CMD - Pathx	-
			V1	State of valve 1	bool

page 25 of 26

Device	*Name of vi*	*Icon*	*Variable*		*Unit*
			V1-8	Array of valves V1-8 indicating their state:0=off (closed) 1=on (opened)	bool array
			V2	State of valve 2	bool
			V3	State of valve 3	bool
			V4	State of valve 4	bool
			V5	State of valve 5	bool
			V6	State of valve 6	bool
			V7	State of valve 7	bool
			V8	State of valve 8	bool
	STATESC	STATES CONTi	*States of the valves continuously*		
			Path cluster	Cluster for path settings: Path, V1-8	-
			STOP	Stop of program	-
			V1	State of valve 1	bool
			V1-8	Array of valves V1-8 indicating their state:0=off (closed) 1=on (opened)	bool array
			V2	State of valve 2	bool
			V3	State of valve 3	bool
			V4	State of valve 4	bool
			V5	State of valve 5	bool
			V6	State of valve 6	bool
			V7	State of valve 7	bool
			V8	State of valve 8	bool